Institut für Nutzpflanzenwissenschaften und Ressourcenschutz
Fachbereich Pflanzenzüchtung

Development of root phenotyping methods and QTL analysis of root traits in grapevine mapping populations

Dissertation

zur Erlangung des Grades
Doktorin der Agrarwissenschaften (Dr. agr.)

der Landwirtschaftlichen Fakultät
der Rheinischen Friedrich-Wilhelms-Universität Bonn

von
Ronja Schmitz
aus
Siegburg

Bonn, 2023

Referentin:	Prof. Dr. Annaliese Mason
Korreferent:	Prof. Dr. Reinhard Töpfer

Tag der mündlichen Prüfung: 06.04.2022

Angefertigt mit Genehmigung der Landwirtschaftlichen Fakultät der Universität Bonn

When solving problems, dig at the roots instead of just hacking at the leaves.

- Anthony J. D’Angelo

Table of Contents

List of Figures

List of Tables

List of Supplementary Figures

List of Supplementary Tables

List of Abbreviations

%	Percentage
°C	Degree Celsius
ARL	Adventitious root length
ARL / LRL	Ratio between adventitious and lateral root length
ARN	Adventitious root number
cM	Centimorgan
cm	Centimeter
g	Gram
IM	Interval mapping
KW	Kruskal-Wallis
l	Liter
LA_LAM	Leaf area measured with leaf are meter
LA_WR	Leaf area measured with WinRhizo image analysis
LG	Linkage group
LRL	Lateral root length
LOD	Logarithm of the odds
mg	Milligram
mm	Millimeter
PCA	Principle components analysis
QTL	Quantitative trait loci
RD	Maximal root diameter
RDW	Root dry weight
RL	Maximal root length
RN	Number of adventitious roots
SDW	Shoot dry weight
SLR	Single-lens reflex
TRL	Total root length
WCD	Woody cutting diameter

Summary

Facing climatic change and upcoming extreme weather events require the adaptation of agricultural crops to conditions like extended drought periods in the future. Therefore, the incorporation of promising morphological and physiological qualities is necessary in crop breeding strategies. Regarding heat and drought, plant roots play an essential role for adequate water uptake and efficient exploitation of water resources in the soils. As plant roots are crucial for crop performance and yield, investigation of phenotypic root traits is a promising approach to promote breeding efforts. However, phenotyping of root systems has proven to be extremely challenging due to their hidden nature. In this study, grapevine adventitious root development from grapevine woody cuttings was investigated by three different phenotyping methods to identify QTL regions linked to grapevine adventitious root formation and root system characteristics.

The first attempt of classifying early adventitious root formation on woody cuttings grown in perlite substrate resulted in the identification of four QTLs. To further investigate sub-traits of root formation, image-based analysis was envisaged. Therefore, a root phenotyping system based on rhizotrons suitable for high throughput root architecture screenings of mapping populations was developed and evaluated. The utilization of rhizotrons for root phenotyping provided a data rich basis for QTL mapping of two mapping populations and revealed 18 QTLs in total for root related traits and four QTLs for leaf area. Thirdly, certain genotypes of a grapevine mapping population grown in the field were analysed regarding root system characteristics resulting in four identified QTLs in total; three QTLs associated with root system characteristics and one QTL associated with shoot biomass. Finally, the three root system phenotyping methods were compared regarding their performance by examining the individual throughput potential, time and cost effort, number of measurable traits, as well as number and quality of resulting QTL regions.

This study describes the development and analysis of phenotyping methods for grapevine root systems. It contributes to the identification of potential genomic regions and candidate genes involved in the regulation of adventitious root formation providing new insights relevant for breeding purposes and breeding research of grapevine rootstocks.

Kurzfassung

Der Klimawandel und zukünftig vermehrt auftretende Extremwetterereignisse erfordern die Anpassung landwirtschaftlicher Nutzpflanzen an besondere klimatische Bedingungen wie anhaltende Dürreperioden. Daher müssen entsprechende morphologische und physiologische Eigenschaften in der modernen Pflanzenzüchtung berücksichtigt werden. Besonders die Entwicklung des Wurzelsystems ist entscheidend für Leistung und Ertrag der Nutzpflanzen. Im Hinblick auf Hitze und Trockenheit spielen die Wurzeln eine essenzielle Rolle für eine ausreichende Wasseraufnahme und effektive Verwertung der Wasserressourcen im Boden. Die phänotypische Untersuchung von Wurzeleigenschaften ist daher eine vielversprechende Strategie in der Pflanzenzüchtung, jedoch mit besonderen Schwierigkeiten verbunden, da Wurzeln unterirdisch wachsen und im Boden nur schwer zugänglich sind. In dieser Arbeit wurde die Entwicklung von Adventivwurzeln an Rebenstecklingen mit Hilfe drei verschiedener Phänotypisierungsmethoden untersucht, um QTL Regionen zu identifizieren, die assoziiert sind mit der Entstehung von Rebenwurzeln und verschiedenen Eigenschaften ihrer Wurzelsysteme.

Zunächst wurden Holzstecklinge in Perlitsubstrat angezogen, um die Entstehung der Adventivwurzeln zu klassifizieren und die phänotypischen Daten zur QTL-Berechnung zu verwenden. Um die Merkmale der Wurzeln mit Hilfe von Bildanalyseverfahren genauer zu erfassen, wurde ein Phänotypisierungssystem basierend auf Rhizotronen entwickelt und evaluiert, das für die Anwendung von Hochdurchsatz-Screenings ganzer Kreuzungspopulationen geeignet war. Insgesamt wurden die Wurzeln von zwei Kreuzungspopulationen phänotypisiert und die folgende QTL-Berechnung ergab insgesamt 18 QTLs für Wurzelmerkmale und vier QTLs für die Blattfläche. In einem weiteren Feldversuch wurden ausgesuchte Genotypen der bereits getesteten Kreuzungspopulation bezüglich ihrer Wurzeleigenschaften untersucht. Durch diesen Feldversuch konnten vier QTLs identifiziert werden, davon waren drei assoziiert mit Wurzeleigenschaften und ein QTL assoziiert mit der Biomasse des Sprosses. Schließlich wurden alle drei Methoden zur Wurzelphänotypisierung an Reben bezüglich ihres Durchsatzes, des Kosten- und Zeitaufwands, der Anzahl und Qualität messbarer Wurzelmerkmale sowie der Anzahl gefundener QTL-Regionen verglichen.

Die vorliegende Studie beschreibt die Entwicklung und Analyse der drei Phänotypisierungs-methoden an Rebenwurzeln. Sie liefert somit einen wichtigen Beitrag zur Identifikation von QTLs und potenziellen Kandidatengenen im Zusammenhang mit Wurzelwachstum und seiner Regulierung. Die so gewonnenen neuen Erkenntnisse tragen zum Fortschritt in der Züchtung und Züchtungsforschung an Rebenunterlagen bei.

1. Chapter 1: General Introduction

1.1. Viticulture and Climate Change

Since hundreds of years, grapevine is one of the most important and valuable horticultural crops in the world. In 2018, 77.8 million tons of grapes were produced on 7.4 million hectares of vineyards worldwide. Wine grapes constituted 57% of the worldwide grape production and were processed mostly into wine or non-alcoholic juice resulting in 292 million hectoliters. In addition, 36% of global grape production accounted to table grapes produced for fresh consumption and 7% were dried into raisins. In Germany, 1.4 million tons of grapes were produced on 103 thousand hectares in 2018 resulting in 10.3 million hectoliters of wine (OIV Statistical Report on World Vitiviniculture, 2019).

Viticulture worldwide mostly consists of *Vitis vinifera* ssp. *vinifera* L. cultivars. In the 19th century, phylloxera (*Daktulospharia vitifoliae* Fitch), an almost microscopic, pale-yellow sap-sucking insect was introduced from North America to Europe. The aphid-like insect (Hemiptera, Sternorrhycha, Aphidoidea and Aphididea) forms pocket-like galls on leaves and hooked galls on root tips, which are called nodosities and serve as physiological nutrient sink for the insect (Granett et al. 2001, Steffan and Rilling, 1981). On older lignified roots, phylloxera causes formation of tuberosities which disrupt water and nutrient uptake. Consequently, phylloxera infestation leads to massive reduction of leaf surface area and yield, ultimately resulting in plant death. As the widespread used *V. vinifera* cultivars in Europe were highly susceptible at their roots, the introduction of phylloxera caused enormous damage and disastrous consequences for European viticulture, especially in France and Germany (Zhang et al. 2009). To overcome the devastating effect of phylloxera, grape species from North America which coevolved with this pest were tested as rootstocks and grafted with scions of high-quality wine-producing *V*. *vinifera* cultivars (Smith et al. 2013). Since the phylloxera crisis, grafting of *V. vinifera* has become standard practice in commercial vineyards in all regions where phylloxera was present by the beginning of the 20th century and still is mandatory today (Zhang et al. 2009; Ollat et al. 2016b).

Most of the current rootstock cultivars are interspecific hybrids of American *Vitis* wild species: *V. riparia*, *V. berlandieri*, and *V. rupestris* (Whiting, 2005). Common rootstock cultivars and their origin of North American crossings are listed in figure 1. The low genetic variability of rootstock varieties is reinforced by the utilization of only a reduced number of rootstocks in respective production areas leading to an even less variability in rootstocks in certain vine growing regions.

V. berlandieri × *V. riparia*	*V. berlandieri* × *V. rupestris*	*V. riparia* × *V. rupestris*	*V. riparia* × *V. cinerea*
Kober 5BB	Richter 110	3309 Couderc	Börner
Selektion Oppenheim 4	Richter 99	101-14 Mgt	
Kober 125 AA	1103 Paulsen	Schwarzmann	
5C Geisenheim	140 Ruggeri		
Teleki 8B			
Binova			
420 A			
Couderc 161-49			
34 E.M.			
R.S.B.1			

Figure 1: Common rootstock cultivars in Germany and their origin from crossings of North American wild species.

Besides phylloxera tolerance, *V. riparia* and *V. rupestris* were selected as rootstock candidates because of their high percentage of adventitious root formation from dormant woody canes (Pongrácz, 1983). However, it turned out they were not appropriate for limestone rich soils of many European wine growing regions. Contrary, *V. berlandieri* shows high tolerance to calcareous soils but does not readily form adventitious roots from dormant canes at a level necessary for commercial purposes (Viala and Ravaz, 1901). Therefore, most crossings were conducted between a limestone tolerant *V. berlandieri* and another vigorous rooting *Vitis* species.

In addition to phylloxera resistance, breeding of grapevine rootstock cultivars aims at several beneficial characteristics as easy growth, resistance to fungal diseases, particularly good lignification and wood maturity, grafting ability, ecological adaptability, suitability for specific locations, nutrient use efficiency, beneficial impact on the scion, and long lifetime (Schmid and Manty, 2005). Both, rootstocks, and scions are propagated vegetatively mostly in commercial nurseries by dormant hardwood cuttings of selected varieties (Nicholas et al. 1992). Therefore, good rooting ability of cuttings is essential for propagation and crucial in today's viticultural practice.

Climate change will challenge grapevine roots and rootstocks in the future. Most important effects are expected to be drought, soil erosion, and salinity (Santos et al. 2020). Southern Europe for instance is suggested to become a hot spot for drought change under climate change (Spinoni et al. 2015). The choice of rootstock cultivar has already been part of the adaptation strategy of viticulture to climate change (van Leeuwen et al. 2019). Future rootstocks will need to cope with water scarcity by improved water use efficiency due to an extensive and deep root system (Medrano et al. 2015). In addition, the interaction of rootstock and scion might be shifted to reduced scion vigor, decreased leaf area, and lower transpiration (Clingeleffer et al. 2019). It is assumed that the genetic variability of current rootstock varieties might be insufficient to cope with future climatic constraints (Peiró et al. 2020). Although,

viticulture can cope in the short term with impacts of climate change, long-term strategies including change of rootstock genotypes need to be envisaged in the near future (Delrot et al. 2020).

1.2. Physiological Functions and Development of Grapevine Roots

Grapevine roots are essential for water and nutrient uptake, anchorage in the soil, storage of reserves, interactions with symbiotic organisms, and production of hormones that control plant functions (Ollat et al. 2016a). Soil-water uptake is induced by two different passive forces driven by 1) the conversion of stored carbohydrates into soluble, osmotically active sugars resulting in a negative, osmotic potential called root pressure in spring; and 2) the transpiration creating negative vascular pressure during the growing season. Contrary to water uptake, nutrient uptake is most often an active process as it usually occurs against a concentration gradient due to a much lower nutrient concentration in soil solution compared to nutrient concentration in root cells (Hellman, 2003).

In addition, grapevines use mycorrhizal associations which influence the mineral uptake of their roots. The vesicular-arbuscular fungi invade grapevine roots and enhance mineral mobilization and uptake by releasing hydroxyamates, oxalate, citrate, and malate. Hereby, mycorrhizal association reduces root-hair formation, increases lateral root production, and promotes dichotomous root branching (Schubert, 1990, Schellenbaum et al. 1991). Whereas water and nutrients are transported upwards to the shoot system, organic nutrients are carried downwards for storage or root growing. The accumulation of organic nutrients in the root system starts after shoot growth decline in mid- to late summer with a peak reached in autumn (Andersen, 2003). During winter, older, mature, and permanent roots of the root system anchor the vine and act as major storage organ (Zapata et al. 2001).

Figure 2 gives a schematic overview of the interaction between grapevine and environment. Factors like soil type, local microclimate, and crop management may influence rootstocks directly or indirectly by scion-rootstock-interaction. Those highly complex and multifactorial interactions complicate the characterization of root systems, as varieties can exhibit multiple manifestations. Therefore, knowledge about root system characteristics and about genetic mechanisms controlling root development and physiology is still very scarce in grapevine (Ollat et al. 2016a). In addition, phenotyping and characterisation of root systems require high investments of time, work force and material costs due to the difficult accessibility of roots in soil, especially of perennial crops (Jeudy et al. 2016).

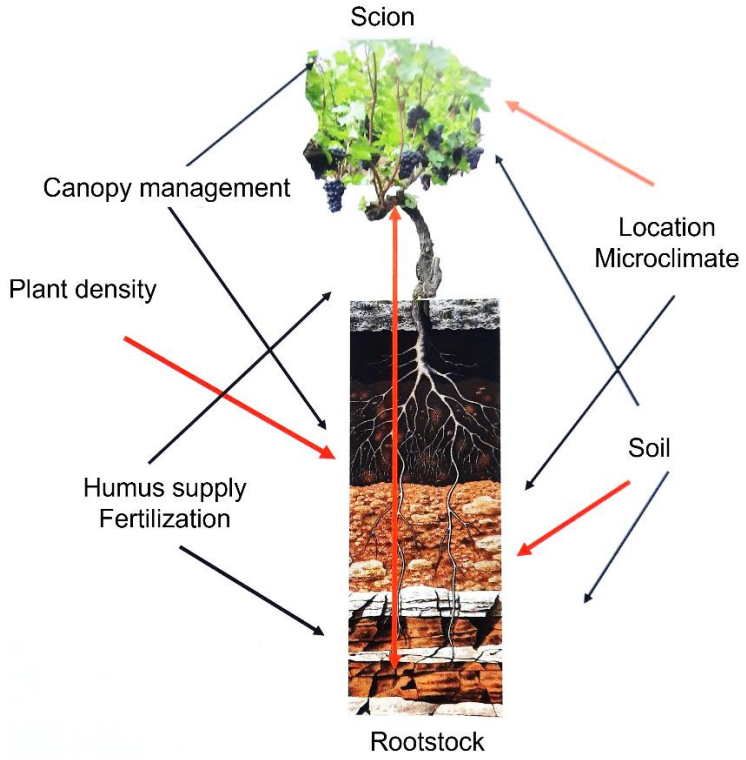

Figure 2: Interactions between scion, rootstock, and environment (modified by Schmid et al. 2019).

1.3. Formation of Adventitious Roots

Whereas root systems of spermatophytes develop from the radicle formed during embryogenesis, post-embryonic roots develop from stems, leaves or other non-root organs are called adventitious roots (Bellini et al. 2014). As grapevines are propagated vegetatively via dormant woody cuttings, ability of adventitious root formation plays an important ecological and economical role in viticulture. Figure 3 shows a grapevine woody cutting with evolved adventitious roots and branching lateral roots.

The biological process of adventitious root formation is affected by several endogenous and exogenous factors like phytohormones, transcription factors, epigenetics, and metabolic signals as well as environmental factors like light, water, and nutrients. Adventitious root formation appears in three phases: 1. Induction phase: Establishment of primordium initial cells and dedifferentiation of pericycle cells or cambium cells; 2. Initiation phase: Cell division of primordia meristematic cells and dedifferentiation into root cell layers for internal root meristem; 3. Extension phase: Elongation and outgrowth of adventitious root primordia through stem cell layers and emerge from the epidermis (De Klerk et al. 1999). During all phases, auxin is suggested to be the main growth-promoting phytohormone involved in adventitious root formation. In apple rootstocks, expression of five genes associated with auxin signal transduction has been identified to change during induction phase of adventitious root formation under exogenous indole-3-butyric acid (auxin precursor) treatment (Li et al. 2018).

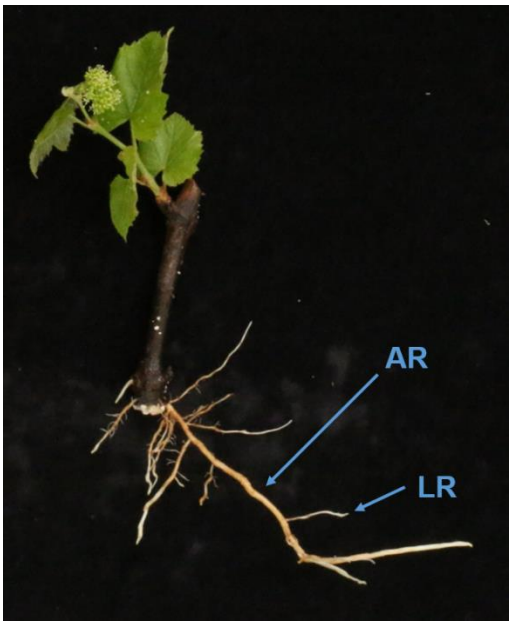

Figure 3: Grapevine woody cutting with adventitious roots (AR) evolved from the stem and lateral roots (LR) branching off the adventitious roots.

Besides auxin, other regulators contribute to the regulation of adventitious root formation: cytokinin, ethylene and gibberellic acid (da Costa et al. 2013). Whereas auxin is known to promote adventitious root formation, cytokinin suppresses the development and represents the antagonist to auxin in several plant species like Arabidopsis and poplar (Werner et al. 2003, Ramirez-Carvajal et al. 2009). This generally applies for adventitious rooting of cuttings, where an increase in auxin and a concomitant decrease in cytokinin are required (da Costa et al. 2013).

It has been shown that ethylene is involved in the regulation of adventitious root formation by controlling the expression pattern of genes coding for PIN-FORMED (PIN) proteins, that form auxin-efflux and -influx carrier, and thereby modifying auxin transport in tomato (Negi et al. 2010). Besides that, ethylene regulates the expression of APETALA/ETHYLENE RESPONSE FACTOR (AP2/ERF) VII transcription factors which are involved in the control of root system architecture in *A. thaliana* seedlings (Eysholdt-Derzsó and Sauter, 2019).

In different plant tissues, gibberellic acid is known to affect auxin accumulation and therefore, plays an important role in regulation of adventitious rooting (Mauriat et al. 2014). However, gibberellins seem to have a negative effect on the formation of adventitious roots, too. Exogenous gibberellin can inhibit the formation of adventitious crown roots in rice and mutants with dysfunctional gibberellins biosynthesis showed additional adventitious roots (Lo et al. 2008).

Even though, insights of the mechanisms behind adventitious root formation have been enhanced in the last years, it still falls short compared to the knowledge about primary root formation and development during embryogenesis (Gonin et al. 2019). As several economically relevant woody crops are propagated vegetatively, a better understanding of adventitious root formation and development can have application in breeding strategies in order to enhance rooting behaviour especially when adventitious root formation is the limiting factor as in propagation of woody and horticultural species like grapevine (Uga et al. 2013).

1.4. QTL Analysis in Grapevine Mapping Populations

QTL (quantitative trait locus) analysis is a statistical method to link phenotypic data and genotypic data in order to identify the genetic basis of variation in complex traits (Falconer and Mackay, 1996). Phenotypic data is collected as trait measurements whereas genotypic data is based on molecular markers. QTL analysis reveals information about the number and location of specific chromosomic regions linked to the investigated phenotypic trait. Common QTL mapping methods are Kruskal-Wallis non-parametric test and interval mapping. The Kruskal-Wallis test detects individual association between markers and traits, whereas interval mapping determines the likelihood for a segregating QTL present at each position within the genome (Van Ooijen, 2004).

The first evidenced molecular marker in grapevine was a microsatellite marker (SSR, Simple sequence repeats) isolated in the early 1990s by Thomas and Scott (1993). The following first genetic map comprising of RAPD (Random amplified polymorphic DNA) and RFLP (Restriciton fragment length polymorphism) markers was published in 1995 (Lodhi et al. 1995). Until now, more than 160 genetic maps of grapevine have been published and over 400 grapevine SSRs are currently publicly available. They have been extensively used in mapping studies because of their multiallelic nature, codominant inheritance, reproducibility, and transferability (Delrot et al. 2020). Also, SNP (Single Nucleotide Polymorphism) markers coupled with SSRs have been used for assessing population genetic structure (Ghaffari, 2014).

The use of genetic polymorphisms among individuals linked to phenotypic traits expedites studies of inheritance and diversity as well as breeding activities (Xu et al. 2016). Only few functional markers have been reported in grapevine, e.g., markers tightly linked to the sex locus (Battilana et al. 2013), gene for muscat flavour (Emanuelli et al. 2014), or berry skin colour (Kobayashi et al. 2004, Migliaro et al. 2014).

Several grapevine traits have been studied for QTL mapping by utilization of segregating F1 mapping populations e.g., the F1 progeny obtained by a cross of the grapevine cultivar ‘V3125’ (‘Schiava Grossa’ × ‘Riesling’) and rootstock cultivar ‘Börner’ (*V. riparia* Gm183 × *V. cinerea* Arnold). The population was crossed and analyzed to localize determinants of phylloxera root

resistance, as rootstock cultivar ‘Börner’ showed high resistance whereas ‘V3125’ was more susceptible to root phylloxera. Zhang et al. (2009) identified one QTL on linkage group 13 for resistance against phylloxera. Besides phylloxera resistance, ‘Börner’ showed high resistance to black rot. QTL analysis based on resistance classification of potted plants revealed two QTLs on linkage group 14 and linkage group 16 and several additional minor QTLs (Rex et al. 2014). Similarly, a resistance locus on linkage group 14 against downy mildew has been identified in this mapping population (Ochssner et al. 2016). Besides resistance traits, QTL mapping also aimed on identification of agronomic traits. Investigation regarding flowering time and ripening related traits resulted in a promising QTL region on linkage group 1 confirmed by QTL analysis in a second mapping population. The corresponding linkage consensus map consisted of 374 markers on 1365 cM and on 19 linkage groups. Marker density was between 6 (LG 16) and 31 (LG 1) marker per chromosome and the average distance between the markers is 3.9 cM (Fechter et al. 2014).

Another grapevine mapping population was derived from a cross between ‘Calardis Musqué’ (‘Bacchus’ × ‘Seyval’) and ‘Villard Blanc’ (Seibel 6468 × ‘Subereux’). A first corresponding genetic map was published by Zyprian et al. (2006) followed by a revised version by Schwander (unpublished). The improved genetic map comprises 394 SSR markers on 1622 cM on 19 linkage groups. The marker density is between 11 (LG 2) and 41 (LG 14) markers per chromosome. The segregating mapping population was analyzed regarding full bloom and QTLs on chromosomes 1, 14, 17, and 9 could be detected (Fechter et al. 2014). Further, the grapevine berry trait cuticle impedance was determined, and one preliminary QTL was identified on linkage group 17 (Herzog et al. 2015). Several QTLs for loose bunch architecture were identified in the same mapping population associated with the traits rachis length, peduncle length, and pedicel length (Richter et al. 2017). Considering disease resistance, a major QTL was identified on chromosome 15 suggested to work together with another QTL on chromosome 18. In the same study a QTL for onset timing of veraison could be localized on chromosome 16 and chromosome 18 (Zyprian et al. 2016).

In total, more than 90 QTL studies of grapevine have been conducted within the last 20 years, but hardly any of them revealed QTLs for root phenology related traits like root biomass or root number (Delrot et al. 2020). Only two studies by Tandonnet et al. (2018) and Alahakoon (2020) identified QTLs related to root traits. The challenging accessibility and difficult characterization of belowground grown root systems limits the successful application of genetic markers in grapevine rootstock breeding. Besides the limiting bottleneck of root phenotyping methods sufficient for large germplasm populations, the polygenic nature of root related traits and complex quantitative inheritance hamper proper investigations. In addition, roots are highly

influenced by the environment and the interaction between genetic background and environment (Delrot et al. 2020). Therefore, variability due to the genotype is not easy to detect.

The use of genetic markers in breeding activities accelerates the breeding process enormously. Especially selection of parents before crossing and selection during juvenile phase is enhanced by marker-assisted selection (MAS) (Yang et al. 2016). Genetic markers associated with beneficial root traits may enable faster breeding for improved rootstocks forearmed for extreme whether events in the future.

1.5. Aim of the Study

The aim of this study was to develop, describe and analyse three different root phenotyping methods and compare their performance and outcome to provide new insights relevant for breeding and breeding research of grapevine rootstocks.

In this study, grapevine adventitious root development was investigated by different phenotyping methods to identify QTL regions linked to grapevine adventitious root formation and further roots system characteristics. Therefore, a root phenotyping system based on rhizotrons suitable for high throughput root architecture screenings of entire mapping populations was developed and evaluated to meet grapevine rootstock breeding purposes. In addition, two other phenotyping methods were used to analyse the grapevine mapping population regarding root system characteristics of grapevines grown in the field and early grapevine woody cuttings planted in perlite substrate.

Afterwards, the gathered phenotypic data of all three root phenotyping methods was utilized for QTL mapping to identify potential genomic regions and candidate genes involved in regulation of adventitious root formation and root system development of grapevine genotypes.

1.6. References

Alahakoon, D. (2020): Exploiring Phenotypic Diversity and Quantitative Trait Loci Mapping for Root Architecture, Freezing Tolerance, Chilling Fulfillment, and Photoperiod Traits in Grapevine Populations. Electronic Theses and Dissertations. 4855

Andersen, C.P. (2003): Source-sink balance and carbon allocation below ground in plants exposed to ozone. New Phytologist, 157(2):213-228

Battilana, J.; Lorenzi, S.; Moreira, F.M.; Moreno-Sanz, P.; Failla, O.; Emanuelli, F.; Grando, M.S. (2013): Linkage Mapping and Molecular Diversity at the Flower Sex Locus in Wild and Cultivated Grapevine Reveal a Prominent SSR Haplotype in Hermaphrodite Plants. Mol. Biotechnol. 54:1031-1037

Bellini, C.; Pacurar, D.I.; Perrone, I. (2014): Adventitious Roots and Lateral Roots: Similarities and Di_erences. Annu. Rev. Plant Biol. 65:639–666.

Clingeleffer, P.; Morales, N.; Davis, H.; Smith, H. (2019): The significance of scion × rootstock interactions. OENO One 53, 335–346

Da Costa, C.T.; de Almeida, M.R.; Ruedell, C.M.; Schwambach, J.; Maraschin, F.S.; Fett-Neto, A.G. (2013): When stress and development go hand in hand: Main hormonal controls of adventitious rooting in cuttings. Front. Plant Sci. 4:133.

De Klerk, G.-J.; van der Krieken, W.; de Jong, J.C. (1999): Review of the formation of adventitious roots: New concepts, new possibilities. Vitr Cell Dev Biol Plant. 35:189-199

Delrot, S.; Grimplet, J.; Carbonell-Bejerano, P. et al. (2020): Genetic and Genomic Approaches for Adaptation of Grapevine to Climate Change. In: Genomic Designing of Climate-Smart Fruit Crops. Edited by Kole, C. Springer

Emanuelli, F.; Sordo, M.; Lorenzi, S.; Battilana, J.; Grando, M.S. (2014): Development of user-friendly functional molecular markers for *VvDXS* gene conferring muscat flavor in grapevine. Molecular Breeding, 33:235-241

Eysholdt-Derzsó, E.; Sauter, M. (2019): Hypoxia and the group VII ethylene responsive transcription factor HRE2 promote adventitious root elongation in Arabidopsis. Plant Biol. 21 (Suppl. 1), 103–108.

Falconer, D.S.; Mackay, T.F.C. (1996): Introduction to Quantitative Genetics. 4th edition, London, Prentice Hall)

Fechter, I.; Hausmann, L.; Zyprian, E.; Daum, M.; Holtgräve, D.; Weisshaar, B.; Töpfer, R. (2014): QTL analysis of flowering time and ripening traits suggests an impact of a genomic region on linkage group 1 in Vitis. Theor. Appl. Genet. 127, 1857-1872

Ghaffari, S.; Hasnaoui, N.; Zinelabidine, L.; Ferchichi, A.; Martínez-Zapater, J.; Ibáñez, J. (2014): Genetic diversity and parentage of Tunisian wild and cultivated grapevines (Vitis vinifera L.) as revealed by single nucleotide polymorphism (SNP) markers. Tree Genetics & Genomes. 10(4):1103-1112

Gonin, M.; Bergougnoux, V.; Nguyen, T.D.; Gantet, P.; Champion, A. (2019): What makes adventitious roots? Plants. 8:240

Granett, J.; Omer, A.D.; Walker, M.A. (2001): Seasonal capacity of attached and detached vineyard roots to support grape phylloxera (Homoptera: Phylloxeridae). Journal of Economic Entomology, 94(1):138-144

Hellman, E.W. (2003): Grapevine Structure and Function. In: Oregon Viticulture, Edited by: Hellman, E.W. Cornvallis: Oregon State University Press.

Herzog, K.; Wind, R.; Töpfer, R. (2015): Impedance of the Grape Berry Cuticle as a Novel Phenotypic Trait to Estimate Resistance to Botrytis Cinerea. Sensors. 15(6), 12498-12512

Jeudy, C.; Adrian, M.; Baussard, C. et al. (2016): RhizoTubes as a new tool for high throughput imaging of plant root development and architecture: test, comparison with pot grown plants and validation. Plant Methods 12, 31.

Kobayashi, S.; Goto-Yamamoto, N.; Hirochika, H. (2004): Retrotransposon-induced mutations in grape skin color. Science 304:982

Li, K.; Liang, Y.; Xing, L.; Mao, J.; Liu, Z.; Dong, F.; Meng, Y.; Han, M.; Zhao, C.; Bao, L.; Zhang, D. (2018): Transcriptome analysis reveals multiple hormones, wounding and sugar signaling pathways mediate adventitious root formation in apple rootstock. Int. J. Mol. Sci. 19(8):2201

Lo, S.-F.; Yang, S.-Y.; Chen, K.-T.; Hsing, Y.-I.; Zeevaart, J.A.D.; Chen, L.-J.; Yu, S.-M. (2008): A Novel Class of Gibberellin 2-Oxidases Control Semidwarfism, Tillering, and Root Development in Rice. Plant Cell 20:2603–2618.

Lodhi, M.A.; Daly, M.J.; Ye, G.N.; Weeden, N.F.; Reisch, B.I. (1995): A molecular marker based linkage map of Vitis. Genome 38:786-794

Mauriat, M.; Petterle, A.; Bellini, C.; Moritz, T. (2014): Gibberellins inhibit adventitious rooting in hybrid aspen and Arabidopsis by affecting auxin transport. Plant J. 78:382-384

Medrano, H.; Tomás, M.; Martorell, S.; Escalona, J.-M.; Pou, A.; Fuentes, S.; Flexas, J.; Bota, J. (2015): Improving water use efficiency of vineyards in semi-arid regions. A review. Agronomy for Sustainable Development 35, 499–517

Migliaro, D.; Crespan, M.; Muñoz-Organero, G.; Velasco, R.; Moser, C.; Vezzulli, S. (2014): Structural dynamics at the berry colour locus in *Vitis vinifera* L. somatic variants. Australian Journal of Grape and Wine Research, Vol. 20(3), 485-495

Negi, S.; Sukumar, P.; Liu, X.; Cohen, J.D.; Muday, G.K. (2010): Genetic dissection of the role of ethylene in regulating auxin-dependent lateral and adventitious root formation in tomato. Plant J. 61:3-15.

Nicholas, P.R.; Chapman, A.P.; Cirami, R.M. (1992): Grapevine propagation, In: Coombe, B.G.; Dry, R.P. eds. Viticulture, Vol. 2, practices. Adelaide, Winetitles. p.1-22.

Ochssner, I.; Hausmann, L.; Töpfer, R. (2016): *Rpv14*, a new genetic source for *Plasmopara viticola* resistance conferred by Vitis cinerea. Vitis, Vol. 55(2), 79-81

OIV Statistical Report on World Vitiviniculture, 2019:
https://www.oiv.int/public/medias/7298/oiv-state-of-the-vitivinicultural-sector-in-2019.pdf

Ollat, N.; Bordenave, L.; Tandonnet, J.P.; Boursiquot, J.M.; Marguerit, E. (2016a): Grapevine rootstocks: origins and perspectives. Acta Hortic. ISHS 2016, Proc. I Int. Symp. On Grapevine Roots. Eds.: Gaiotti, F. et al.

Ollat, N.; Peccoux, A.; Papura, D.; Esmenjaud, D.; Marguerit, E.; Tandonnet, J.-P.; Bordenave, L.; Cookson, S.J.; Barrieu, F.; Rossdeutsch, L.; Lecourt, J.L.; Lauvergeat, V.; Vivin, P.; Bert, P.-F.; Delrot, S. (2016b): Rootstocks as a component of adaptation to environment. In: Grapevine in a Changing Environment: A Molecular and Ecophysiological Perspective, First Edition. Edited by Gerós, H.V.; Chaves, M.M.; Gil, H.M.; Delrot, S. John Wiley & Son, Ltd.

Peiró, R.; Jiménez, C.; Perpiña, G.; Soler, J.X.; Gisbert, C. (2020): Evaluation of the genetic diversity and root architecture under osmotic stress of common grapevine rootstocks and clones. Scientia Horticulturae 266

Pongrácz, D.P. (1983): Rootstocks for grapevines. David Philip, Cape Town.

Ramirez-Carvajal, G.A.; Morse, A.M.; Dervinis, C.; Davis, J.M. (2009): The cytokinin type-B response regulator PtRR13 is a negative regulator of adventitious root development in Populus. Plant Physiol. 150:759-771

Rex, F.; Fechter, I.; Hausmann, L.; Töpfer, R. (2014): QTL mapping of black rot (*Guignardia bidwellii*) resistance in the grapevine rootstock 'Börner' (*V. riparia* Gm183 × *V. cinerea* Arnold). Theoretical and Applied Genetics. 127, 1667-1677

Richter, R.; Rossmann, S.; Töpfer, R.; Theres, K.; Zyprian, E. (2017): Genetic analysis of loose cluster architecture in grapevine. BIO Web of Conferences. 9, 01016. 40th World Congress of Vine and Wine.

Santos, J.A.; Fraga, H.; Malheiro, A.C.; Moutinho-Pereira, J.; Dinis, L.-T.; Correia, C.; Moriondo, M.; Leolini, L.; Dibari, C.; Costafreda-Aumedes, S.; Kartschall, T.; Menz, C.; Molitor, D.; Junk, J.; Beyer, M.; Schultz, H.R. (2020): A review of the potential climate change impacts and adaptation options for European viticulture. Applied Sciences 10, 3092

Schellenbaum, L.; Berta, G.; Ravolanirina, F.; Tisserant, B.; Gianinazzi, S.; Fitter, A.H. (1991): Influence of Endomycorrhizal Infection on Root Morphology in a Micropropagated Woody Plan Species (*Vitis vinifera* L.). Annals of Botany, Vol. 68(2), 135-141

Schmid, J.; Manty, F. (2005): Abschlussbericht zum BML-Forschungsvorhaben 115-0940-2/7, Züchtung und Prüfung von Unterlagssorten. Hochschule Geisenheim University.

Schmid, J.; Manty, F.; Lindner, B. (2019): Geisenheimer Rebsorten und Klone. Geisenheimer Berichte, 90, Auflage 3. Hochschule Geisenheim University.

Schubert, A. (1990): Effects of vesicular arbuscular mycorrhizal fungi on micropropagated grapevines: Influence of endophyte strain, P fertilization and growth medium. Vitis, 29(1), 5-13

Smith, B.P.; Wheal, M.S.; Jones, T.H.; Morales, N.B.; Clingeleffer, P.R. (2013): Heritability of adventitious rooting of grapevine dormant canes. Tree Genetics and Genomes, 9:467-474

Spinoni, J.; Naumann, G.; Vogt, J. (2015): Spatial patterns of European droughts under a moderate emission scenario. Adv. Sci. Res. 12, 179-186

Steffan, H. and Rilling, G. (1981): The effect of phylloxera leaf and root galls on the pattern of assimilate distribution in grapevine (Dactylosphaera-vitifolii shimer on *Vitis rupestris* 187 G.). Vitis. 20(2), 146-155

Tandonnet, J.P.; Marguerit, E.; Cookson, S.J.; Ollat, N. (2018): Genetic architecture of aerial root traits in field-grown grafted grapevines is largely independent. Theor. Appl. Genet. 131:903-915

Thomas, M.R. and Scott, N.S. (1993): Microsatellite repeats in grapevine reveal DNA polymorphisms when analysed as sequence-tagged sites (STSs). Theor. Appl. Genet. 86:985-990

Uga, Y.; Sugimoto, K.; Ogawa, S.; Rane, J.; Ishitani, M.; Hara, N.; Kitomi, Y.; Inukai, Y.; Ono, K.; Kanno, N.; (2013): Control of root system architecture by DEEPER ROOTING 1 increases rice yield under drought conditions. Nat. Genet. 45:1097–1102

van Leeuwen, C.; Destrac-Irvine, A.; Dubernet, M.; Duchêne, E.; Gowdy, M.; Marguerit, E.; Pieri, P.; Parker, A.; de Rességuier, L.; Ollat, N. (2019): An update on the impact of climate change in viticulture and potential adaptations. Agronomy 9, 514.

Van Ooijen (2004): MapQTL5: Software for the mapping of quantitative trait loci in experimental populations. (Kyazma BV, Wageningen.

Viala, P. and Ravaz, L. (1901): American vines: their adaptation, culture, grafting, and propagation. Robert S. Brain, Melbourne.

Werner, T.; Motyka, V.; Laucou, V.; Smets, R.; Van Onckelen, H.; Schmulling, T. (2003): Cytokinin-deficient transgenic Arabidopsis plants show multiple developmental alterations indicating opposite functions of cytokinins in the regulation of shoot and root meristem activity. *Plant Cell*, *15*:2532–2550

Whiting, J.R. (2005): Grapevine rootstocks. In *Viticulture*, Vol.1: *Resources* (eds. P.R. Dry and B.G. Coombe), Winetitles Pty Ltd, Ashford, Australie, pp. 167-188.

Xu, Y.; Gao, Z.; Tao, J.; Jiang, W.; Zhang, S.; Wang, Q.; Qu, S. (2016): Genome-wide detection of SNP and SV variations to reveal early ripening-related genes in grape. PLoS ONE 11:e0147749

Yang, S.; Fresnedo-Ramírez, J.; Wang, M. et al. (2016): A next-generation marker genotyping platform (AmpSeq) in heterozygous crops: a case study for marker-assisted selection in grapevine. Hortic. Res. 3, 16002

Zapata, C.; Magné, C.; Deléens, E.; Brun, O.; Audran, J.C.; Chaillou, S. (2001): Grapevine culture in trenches. 1. Root growth and dry matter partitioning, Australien Journal of Grape and Wine Research. Vol. 7, 127-131

Zhang, J.; Hausmann, L.; Eibach, R.; Welter, L.J.; Töpfer, R.; Zyprian, E.M. (2009): A framework map from grapevine V3125 (*Vitis vinifera* 'Schiava grossa' × 'Riesling') × rootstock cultivar 'Börner' (*Vitis riparia* × *Vitis cinerea*) to localize genetic determinants of phylloxera root resistance. Theor. Appl. Genet., 119:1039-1051.

Zyprian, E.; Welter, L.J.; Akkurt, M.; Ebert, S.; Salakhutdinov, I.; Gokturk-Baydar, N.; Eibach, R.; Töpfer, R. (2006): Genetic Analysis of Fungal Disease Resistance in Grapevine. Acta Horticulturae 827, 535-538

Zyprian, E.; Ochssner, I.; Schwander, F.; Šimon, S.; Hausmann, L.; Bonow-Rex, M.; Moreno-Sanz, P.; Grando, M.S.; Wiedemann-Merdingoglu, S.; Merdinoglu, D.; Eibach, R.; Töpfer, R. (2016): Quantitative trait loci affecting pathogen resistance and ripening of grapevines. Molecular Genetics and Genomics. 291, 1573-1594

2. Chapter 2: Grapevine Root Development in Perlite Substrate

2.1. Introduction

2.1.1. Propagation and Adventitious root formation of Grapevines

Today's premium wines are derived almost exclusively from the classic cultivars of V. *vinifera* (This et al. 2006). Like several domesticated hardwood and semi-hardwood species, grapevines are propagated vegetatively by woody cuttings. Characteristics that enable the propagation of grapevine cuttings are influenced by genotype, environmental conditions, and management of the mother vine in the previous season, where the canes are grown and cut during winter pruning (Winkler et al. 1974, Hartmann et al. 2001). Besides health status and grafting ability, the ability to form adventitious roots is a key component for successful propagation of grapevines, especially regarding the propagation of rootstock varieties (Smart et al. 2003).

The development of adventitious roots of woody cuttings is initiated at pericycle-like tissue adjacent to the vascular bundles of the stem (Li et al. 2009). In case of wounding, adventitious roots can also develop from calli that differentiate after wounding (Xu, 2018). The complex process and regulation of adventitious root formation from woody stem cuttings includes several endogenous and exogenous factors e.g., plant hormones and growth regulators, the extent and duration of dormancy, carbohydrate storage, genetic background, and preconditioning treatments (Smart et al. 2003).

The influence of the genetic background of poor rooting ability has been described in rootstock cultivars 'Ramsay' and '140 Ruggeri' and is also known for cuttings of *V. berlandieri* (Smith et al. 201, Kracke et al. 1981, Rives, 1971). Although, those phenotypic observations of rooting behaviour are known, the genetic origin and genomic regions of adventitious root formation ability in grapevine remain not fully elucidated.

2.1.2. Classification of Grapevine Adventitious Root Formation

Vitis varieties and species were described among their morphological characteristics by various ampelographists for years. The standard work of many grapevine descriptive characteristics was given by the Office International de la Vigne et du Vin (OIV). The second edition of the 'OIV descriptor list for grape varieties and *Vitis* species' comprises 151 characteristics ranked concerning their certain expression levels from low to high (https://www.oiv.int/public/medias/2274/code-2e-edition-finale.pdf). Besides distinguishing grape varieties with help of these standardized descriptors, OIV descriptors are a widely used instrument for classification of grapevine phenotypic characteristics to identify their genomic origin.

OIV descriptor 553 scores the ability to form adventitious roots from grapevine dormant woody cuttings after 14 days at 30°C under wine nursery conditions. The classification levels range from “very low” (1) to “very high” (9). In addition, certain varieties are given as reference for classification levels; namely *V. berlandieri* (1, “very low”), ‘Millardet et. Grasset’ (3, “low”), ‘Kober 5BB’ (5, “medium”), and ‘Gloire de Montpellier’ (9, “very high”).

2.2. Aim of the Study

Aim of this study was to score the ability to form adventitious roots of grapevine woody cuttings of a biparental mapping population in three experimental years based on OIV descriptor 553. Images taken of the adventitious roots provided additional data such as the number of adventitious roots and the cumulative length of adventitious roots. Finally, the gathered root phenotypic data was utilized for subsequent QTL mapping to provide new insights into the identification of potential genomic regions relevant for adventitious root formation in grapevine woody cuttings.

2.3. Material and Methods

2.3.1. Plant material

136 genotypes of the F1 progeny descending from a cross between ‘V3125’ (Schiava Grossa’ × ‘Riesling’) and rootstock cultivar ‘Börner’ (*V. riparia* Gm183 × *V. cinerea* Arnold) (‘VB2001’) were analysed regarding their adventitious root formation ability. In addition to the population genotypes, the parental genotypes ‘V3125’ and ‘Börner’ as well as the OIV reference varieties ‘*V. berlandieri*’, ‘Kober 5BB’, and ‘Gloire de Montpellier’ were scored regarding their adventitious root formation in this study. Therefore, dormant, two-bud woody cuttings were collected during winter pruning and subsequently sterilized with a 0.5% solution of Chinosol (Riede de Haen AG, Seelze, Germany). Afterwards cuttings were stored at 5°C until they were utilized for experiments.

2.3.2. Experimental Setup

The experiment was conducted at Geisenheim University (Department of grapevine breeding) in three consecutive years: 2017, 2018, and 2019. Ten replicates of each genotype were classified in each experimental year. Therefore, dormant woody cuttings were planted in plastic trays (PP/PE, 600 x 400 x 125 mm) filled with ca. 30 l watered perlite (Perligran Classic, Knauf Performance Materials GmbH) per tray and placed in the green house with constant air humidity of 70 %. Figure 4 shows the setup of perlite-filled boxes in the green house. After four weeks, vines were carefully taken out from the trays and remaining perlite particles attached to the roots were removed by washing with tap water. In all three experimental years, adventitious root formation was assessed according to a classification scheme slightly modified from OIV descriptor 553, scoring the adventitious root formation ranging from 1 “very

low" to 5 "very high". Cuttings without any roots, but with leaves were ranked as 0 "no roots"; cuttings without any roots or leaves were not considered. Additionally, in experimental years 2018 and 2019, images of all woody cuttings were taken with a SLR camera (Canon EOS 70D) to enable further investigation of adventitious root formation after completion of the experiment.

*Figure 4: Experimental setup: **A**: Perlite filled tray with planted woody cuttings, 10 replicates per genotype; **B**: Perlite boxes placed within the green house of Geisenheim University.*

2.3.3. Image Analysis

Images taken in 2018 and 2019 were analysed with ImageJ software (ImageJ 1.5r, Wayne Rasband, National Institutes of Health, USA) by use of '*Freehand Line'* tool getting the following sub-traits: number of adventitious roots (ARN) and cumulated length of adventitious roots (ARL). In addition, the same tool was used to measure the diameter of each woody cutting in the middle of the internode (see figure 5).

*Figure 5: **A**: Original image, **B**: Image analysis with ImageJ: digital tracing of adventitious roots (indicated in yellow) and counting of adventitious roots, **C**: Sample with arrow indicating the position of woody cutting diameter measurement.*

2.3.4. Statistical Analysis

Differences in adventitious root formation between the population parents ‘V3125’ and ‘Börner’ were analysed by applying non-parametric Kruskal-Wallis test for classification scheme data and ANOVA for adventitious root number, adventitious root length and woody cutting diameter. Statistics were performed in RStudio (Version 3.5.1; R Core Team, 2020) by use of the package ‘stats’. Residuals were checked visually as QQ-plot and variance homogeneity was verified with Levene’s test using ‘car’ package (Fox and Weisberg, 2019).

Phenotypic data of the mapping population genotypes was analysed by statistical modelling. A cumulative link mixed model was fitted with ordinal data gathered by classification scheme by using the ‘ordinal’ package (Christensen, 2018). Generalized linear mixed effect models were fitted for traits adventitious root number and adventitious root length with ‘glmmTMB’ package (Brooks et al. 2017). In all models, the genotype was included as random effect, while woody cutting diameter and experimental year were included as fixed effects. There was no effect of woody cutting diameter on classification scheme data and therefore, the cumulative link mixed model was fitted without this factor. Model assumptions for cumulative link mixed model were checked with nominal and scale test of the corresponding cumulative link model. Model diagnostics for generalized linear mixed effect models were performed by plotting Pearson residuals versus fitted values to inspect variance homogeneity (see supplementary figure S1).

2.3.5. QTL Mapping

Package ‘lme4’ (Bates et al. 2015) was utilized to extract best linear unbiased prediction estimates (BLUP) for each genotype of all replicates over three experimental years. QTL mapping was carried out with BLUP values and the consensus map of ‘VB2001’ by Fechter et al. (2014) based on 195 F1 individuals. The genetic map is illustrated in figure S12. QTL detection was performed with MapQTL 6 (MapQTL 6.0; Van Ooijen 2009) using interval mapping. The significant LOD threshold was calculated with $\alpha = 0.05$ (5 %) for each linkage group through 1000 permutations. Additionally, Kruskal-Wallis test was performed to further verify significance of genomic regions detected by interval mapping.

2.4. Results

2.4.1. Experimental Setup

Adventitious root formation of woody cuttings of the reference varieties is shown in figure 6. The classification of adventitious root formation corresponds to the ranking given by OIV descriptor 553 assessing ‘V. *berlandieri*’ with the lowest (≙ 1), ‘Gloire de Montpellier’ with the highest (≙ 5), and ‘Kober 5BB’ with a medium rating (≙ 3).

Figure 6: Adventitious root formation of woody cuttings of the OIV reference cultivars V. berlandieri, 'Kober 5BB' and 'Gloire de Montpellier'.

2.4.2. Population Parents

Table 1 shows the results of the populations parental genotypes 'V3125 and 'Börner'. Comparing 'V3125' (n = 19) and 'Börner' (n = 20) revealed no significant differences between both genotypes in the considered traits: classification of adventitious root formation, adventitious root number, adventitious root length, and woody cutting diameter. Kruskal-Wallis test was used for ordinal classification scheme data (Class: $H(1) = 0.22$; $p = 0.64$). ANOVA was performed for adventitious root number (ARN: $F(1,16) = 0$; $p = 0.99$), adventitious root length (ARL: $F(1,13) = 1.48$; $p = 0.25$), and woody cutting diameter (WCD: $F(1,17) = 1.65$; $p = 0.22$).

Table 1: Mean value / median, range and standard deviation of phenotypic variation of classification scheme data (Class), adventitious root number (ARN), adventitious root length (ARL, [cm]), and woody cutting diameter (WCD, [mm]) of the populations parental genotypes 'V3125' (n=19) and 'Börner' (n=20).

Trait	Median		Minimum		Maximum			
	'Börner'	'V3125'	'Börner'	'V3125'	'Börner'	'V3125'		
Class	4	3	1	0	5	5		
Trait	**Mean**		**Minimum**		**Maximum**		**SD**	
	'Börner'	'V3125'	'Börner'	'V3125'	'Börner'	'V3125'	'Börner'	'V3125'
ARN	5.4	5.4	0	0	12	12	3.6	4.4
ARL	36.0	23.0	5.00	1.3	73.7	40.1	21.1	15.0
WCD	7.6	8.5	5.8	5.5	9.5	10.1	1.3	1.3

2.4.3. Phenotypic Data of Mapping Population 'VB2001'

Considering the phenotypic data collected via the classification scheme, woody cutting diameter had no significant effect on the ability for adventitious root formation ($p = 0.147$). In contrast, the effect of the experimental year was significant ($p = 2.39e^{-15}$) and is shown in figure 7.

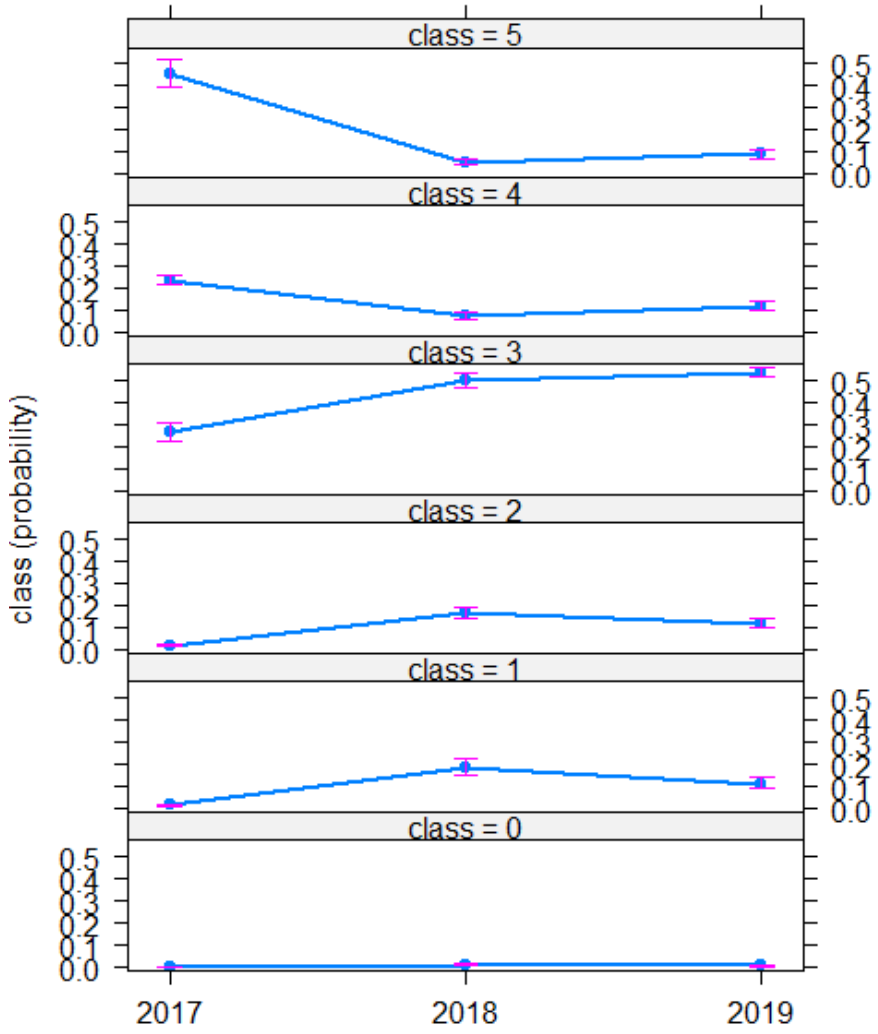

Figure 7: Effect plot presenting the effects of the experimental year on the ability to form adventitious roots, assessed by the following classification scheme:

class 5 = very high;
class 4= high;
class 3 = medium;
class 2 = low;
class 1 = very low;
class 0 = no roots.

The experimental year had the lowest effect on class 0 (“woody cutting without roots”). Results of 2018 and 2019 were similar throughout all classes. However, the probability of classes 1, 2, and 3 was lower in 2017 compared to the years 2018 and 2019. Contrary, the probability of class 4 and 5 rankings was higher in 2017 compared to the years 2018 and 2019.

Besides the classification scheme data, adventitious root number and adventitious root length were determined from images in experimental years 2018 and 2019 only. Woody cutting diameter had a significant positive effect on both traits and is visualized in figure 8.

Effect of the experimental year on adventitious root number and adventitious root length are shown in figure 9. Adventitious root number as well as adventitious root length tended to be higher in 2019 compared to 2018. The adventitious root number was significantly higher in 2019 compared to 2018, whereas the adventitious root length did not differ significantly between both years.

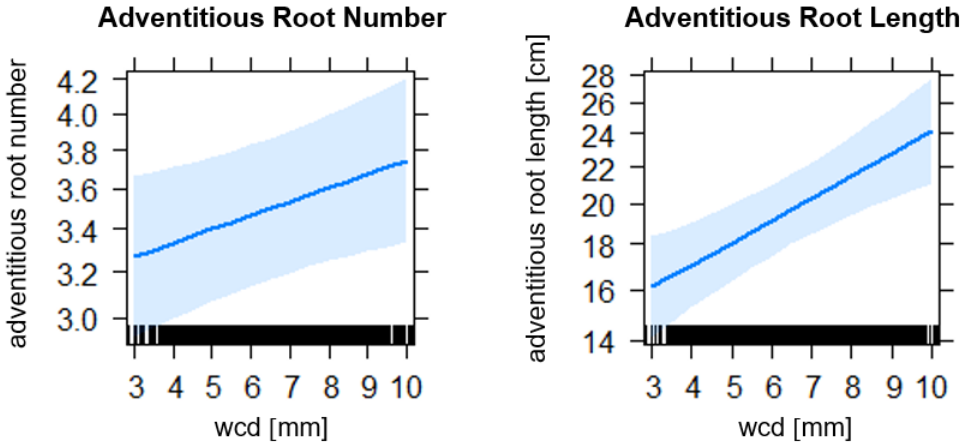

Figure 8: Effect of woody cutting diameter (wcd) on adventitious root number and adventitious root length in mapping population ‘VB2001’ (data of 2018 and 2019).

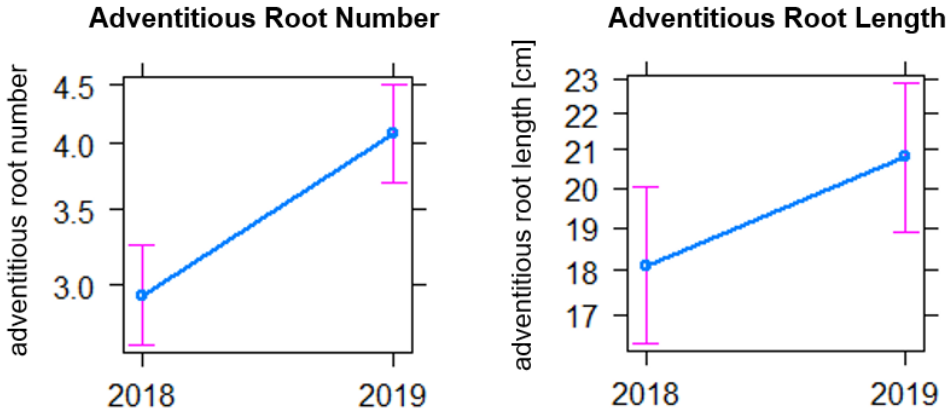

Figure 9: Effect of the experimental year on adventitious root number and adventitious root length in mapping population ‘VB2001’.

Both, woody cutting diameter and experimental year, were included into statistical modelling as fixed effects. Genotype was included as random effect. By extracting the best linear unbiased prediction values (BLUP values), the best predictive value for each genotype was generated while the variance resulting from woody cutting diameter and experimental year was reduced. Histograms in figure 10 show the distribution of adventitious root formation observed by the classification scheme as well as the distribution for adventitious root number and adventitious root length of mapping population 'VB2001'. The parental genotypes 'V3125' and 'Börner' are indicated by arrows and exhibit similar rankings within the upper half of the F1 population genotypes. The rankings of all individual F1 genotypes of the mapping population are given in figure S2.

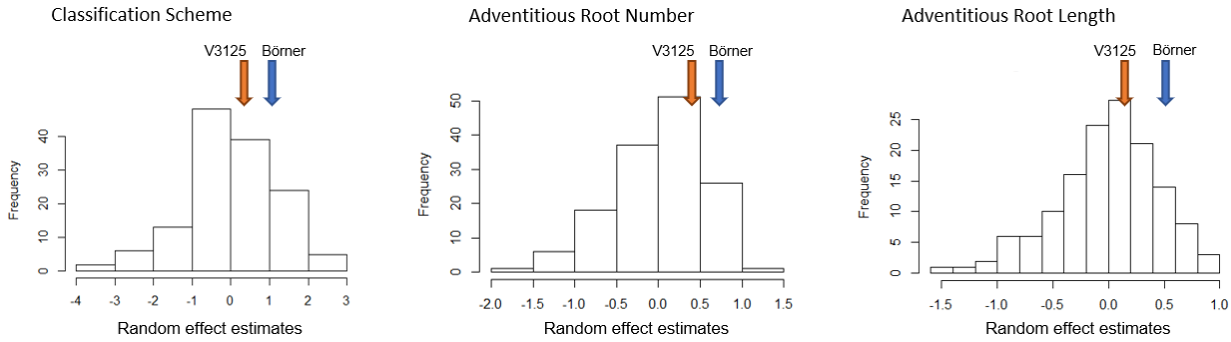

Figure 10: Frequency distribution of adventitious root formation classification, adventitious root number and adventitious root length in population 'VB2001'. Phenotypic data is given as best linear unbiased prediction estimates (BLUP) derived from the respective statistical model. Parental values are indicated by arrows. Frequency is the number of genotypes.

2.4.4. QTL Mapping

QTL mapping was performed with BLUP values extracted from the statistical models and revealed four QTLs linked to adventitious root formation. Results of QTL mapping are shown in table 2. The QTL position (cM) was derived from the corresponding LOD_{max} (logarithm of the odds) value and the confidence interval (cM) is given as the interval of LOD_{max} ± 1. The LOD threshold is presented on linkage group level as well as genome-wide produced by permutations tests. Linked genetic markers were identified by interval mapping and resulting genomic regions were confirmed by Kruskal-Wallis mapping. When a neighbouring marker was found through Kruskal-Wallis mapping, marker name and significance level are presented as asterisks. Otherwise, in case Kruskal-Wallis mapping did not confirm the linked marker previously found by interval mapping, positions are indicated as "-".

QTL mapping with classification scheme data revealed one QTL on linkage group 6 with a LOD_{max} value of 3.27. Neither interval mapping nor Kruskal-Wallis mapping confirmed a linked genetic marker. Even though, explained variance was 9.1%.

In addition, two QTLs were found for adventitious root number on linkage groups (LG) 2 and 17, from which Kruskal-Wallis test confirmed the genomic region on LG 2. Both QTLs were significant at the threshold of 2.9 and 2.7 on linkage group level, respectively; with LOD_{max} values of 2.95. They explained 9.6% (LG 2) and 9.7% (LG 17) of the phenotypic variance.

One QTL could be identified for adventitious root length on linkage group 9, not linked to a marker after interval mapping and Kruskal-Wallis mapping. The QTL showed a LOD_{max} value of 2.88 (significance threshold on linkage group level: 2.7) while explaining 9.4% of the phenotypic variance.

*Table 2: List of identified QTLs linked to the ability of adventitious root formation revealed by interval mapping (permutations = 1000) of mapping population 'VB2001' with classification scheme data, adventitious root number, and adventitious root length. Confidence intervals are confined by ±1 LOD, given by position (in cM), or by the end of the chromosome (x) if ±1 LOD exceeded the chromosome. Kruskal-Wallis significance levels are given as asterisks *** < 0.01; **** < 0.005; ***** < 0.001.*

Trait	LG	QTL position (cM)	Confidence Interval ± 1 LOD in cM	LOD max	LOD threshold (LG)	LOD threshold genome	linked marker Interval Mapping	Kruskal-Wallis	Explained variance (%)
Classification scheme	06	65.0	55.5 - x	3.27	2.7	4.5	-	-	9.1
Adventitious root number	02	70.1	63.7 - x	2.95	2.9	4.4	GF02-20_268	GF02-20_345 ****	9.6
	17	45.9	37.7 - x	2.95	2.7		UDV_018a	-	9.7
Adventitious root length	09	25.7	13.4 - 42.2	2.88	2.7	4.4	-	-	9.4

Chapter 2: Grapevine Root Development in Perlite SubstrateFigure 11 shows a schematic illustration of the physical positions (confidence interval LOD max. ± 1) of all four QTLs related to adventitious root formation which were found after evaluation of woody cuttings grown in perlite substrate. The determination of the physical positions was based on the grapevine reference genome sequence of 'Pinot Noir', PN40024 12X v.2 (GENOSCOPE, CRIBI Consortium VIGNA and IGA; Jaillon et al. 2007; Goremykin et al. 2008). QTLs were found on LG 2, LG 6, LG 9, and LG 17. Out of four QTLs identified via interval mapping, one QTL was confirmed by Kruskal-Wallis mapping: QTL for adventitious root number on chromosome 2.

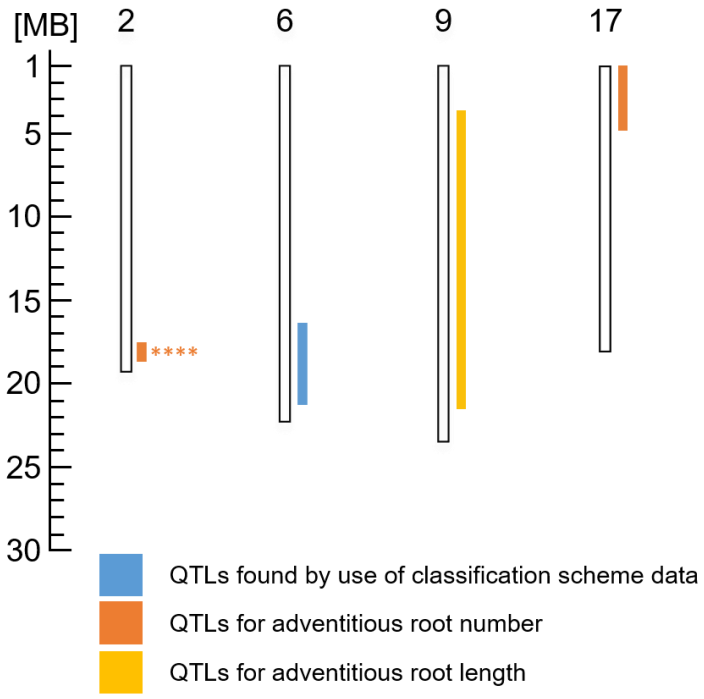

*Figure 11: Schematic figure of physical positions of QTLs identified via interval mapping by use of classification scheme data, adventitious root number and adventitious root length of mapping population 'VB2001' grown in perlite substrate. Levels of significant correlations of Kruskal-Wallis mapping are given as asterisks *** < 0.01; **** < 0.005; ***** < 0.001.*

2.5. Discussion

OIV descriptor 553 scores the ability to form adventitious roots from dormant woody cuttings after 14 days at 30°C under wine nursery conditions. The experimental setup of this study varied slightly from the OIV guidelines because plant samples were four weeks old when determined and temperature varied slightly depending on the outdoor temperature. Nevertheless, classification of the reference cultivars *V. berlandieri 10594* (*V. berlandieri*), 'Kober 5BB' (*V. berlandieri* × *V. riparia*) and 'Gloire de Montpellier' (*V. riparia*) was in general accordance with the reference classification given by OIV. It also corresponds to the general observation of different *Vitis* species exhibiting different ability to form adventitious roots. *V. vinifera* is known to show extremely prolific adventitious root formation (Smart et al. 2002),

whereas North American *V. berlandieri* is highly recalcitrant to root and was crossed with easily rooting species like *V. riparia*, *V. rupestris* or *V. vinifera* in the past (Olmo, 1976). Therefore, the experimental setup could be confirmed by the observations of the standard varieties as references.

The cumulative link model revealed a significant effect of the experimental year on root classification. In fact, classification of adventitious root formation in 2017 showed more individuals corresponding to classification levels 4 (high) and 5 (very high) and less individuals corresponding to classification levels 1 (very low), 2 (low) and 3 (medium) compared to years 2018 and 2019. This effect might be explained by the later experimental date in 2017. Even though the duration of all three experiment was 4 weeks, classification date in 2017 (19.06.17) was 8 weeks later than in 2018 (18.04.18) and 10 weeks later than 2019 (03.04.2019). Due to the later date, warmer temperatures and promoting light conditions could have positively affected the formation of adventitious roots on woody cuttings in 2017.

Besides the experimental year, diameter of the woody cuttings can possibly influence the initiation of adventitious roots. Even though, the woody cutting diameter had no effect on classification scheme data, the number and length of adventitious roots was positively affected by a bigger woody cutting diameter. The diameter of woody cuttings from canes is influenced by seasonal conditions and management of their mother vine (Hartmann et al. 2001). For instance, vines grown under drought stress and under-fertilisation show thinner canes and lower rooting performance (Smart et al. 2002). In addition, it has been shown that cuttings from the thinner distal end of the cane exhibited poorer rooting performance than cuttings from the thicker basal end (Nicholas et al. 1992). Therefore, both, experimental year and woody cutting diameter were included as fixed factors into statistical modelling to give an improved assessment of the population genotypes. In addition, using best linear unbiased prediction values shrunk the variance resulting from testing in different replicates and environments and subsequently generated the best predictive value for each genotype (Razar and Missaoui, 2020).

Utilization of a classification scheme offers fast assessment of a certain trait and has been conducted for grapevine phenotyping and genotyping of several traits. Fungal disease resistances were classified by use of OIV descriptors against *Plasmopara viticola* and *Uncinula necator* at leaves (OIV descriptor 452 and 455) and at berries (OIV descriptor 453 and 456) (Fisher et al. 2004). With help of this phenotypic data, QTL mapping revealed two major QTLs for resistance to *Uncinula necator* on chromosome 16 and *Plasmopara viticola* on chromosome 9. Besides disease resistances, agronomic traits like berry size, axillary shooting, and onset of ripening (“veraison”) were scored according to OIV scales in the past, identifying QTLs on chromosome 1 (“veraison”), 3 (berry size, axillary shoot formation), 6 (“veraison”), 10

(berry size), and 11 (“veraison”). However, phenotyping by using classification schemes is highly subjective and in addition, it does not provide any quantitative information about sub-traits e.g. no distinguishing between root number and root length. A plant sample with only few but long roots will possibly be ranked into the same classification group as a sample with many but only short roots, even though the mechanisms of initiation of adventitious roots at the stem and elongation of certain roots at the root tip may underlie quite different molecular processes and regulations.

Therefore, the number of adventitious roots and adventitious root length were additionally evaluated by image analysis in the last two experimental years. In fact, using phenotypic data resulting from the use of the classification scheme, revealed only one single QTL region on linkage group 6, whereas two additional QTLs were found for the number of adventitious roots (LG 2, LG 17) and one additional QTL for adventitious root length (LG 9). Each QTL explained almost 10 % of the phenotypic variation, with LOD_{max} values between 2.88 (ARL) and 3.27 (classification scheme). Similar ranges and LOD scores corresponding to adventitious root number were found in poplar: Ribeiro et al. (2016) combined QTL analysis of a segregating population with genome and transcriptome data to identify putative regulators of the adventitious root development and identified two QTLs for adventitious root number with LOD scores reaching 5.60 and 4.99 and explained phenotypic variance of 7 - 10 %. In accordance, Sun et al. (2019) found in total 150 QTLs for eight adventitious root traits explaining 3.1 - 6.1% phenotypic variance and LOD scores from 3.0 to 5.95 in poplar cuttings. It was enunciated that adventitious root formation is driven by differentially expressed genes in the IAA biosynthesis pathway (Ribeiro et al. 2016). Although, the mechanisms behind adventitious root formation are not fully investigated yet, comparing genotypes differing in their ability to form adventitious roots and the identification of QTLs associated with the development of adventitious roots and underlying genes are promising methods to understand regulatory mechanisms.

Interestingly, the *V. riparia* derived rootstock Gloire de Montpellier is known as a drought-sensitive rootstock (Fort and Fraga, 2017) and *V. riparia*- based rootstocks are stated as in general not recommended in drought-prone regions (Dry and Coombe, 2005). Therefore, a rapid adventitious root formation from woody cuttings is not automatically accompanied by deep rooting and dehydration tolerance in viticultural practice. These observations point out the need to elucidate the exact circumstances as well as genetic and molecular processes involved in adventitious rooting of grapevine woody cuttings. In addition, environmental factors affecting root system development in the field and at later time points need to be taken into consideration.

2.6. References

Dry, P. and Coombe, B. (2005): Viticulture. Vol 1-Resources, Wintitles, Adelaide, Australia.

Fechter, I.; Hausmann, L.; Zyprian, E.; Daum, M.; Holtgräve, D.; Weisshaar, B.; Töpfer, R. (2014): QTL analysis of flowering time and ripening traits suggests an impact of a genomic region on linkage group 1 in Vitis. Theor. Appl. Genet. 127, 1857-1872

Fisher, B.M.; Salakhutdinov, I.; Akkurt, M.; Eibach, R.; Edwards, K.J.; Töpfer, R.; Zyprian, E.M. (2004): Quantitative trait locus analysis of fungal disease resistance factors on a molecular map of grapevine. Theor. Appl. Genet. 108:201-515

Fort, B. and Fraga, B. (2017): Early Measures of Drought Tolerance in four Grapevine Rootstocks. J. Amer. Soc. Hort. Sci. 142(2):36-46

Goremykin, V.V.; Salamini, F.; Velasco, R.; Viola, R. (2008): Mitochondrial DNA of Vitis vinifera and the issue of rampant horizontal gene transfer. Molecular Biology and Evolution, 26(1):99-110

Hartmann, H.T.; Kester, D.E.; Davies, F.E.; Geneve, R. (2001): Hartmann and Kester's plant propagation: principles and practices. 8th edition. Englewood Cliffs, New Jersey, Prentice-Hall. 928 p.

Jaillon, O.; Aury, J.M. et al. (2007): The grapevine genome sequence suggests ancestral hexaploidization in major angiosperm phyla. Nature, 449(7161):463-467

Kracke, H.; Cristoferi, G.; Marangoni, B. (1981): Hormonal changes during the rooting of grapevine rootstocks. American Journal of Enology and Viticulture 32:135–137.

Li, S.W.; Xue, L.; Xu, S.; Feng, H.; An, L. (2009): Mediators, genes and signaling in adventitious rooting. Bot. Rev. 75:230–247.

Nicholas, P.R.; Chapman, A.P.; Cirami, R.M. (1992): Grapevine propagation, In: Coombe, B.G.; Dry, R.P. eds. Viticulture, Vol. 2, practices. Adelaide, Winetitles. p.1-22.

Olmo, H.P. (1976): Grapes. In: Simmonds NW, editor. Evolution of Crop Plants. London & NY: Longman, p 86-90

Razar, R.M.; Missaoui, A. (2020): QTL mapping of winter dormancy and associated traits in two switchgrass pseudo-F1 populations: lowland x lowland and lowland x upland. BMC Plant Biology, 20:537

Ribeiro, C.L.; Silva, C.M.; Drost, D.R.; Novaes, E.; Novaes, C.R.; Dervinis, C.; Kirst, M. (2016): Integration of genetic, genomic, and transcriptomic information identifies putative regulators of adventitious root formation in Populus. BMC Plant Biol. 16:66.

Rives, M. (1971): Statistical analysis of rootstock experiments as providing a definition ot the terms vigour and affinity in grapes. VITIS 9, 280-290

Smart, D.R.; Kocsis, L.; Walker, M.A.; Stockert, C. (2002): Dormant buds and adventitious root formation by *Vitis* and other woody plants. J. Plant Growth Regul. 21:296-314

Smart, D.R.; Kocsis, L.; Walker, M.A.; Stockert, C. (2003): Dormant Buds and Adventitious Root Formation by *Vitis* and Other Woody Plants. J. Plant Growth Regul. 21:296-314

Smith, B.P.; Wheal, M.S.; Jones, T.H.; Morales, N.B.; Clingeleffer, P.R. (2013): Heritability of adventitious rooting of grapevine dormant canes. Tree Genetics and Genomes, 9:467-474

Sun, P.; Jia, H.; Zhang, Y.; Li, J.; Lu, M.; Hu, J. (2019): Deciphering Genetic Architecture of Adventitious Root and Related Shoot Traits in *Populus* Using QTL Mapping and RNA-Seq Data. Int. J. Mol. Sci. 20, 6114

This, P.; Lacombe, T.; Thomas, M.R. (2006): Historical origins and genetic diversity of wine grape. Trends in Genetics 22: 511–519.

Winkler, A.J.; Cook, J.A.; Kliewer, W.M.; Lider, L.A. (1974): General viticulture, Berkeley, California, University of California Press.

Xu, L. (2018): De novo root regeneration from leaf explants: Wounding, auxin, and cell fate transition. Curr. Opin. Plant Biol. 41:39–45.

Software

ImageJ:

ImageJ 1.5r, Wayne Rasband, National Institutes of Health, USA. http://imagej.nih.gov/ij

MapQTL6:

Van Ooijen, J.W. (2009): MapQTL 6, Software for the mapping of quantitative trait loci in experimental populations of diploid species. Kyazma BV; Wageningen, Netherlands

R Studio:

R Core Team (2020): R: A language and environment for statistical computing. R Foundation for Statistical Computing, Vienna, Austria. URL https://www.R-project.org/

- **Bates, D.; Mächler, M.; Bolker, B.; Walker, S. (2015):** Fitting Linear Mixed-Models using lme4. Journal of Statistical Software. 67(1), 1-48.
- **Brooks, M.E.; Kristensen, K.; van Benthem, K.J.; Magnusson, A.; Berg, C.W.; Nielsen, A.; Skaug, H.J.; Maechler, M.; Bolker, B.M. (2017):** glmmTMB Balances Speed and Flexibility Among Packages for Zero-inflated Generalized Linear Mixed Modeling. The R Journal. 9(2), 378-400.

- **Christensen, R.H.B. (2018):** Ordinal-Regression Models for Ordinal Data. R package version 2015. 6-28
- **Fox, J.; Weisberg, S. (2019):** An R Companion to Applied Regression, Third edition. Sage, Thousand Oaks CA.

Internet Sources:

Datenbank EnsemblPlants: http://plants.ensembl.org/index.html

3. Chapter 3: Grapevine Root Development in Rhizotrons

3.1. Introduction

Plant roots' major function is the access to water and nutrient uptake, but they also serve as anchorage in soil medium and storage organs, and they contribute to the formation of beneficial symbioses with microbes of the rhizosphere (Smith and De Smet, 2012; Khan et al. 2016). Therefore, roots play a crucial role for maintenance of plant health and constant yield (Adeleke et al. 2020). Consequences of climate change will show a multifaceted nature including the rise of atmospheric CO_2 concentrations, higher temperatures, and extreme weather events like extensive drought periods (Gray and Brady, 2016). A study of Ray et al. (2019) found that climate change already has impact on crop yield: The statistic modelling approach analysed global crop production data of ten crops accounting for approx. 83% kilocalorie production worldwide for the time period from 1974 - 2013. Regarding the European region, yields of major crops like wheat, barley, maize, and rapeseed were reduced by 6.3 to 21.2% in western and southern Europe. For Germany, they calculated a reduction of 11% of consumable food calories due to climate change.

To cope with future consequences of climate change, complex phenotypic plant traits need to be dissected and combined with high-throughput genotyping approaches (Delrot et al. 2020). The incorporation of image-based quantification methods potentially standardizes accuracy and therefore, enhances the performance of mapping genotype to phenotype (Houle et al. 2010). In grapevine, image-based phenotyping methods have been developed for different utilization, e.g., identification of virus diseases using hyperspectral imaging (Bendel et al. 2020) or description of bunch architecture with a 3D scanner (Rist et al. 2018). However, most of grapevine phenotyping methods are limited to aerial plant parts.

Contrary to aerial plant parts, plant roots are the hidden half of the plant making investigation of roots even more challenging and time costly. Nevertheless, for appropriate breeding approaches, screening of whole mapping populations, and therefore in a high throughput manner are required. Phenotyping plant roots will help to find heritable traits correlated with resource use efficiency, performance, and yield of plants (Nagel et al. 2012). For this purpose, so-called rhizotrons have been invented in the last years to non-destructively analyse root systems based on 2D images. The rhizotron boxes, filled with soil or growth medium are positioned at an angle of approximately 45° and allow inspection of root growth along the bottom side of the box through a transparent or removable lid. Rae et al. (2007) used rhizotrons to analyse root density responses to elevated CO_2 levels in poplar, finding a stronger magnitude of root density in response to increased CO_2 levels and identified three QTLs associated with root growth and root density. In hydroponic rhizotrons, total root length of maize was significantly increased with rising temperature from 13°C to 22°C and stagnated at

22 - 25°C. In addition, oilseed rape exhibited increased tap root length and number of lateral roots induced by a temperature rise from 10°C to 20°C (Nagel et al. 2009). Another rhizotron study of Zang et al. (2014) examined fine roots of beech tree saplings during drought treatments. A tendency towards an increased proportion of roots with diameter < 0.2 mm was detected, indicating a possible strategy of the plant to enhance root surface area per unit carbon investment in drought stress situations.

Rhizotrons have brought new insights into functional changes of root systems during the major forces driven by climate change: CO_2, temperature rise, and drought stress periods. Until now, grapevines have only rarely been studied in rhizotrons either to evaluate the extent of root ramification or the root diameter (de Herralde et al. 2010; Dumont et al. 2016). De Herralde et al. (2010) examined three different grapevine rootstocks in rhizotron containers (1.2 m deep, 0.6 m × 0.5 m surface) comparing root length at two different time points in September and November. In addition, they determined depth distribution, root type and phenological state and documented a certain amount of root growth after harvest and a clear ageing process shown by lignification (Fortea et al. 2009). In another study, grapevine root systems were analyzed in rhizotron containers of acrylic sheets (0.4 m high × 0.3 m wide) filled with perlite substrate. Two grafted rootstock cultivars were compared regarding their two-dimensional root morphology under PEG (polyethylene glycol)-induced osmotic stress. Even though grapevine roots could be observed in rhizotrons, the throughput in both experiments was only 16 plant samples in the study by Fortea et al. (2009). Regarding drought stress, Fort and Fraga (2017) conducted experiments with four grapevine rootstock cultivars in 32 rhizotrons and therefore, severely limited number of plant samples. For determination of mapping populations in breeding approaches, rhizotrons with high-throughput potential are required to provide appropriate information for QTL mapping. Similar to rhizotrons, Jeudy et al. (2016) successfully tested suitability of grapevine herbaceous cuttings for root phenotyping in RhizoTubes and analysed the level of mycorrhization. However, grapevine roots were hydroponically grown with nutrient solution, but root growth and architecture are not only modulated by the availability of nutrients. Physical constraints in soil and soil microorganisms impact root growth, too and these factors can be considered by using soil-filled rhizotrons.

3.2. Aim of the Study

The aim of this study was to design and develop a rhizotron system for phenotyping grapevine root systems grown from woody cuttings, appropriate for high-throughput phenotyping of grapevine mapping populations with approximately 150 individual genotypes and a sufficient number of replicates. Therefore, method development focussed on 1.) the optimization of experimental setup including cost-saving materials, and 2.) the development of a workflow for objective and automated image-based analysis of root systems. Subsequently, the study

aimed on utilizing the gathered phenotypic data for QTL mapping in order to identify genomic regions associated with root system related traits. Roots of two mapping populations were phenotyped in three experimental replications within two years to evaluate the rhizotron system and conduct QTL analysis.

3.3. Material and Methods

3.3.1. Rhizotron Setup and Experimental Design

Dormant, two-bud woody cuttings were collected during winter prune and subsequently sterilized with a 0.5% solution of Chinosol (Riede de Haen AG, Seelze, Germany). Afterwards cuttings were stored at 5°C until they were utilized for experiments but not longer than 8 weeks. Woody cuttings were pre-planted for rooting initiation in jiffy peat pellets (Jiffy-7 Peat Pellets, Jiffy Products International BV, Zwijndrecht, Netherlands) for three weeks before they were placed into rhizotrons. Black sealed trays of polypropylene (PP 1/2, 325 x 265 x 40 mm, packpack.de GmbH, Jever, Germany) were used as rhizotron boxes. The rhizotron setup is illustrated step by step in figure 12. Three openings at the upper site of each rhizotron provided the planting spot for a single woody cutting sample in the middle and irrigation wholes at both sites of it (see figure 12 A). In addition, smaller drainage holes at the bottom end ensured gravimetrically release of excess water after irrigation. Stripes of hygroscopic foam (big-®mosy, mosy GmbH, Thedinghausen, Germany) placed at the bottom end avoided water logging (see figure 12 B).

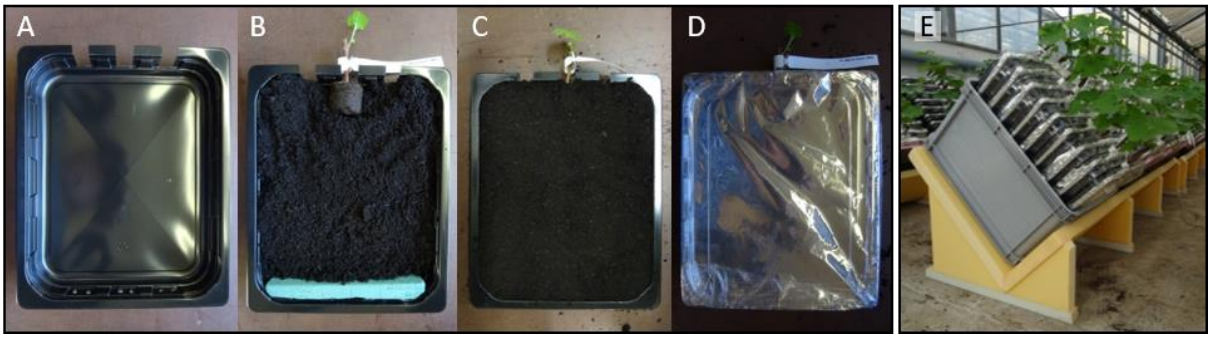

*Figure 12: **A**: Rhizotron trays with openings for plant sample and irrigation, **B**: floral foam stripe, **C**: filled with soil and **D:** closed with two layers of foil and their lid. **E**: Positioning of rhizotrons in 45° angle on benches in the green house.*

All rhizotrons were filled with approximately 4 l of sieved (mesh < 5 mm) black peat soil (gartenkraft, Raiffeisen Webshop GmbH & Co. KG, Münster, Germany; see table 3 for details of soil composition) and closed with one layer of plastic foil (Toppits bag 6 l, Cofresco Frischhalteprodukte GmbH & Co. KG), followed by a layer of aluminium foil (thickness: 0.03 mm, VWR, Darmstadt, Germany), and finally sealed with a polypropylene lid (packpack.de)

(see figure 12 C, D). Rhizotrons were set up in the green house with an inclination angle of 45° with their lid facing downwards (see figure 12 E).

Table 3: Composition of the black peat soil used for rhizotron experiments

Black peat soil by 'gartenkraft', Raiffeisen	
pH value ($CaCl_2$)	5,3
Salt content (KCL)	2,6 g/l
Nitrogen (N)	130 mg/l
Phosphate (P_2O_5)	100 mg/l
Potassium oxide (K_2O)	220 mg/l
Magnesium	90 mg/l
Sulphur	850 mg/l
Volume	50 l per bag

After 3 weeks, rhizotrons were opened and images of roots and shoots were taken in a photo box. This box provided consistent lightening conditions by installed lamps and closable doors, a device for attaching the cameras. In addition, the red coloured ground offered a good contrast to the green leaves and dark rhizoboxes ideal for following image analysis. Images of roots and shoots were taken simultaneously by use of two single-lens reflex cameras with remote control trigger (see figure 13). Every sample was unambiguously labelled with genotype number, plant organ (root or shoot) and replicate number by a data matrix barcode. With help of these barcodes, image files were automatically renamed according to their corresponding data matrix barcodes after implementation of the experiment by using 'bardecode' software (Softek Software, Sheffield, UK).

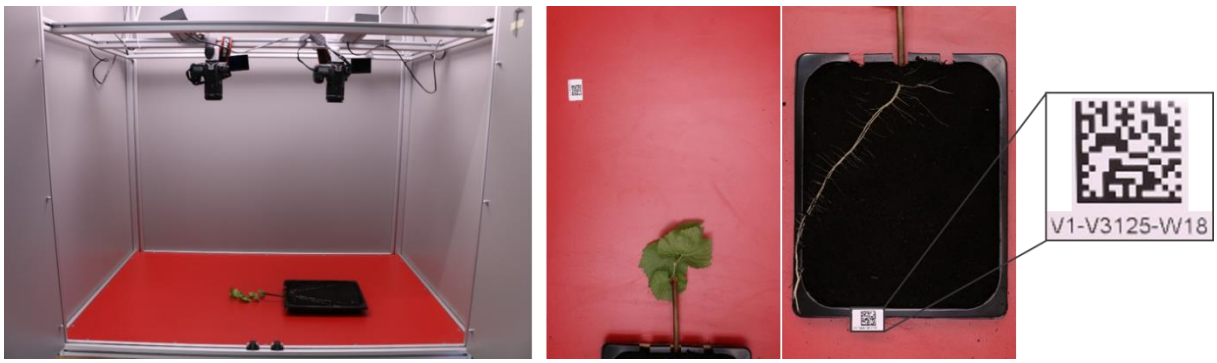

Figure 13: Photo box with installed lamps for consistent lightening conditions and two single-lens reflex cameras. Cameras are triggered simultaneously by remote control for taking images of roots and aerial shoot part of the plant sample at the same time.

3.3.2. Image Analysis

Root images were automatically analysed with WinRHIZO software (WinRHIZO™ Pro 2019a, Regent Instruments Inc., Québec, Canada) by colour analysis. Roots were detected by pixel colour and *'root morphology'* adjustment. By clicking onto a pixel of a root in the image, the colour of the pixel was defined as root colour. In the further image analysis process, pixels with similar colour (10% tolerance) were automatically detected as root. In this way, roots could be distinguished from the dark background of the image by pixel colour. Cumulated total root length was measured and root parts were classified into diameter classes. Roots with diameter > 0.5 mm were classified as adventitious roots, whereas roots with diameter < 0.5 mm were classified as lateral roots. With a set of 94 images, accuracy of this classification was checked by comparing WinRHIZO analysis with manual image analysis with help of ImageJ (ImageJ 1.51r, Wayne Rasband, National Institute of Health, USA) software. Utilization of ImageJ enables manual tracing of roots in digital images and subsequent measurement of the traced root line. Adventitious roots and lateral roots were measured separately in ImageJ.

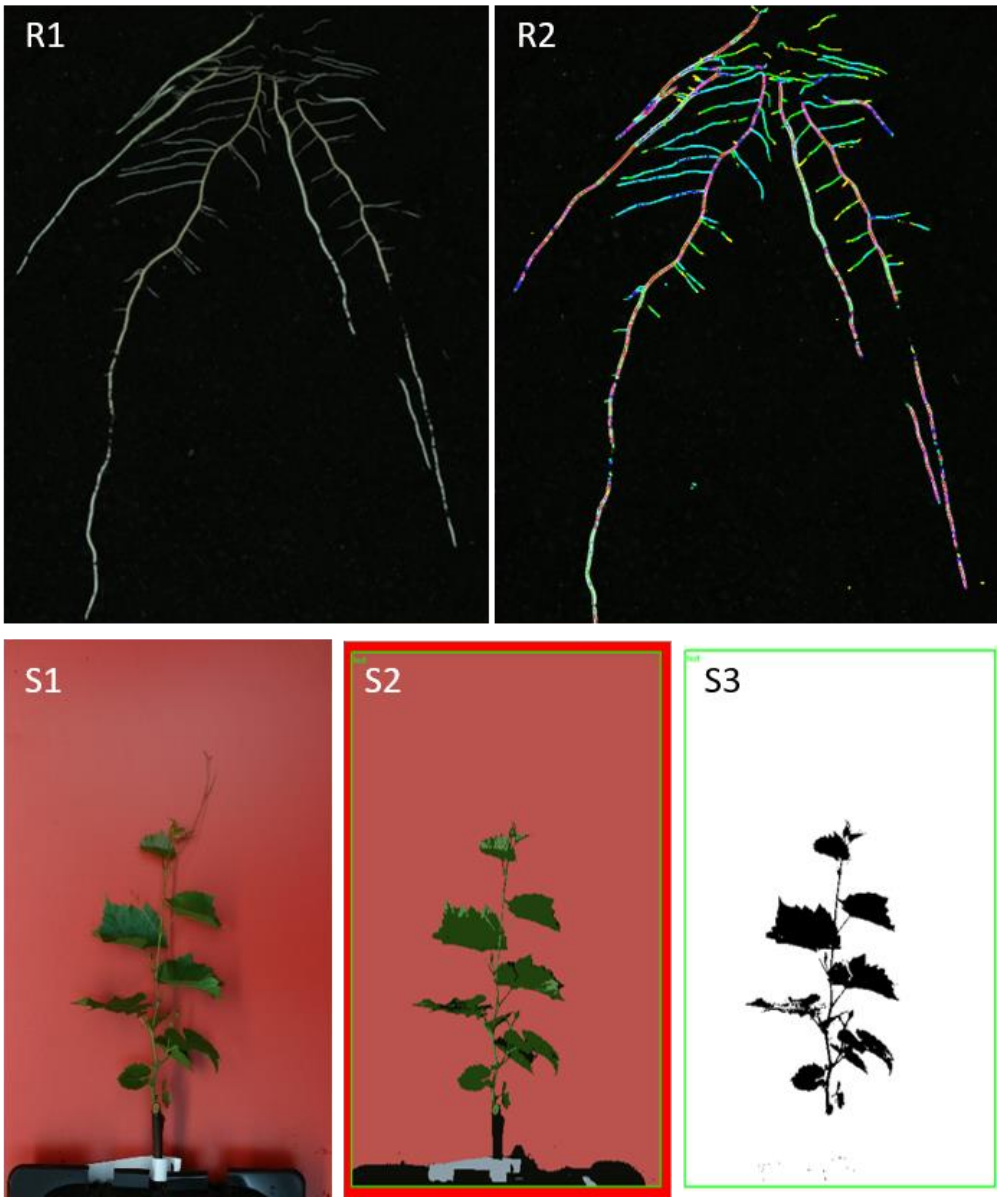

Figure 14: WinRHIZO image analysis of roots (R) and shoots (S). ***R1****: original RGB image.* ***R2****: Roots are segmented from the black background and marked in different colours depending on their diameter class.* ***S****: Win RHIZO image analysis of aerial plant parts.* ***S1****: original RGB image.* ***S2****: pixels are segmented by prior defined colour classes.* ***S3****: Area of green plant parts are segmented from the background and quantified as leaf area.*

Shoot images were also analysed with WinRHIZO software, but without '*root morphology'* adjustment. Area of green shoot parts was quantified based on pixel colour and previously defined colour classes. WinRHIZO settings including defined colour classes are given in table S1. In addition, leaves of a subset of samples were manually measured with a leaf area meter (LI-3100 Area Meter, LI-COR, inc. Lincoln, Nebraska, USA). The subset consists of 478 samples in total, made up of biological replicates of 45 different genotypes (F1 individuals of both populations and reference cultivars). The number of replicates per genotype differed due to different ability of leaf emergence because samples without leaves were not considered. The subset served as ground truth data in order to validate data of image analysis. Roots of

the same subset of samples (n = 342, not all woody cuttings with leaves had roots) were washed out from soil after image acquisition and both, leaves and roots were dried at 60°C to a constant mass to quantify their dry weight. Woody cutting diameter was measured by using *'straight line*' function in ImageJ. Table 4 presents a list of all traits obtained during the rhizotron experiment with their abbreviations and measurement description.

Table 4: List of traits obtained in rhizotron experiments with abbreviations and descriptions.

Trait	Abbreviation	Unit	Description
Total root length [1]	TRL	cm	Cumulated root length of all roots visible at rhizotron surface. Measured by WinRHIZO image analysis.
Adventitious root length [1]	ARL	cm	Cumulated root length of all adventitious roots visible at rhizotron surface. Measured by WinRHIZO image analysis.
Lateral root length [1]	LRL	cm	Cumulated root length of all lateral roots visible at rhizotron surface. Measured by WinRHIZO image analysis.
Leaf area (image analysis) [1]	LA_WR	cm²	Leaf area measured by WinRHIZO image analysis.
Leaf area (leaf area meter) [2]	LA_LAM	cm²	Leaves were cut off the shoot and quantified in a leaf area meter.
Root dry weight [2]	RDW	g	Roots were washed from soil, cut off the woody cutting and dried to detemine root dry weight.
Shoot dry weight [2]	SDW	g	Leaves and shoots were cut off the woody cutting and dried to detemine shoot dry weight.
Woody cutting diameter [1]	WCD	mm	Woody cutting diameter was measured in shoot images. A straight line was drawn at the center of the woody cutting avoiding the thicker bud regions at the ends

[1]Traits measured from images of all genotypes and replicates
[2]Traits measured manually of only selected number of reference genotypes

3.3.3. Plant Material

Root system of the following two mapping populations were tested and phenotyped within the developed rhizotron system:

- 'VB2001': 136 genotypes of the F1 progeny descending from a cross between 'V3125' ('Schiava Grossa' × 'Riesling') and rootstock cultivar 'Börner' (*V. riparia* Gm183 × *V. cinerea* Arnold)
- 'CMVB1989': 151 genotypes of the F1 progeny descending from a cross between 'Calardis Musqué' ('Bacchus Weiß' × 'Seyval') and 'Villard Blanc' ('Seibel 6468' × 'Subéreux')

Three independent experiments were conducted ('VB2001': 2018.1, 2018.2, 2019; and 'CMVB1989': 2018, 2019.1, 2019.2) with 5 replications per genotype in each experiment, making a total of 15 replicates per genotype.

3.3.4. Statistical Analysis

Validation of Automated Image Analysis

Statistical analyses were performed with R Studio (Version 3.5.1; R Core Team, 2020) and several packages. To determine the relationship between data acquired by automated image analysis and from manual analysis, results were compared by using Pearson correlation coefficients ($\alpha = 0.05$) with 'stats' package. For this purpose, root system images of a subset of 95 samples (biological replicates of 14 genotypes of reference cultivars) were analysed as well as 496 shoot images (biological replicates of 43 genotypes of F1 individuals of both mapping populations and reference cultivars).

In addition, linear models were fitted to compare measurements of roots (TRL, ARL, LRL) executed manually with ImageJ and measurements of roots gathered by automated image analysis by WinRHIZO. Similarly, leaf area measured by leaf area meter (LA_LAM) was compared to leaf area measured by WinRHIZO image analysis (LA_WR). Model diagnostics were performed by visual inspection of residuals versus fitted values and Breusch-Pagan test by using 'lmtest' package (Zeileis and Hothorn, 2002). In case of variance heteroscedasticity (TRL, LRL, LA_WR, and LA_LAM), model was transformed into a model with homoskedastic errors by applying weighted least squares. The same procedure was applied on relationships of both biomass traits: of root dry weight (RDW) and shoot dry weight (SDW).

Significant differences between groups were tested by either two sample ANOVA or Wilcoxon test (p value adjustment bonferroni) at significance level of 0.05 after applying Shapiro-Wilk test to check normal data distribution and Levene's test to varify homoscedasticity.

Analysis of Mapping Populations 'VB2001' and 'CMVB1989'

Phenotypic differences between the population parents 'V3125' and 'Börner' as well as 'Calardis Musqué' and 'Villard Blanc' were analysed by comparing total root length, adventitious root length, lateral root length, leaf area, woody cutting diameter, shoot and root dry weight by two sample ANOVA or Kruskal-Wallis test after verification of homoscedasticity by applying Levene's test. Statistics were performed in R Studio using the 'stats' package. Residuals were checked visually as QQ-plot and variance homogeneity was verified with Levene's test using the 'car' package (Fox and Weisberg, 2019).

Phenotypic measurements of both populations were visualized using 'ggplot2' package (Wickham, 2016). Generalized linear mixed effect models were fitted with 'glmmTMB' package (Brooks et al. 2017). Package 'effects' displayed fixed effects from the fitted models (Fox and Weisberg, 2019). Random effects were extracted and visualized with 'ggpubr' (Kassambara 2020). Generalized linear mixed effect models were fitted with the following phenotypic traits measured by automated image analysis as dependent variable: total root length, adventitious

root length, lateral root length and leaf area. The genotype was included as random effect, while woody cutting diameter and experimental replication were included as fixed effects. Model diagnostics were performed by plotting Pearson residuals versus fitted values to inspect variance homogeneity. Secondly, models were compared by assessing the Akaike Information Criterion (AIC), where lower values indicate the better fit. Model diagnostics are visualized in supplementary figure S4 and S5.

3.3.5. QTL Mapping and *in silico* Candidate Gene Analysis

Best linear unbiased prediction values (BLUP values) were extracted from the respective statistical model and utilized for QTL mapping with the consensus map of 'VB2001' (Fechter et al. 2014) and 'CMVB1989' (Schwander, unpublished), respectively. The utilized genetic maps are illustrated in figure S12 and figure S13. QTL detection was performed with MapQTL6 (MapQTL 6.0; Van Ooijen 2009) using interval mapping. The significant LOD threshold was calculated with α = 0,05 (5 %) for each linkage group through 1000 permutations.

For *in silico* candidate gene analysis, the Ensembl online platform (Yates et al. 2020) was utilized for searching putative candidate genes involved in processes of root growth and development within the identified QTL regions.

3.4. Results

3.4.1. Validation of Automated Image Analysis

Comparison of automated (WinRHIZO) and manual (ImageJ or leaf area meter) image analysis resulted in high correlations of r = 0.99 for total root length, r = 0.93 for adventitious root length, r = 0.96 for lateral root length, and r = 0.84 for leaf area (see table 5). However, these correlations do not describe shape and slope of the relationships and therefore, linear regression models were fitted and revealed R^2-values of 0.99 (TRL), 0.86 (ARL), 0.92 (LRL) and 0.74 (LA) (see figure 15). As given in table 6, comparing both methods showed no significant shift in mean values of the root-related traits total root length, adventitious root length and lateral root length. However, leaf area was significantly underestimated by image-based automated quantification. Data is shown in figure 14 and visualized as boxplots.

Table 5: Pearson correlation coefficients (α = 0.05) of traits measured manually and traits measured by automated image analysis. Total root length (n = 95), adventitious root length (n = 95), lateral root length (n = 75), and leaf area (n = 496).

Manual vs. Automated Image Analysis	r
Total Root Length	0.99
Adventitious Root Length	0.93
Lateral Root Length	0.97
Leaf Area	0.84

Table 6: Comparison of manual measurements and automated image analysis for root parameters and leaf area.

Trait	n	Shapiro-Wilk	Levene-Test	Wilcoxon-Test „bonferroni“	
		p-value	p-value	W	p-value
TRL	95	2.961*e-10	0.34	4711	0.60
ARL	95	9.603*e-07	0.44	4391	0.75
LRL	75	1.505*e-13	0.08	3177	0.17
LA	496	< 2*e-16	< 2.2*e-16	169904	< 2*e-16

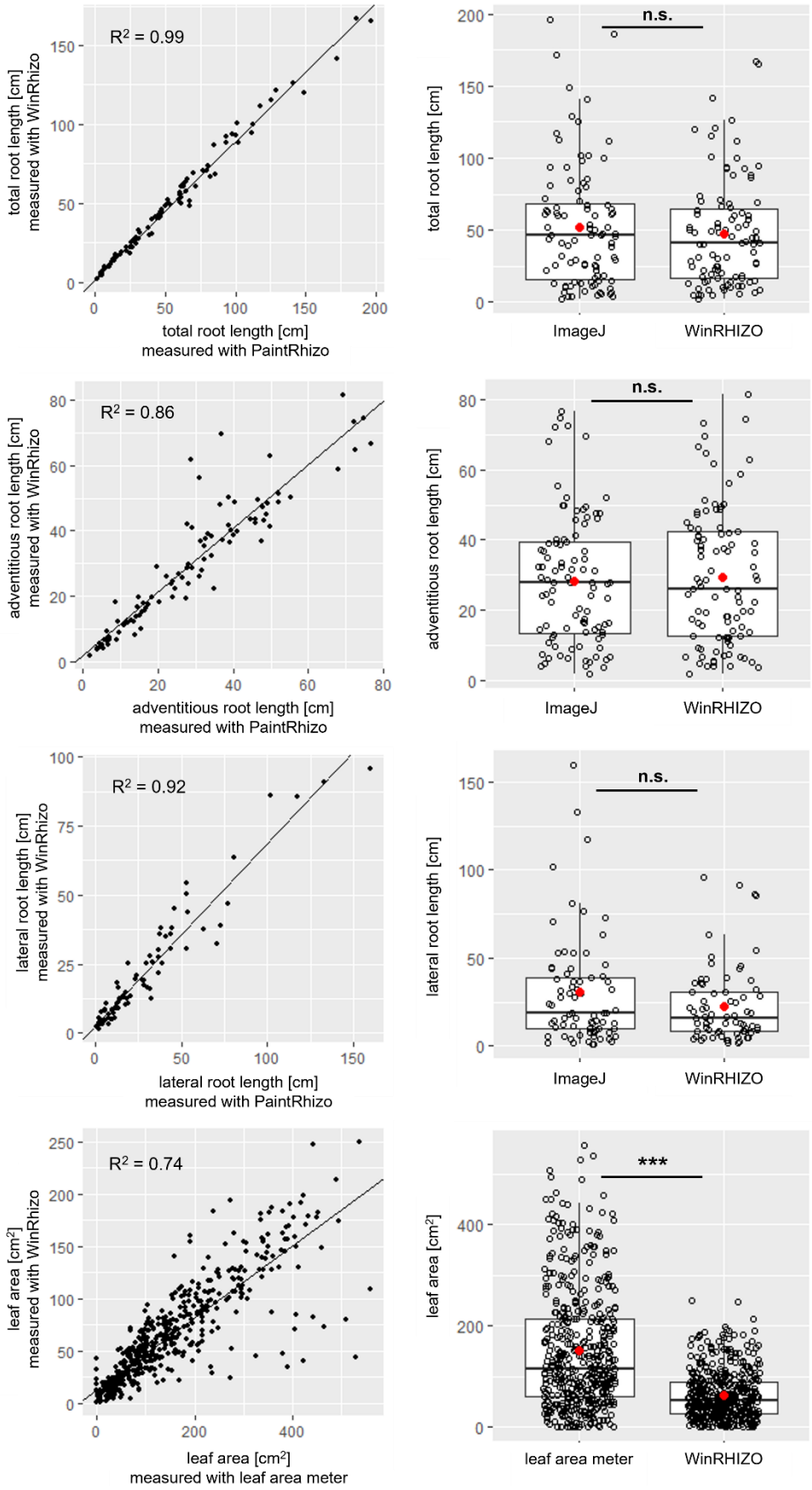

Figure 15: Comparison of measurements based on manual measurements and based on automated image analysis. Correlation was performed for total root length (n = 95), adventitious root length (n = 95), lateral root length (n = 75), and leaf area (n = 496).

3.4.2. Correlation Between Image Analysis and Plant Biomass

A moderate linear correlation was found between root dry weight and visible total root length and the fitted linear regression model explained 59% of the variance (see figure 16). Figure 17 shows relation of shoot dry weight and leaf area measured by WinRHIZO (R^2 = 0.36) and measured by leaf area meter (R^2 = 0.55) based on linear regression models.

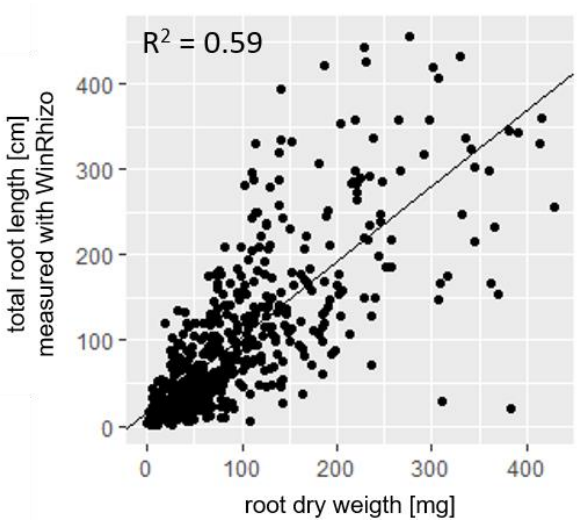

Figure 16: Correlation between root dry weight and total root length measured by automated image analysis with WinRHIZO (n = 342) based on the fitted linear regression model.

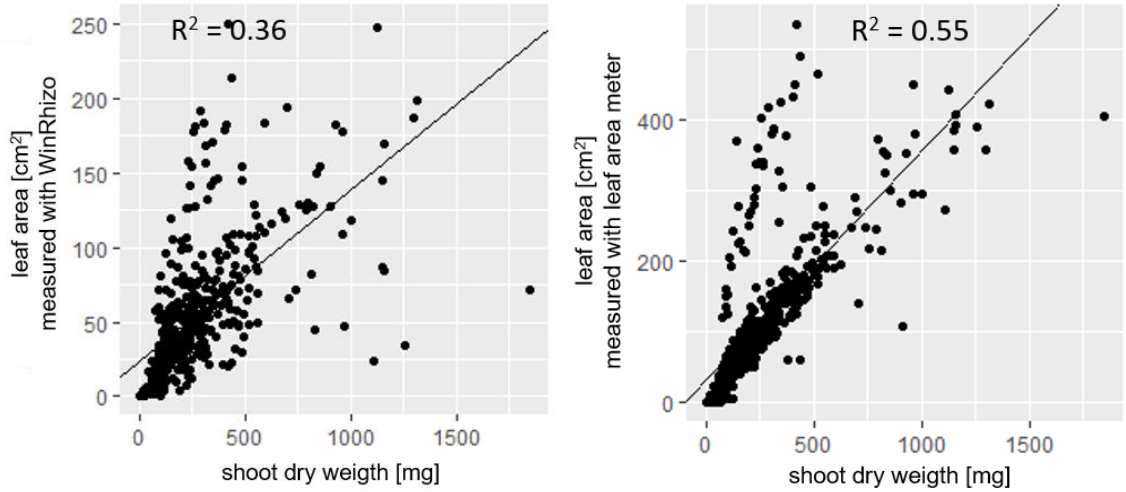

Figure 17: Correlation between shoot dry weight and leaf area measured by automated image analysis with WinRHIZO (n = 388) and leaf area measured manually with leaf area meter (n = 478) based on linear regression models.

3.4.3. Correlation Between Belowground and Aboveground Plant Parts

Root dry weight exhibited moderate linear correlations with shoot dry weight as well as leaf area measured manually with leaf area meter (both: $R^2 = 0.52$) (see figure 18). Using image analysis based phenotypic data, simple linear regression model of leaf area depending on total root length explained 47% of variance. Coefficient of determination of leaf area measured manually and total root length measured with automated image analysis was $R^2 = 0.69$ (see figure 19).

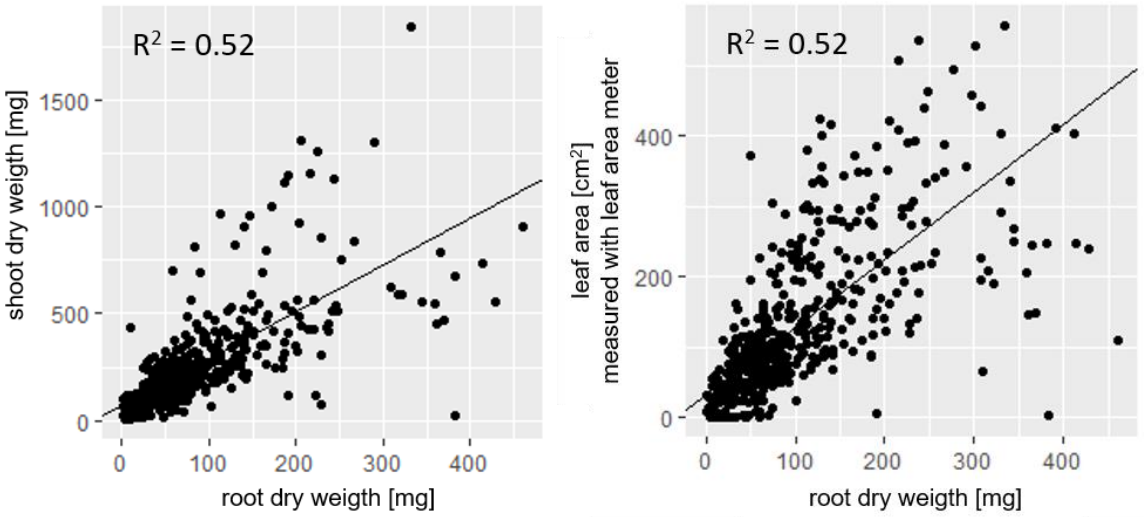

Figure 18: Correlation between root dry weight and shoot dry weight (n = 428) and between root dry weight and leaf area measured manually with leaf area meter (n = 485) based on linear regression models

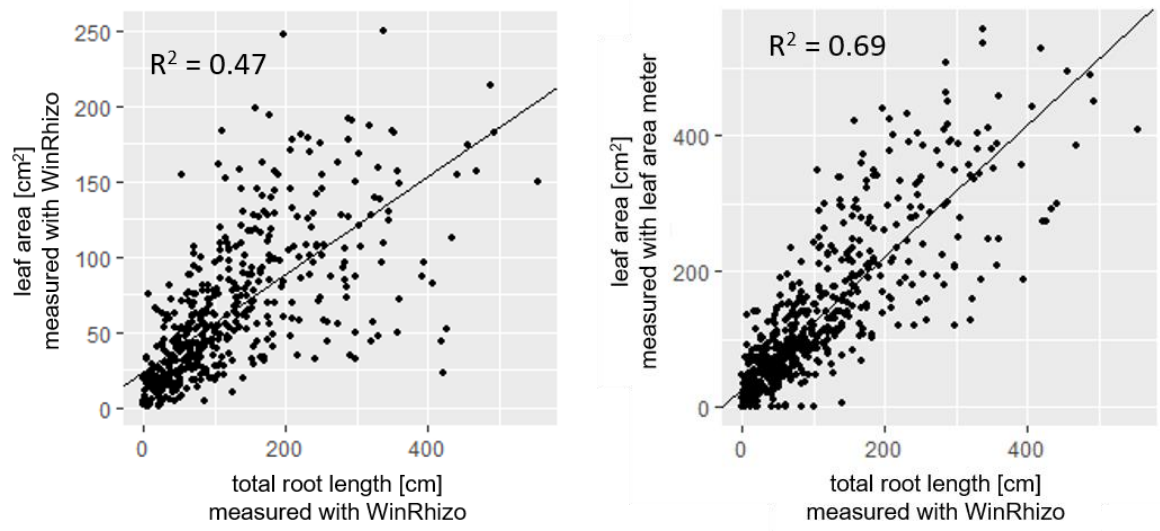

Figure 19: Correlation between total root length based on automated image analysis with leaf area measured by image analysis (n = 460) and with leaf area measured with leaf area meter (n = 552).

3.4.4. Analysis of Mapping Populations ‘VB2001’ and ‘CMVB1989’

Table 7 shows means, ranges and standard deviations of the population parental genotypes ‘V3125’ and ‘Börner’ as well as ‘Calardis Musqué’ and ‘Villard Blanc’. Comparing ‘V3125’ and ‘Börner’ revealed no significant differences between both genotypes in the considered traits except in the ratio between lateral and adventitious root length. ANOVA was conducted for comparing the total root length ($F(1, 15) = 0.11$; $p = 0.745$), adventitious root length ($F(1, 15) = 0.207$; $p = 0.656$), lateral root length ($F(1, 15) = 0.126$; $p = 0.727$), ratio between lateral and adventitious root length ($F(1, 15) = 5.981$; $p = 0.0273$), leaf area measured by WinRHIZO image analysis ($F(1, 16) = 1.123$; $p = 0.305$), leaf area measured by leaf area meter ($F(1, 16) = 0.196$; $p = 0.664$), and woody cutting diameter ($F(1, 18) = 0.083$; $p = 0.777$). Due to violated assumption of normal distribution of residuals, Kruskal-Wallis test was conducted for root dry weight ($H(1) = 0.83333$; $p = 0.3613$) and shoot dry weight ($H(1) = 0.19737$; $p = 0.6569$) instead of ANOVA.

Contrary to ‘V3125’ and ‘Börner’, comparison of ‘Calardis Musqué’ and ‘Villard Blanc’ showed significant differences in all traits with exception of ratio between lateral and adventitious root length as well as woody cutting diameter. Kruskal-Wallis test was performed for total root length ($H(1) = 9.20$; $p = 0.0024$), adventitious root length ($H(1) = 12.60$; $p = 0.0003849$), lateral root length ($H(1) = 5.4$; $p = 0.02014$), ratio between lateral and adventitious root length ($H(1) = 0.0375$; $p = 0.8465$), root dry weight ($H(1) = 11.006$; $p = 0.0009082$), leaf area measured by leaf area meter ($H(1) = 13.696$; $p = 0.000215$), and shoot dry weight ($H(1) = 14.143$; $p = 0.0001694$). ANOVA was performed for leaf area measured by WinRHIZO image analysis ($F(1, 20) = 7.923$; $p = 0.0107$) and woody cutting diameter ($F(1, 20) = 0.542$; $p = 0.47$).

Table 7: Mean value, range and standard deviation (SD) of total root length (TRL [cm]), adventitious root length (ARL [cm]), lateral root length (LRL [cm]), ration between lateral and adventitious root length (LRL/ARL), leaf area measured in images with WinRHIZO (LA_WR [cm^2]), leaf area measured with leaf area meter (LA_LAM [cm^2]), woody cutting diameter (WCD [mm]), shoot dry weight (SDW [g]), and root dry weight (RDW [g])] of mapping population parental genotypes 'V3125' (V), 'Börner' (B), 'Calardis Musqué' (CM), and 'Villard Blanc' (VB). Significantly differing means are highlighted in bold.

Trait	n				Mean				Minimum				Maximum				SD			
	V	B	CM	VB	V	B	CM	VB	V	B	CM	VB	V	B	CM	VB	V	B	CM	VB
TRL	7	10	15	8	56.79	50.35	**203.18**	**54.10**	1.09	21.42	54.01	6.02	146.56	102.42	395.03	102.09	48.17	26.55	114.87	29.56
ARL	7	10	15	8	10.25	12.05	**50.24**	**13.71**	0.17	4.87	11.00	0.81	28.27	25.60	90.22	25.54	8.59	6.75	19.62	7.61
LRL	7	10	15	8	55.83	49.09	**152.94**	**40.39**	1.09	20.27	15.86	5.22	141.38	100.34	333.15	80.61	46.86	26.12	106.19	23.82
LRL/ARL	7	10	15	8	**5.52**	**4.22**	3.27	3.51	3.27	3.06	0.40	0.99	7.07	6.11	6.10	6.47	1.21	0.85	2.04	1.61
LA_WR	7	10	15	7	38.53	56.34	**62.95**	**24.53**	1.67	0.66	7.50	0.55	73.70	154.45	145.00	42.66	26.62	37.96	32.97	14.49
LA_LAM	7	10	15	7	86.70	98.24	**146.37**	**0.11**	8.74	7.86	50.57	0.02	185.05	191.77	304.87	0.18	58.37	45.90	61.06	0.05
WCD	9	10	15	8	6.86	6.69	7.33	7.90	5.02	4.36	5.58	5.58	8.92	9.21	9.75	12.35	1.07	1.43	1.18	2.38
SDW	7	10	15	7	0.24	0.21	**0.37**	**0**	0.04	0.03	0.15	0	0.70	0.48	0.56	0	0.21	0.11	0.13	3.23
RDW	6	5	12	8	0.06	0.17	**0.14**	**0.04**	0.01	0.04	0.04	0.01	0.16	0.65	0.37	0.06	0.05	0.24	0.09	0.02

Root parameter of both population genotypes are visualized in figure 20. Depending on the compliance of homoscedasticity, ANOVA or Kruskal-Wallis test was performed to invest the differences between both populations. Overall, genotypes of 'CMVB1989' showed significantly higher values of total root length ($H(1) = 324.5$; $p < 2.2e^{-16}$), root dry weight ($F(1, 340) = 7.44$; $p = 0.0067$), adventitious root length ($F(1, 3701) = 51.67$; $p = 7.9e^{-13}$), and lateral root length ($H(1) = 371.3$; $p < 2.2e^{-16}$) compared to 'VB2001'. Comparably, quantified aboveground plant parts showed a similar trend, revealing higher values of leaf area (LA_WR: $H(1) = 414.2$; $p < 2.2e^{-16}$; LA_LAM: $H(1) = 57.8$; $p = 2.974e^{-14}$), shoot dry weight ($F(1, 306) = 6.6$; $p = 0.01$) and woody cutting diameter ($F(1, 3715) = 500.8$; $p < 2e^{-16}$) in population genotypes of 'CMVB1989' compared to genotypes of 'VB2001' (see figure 21).

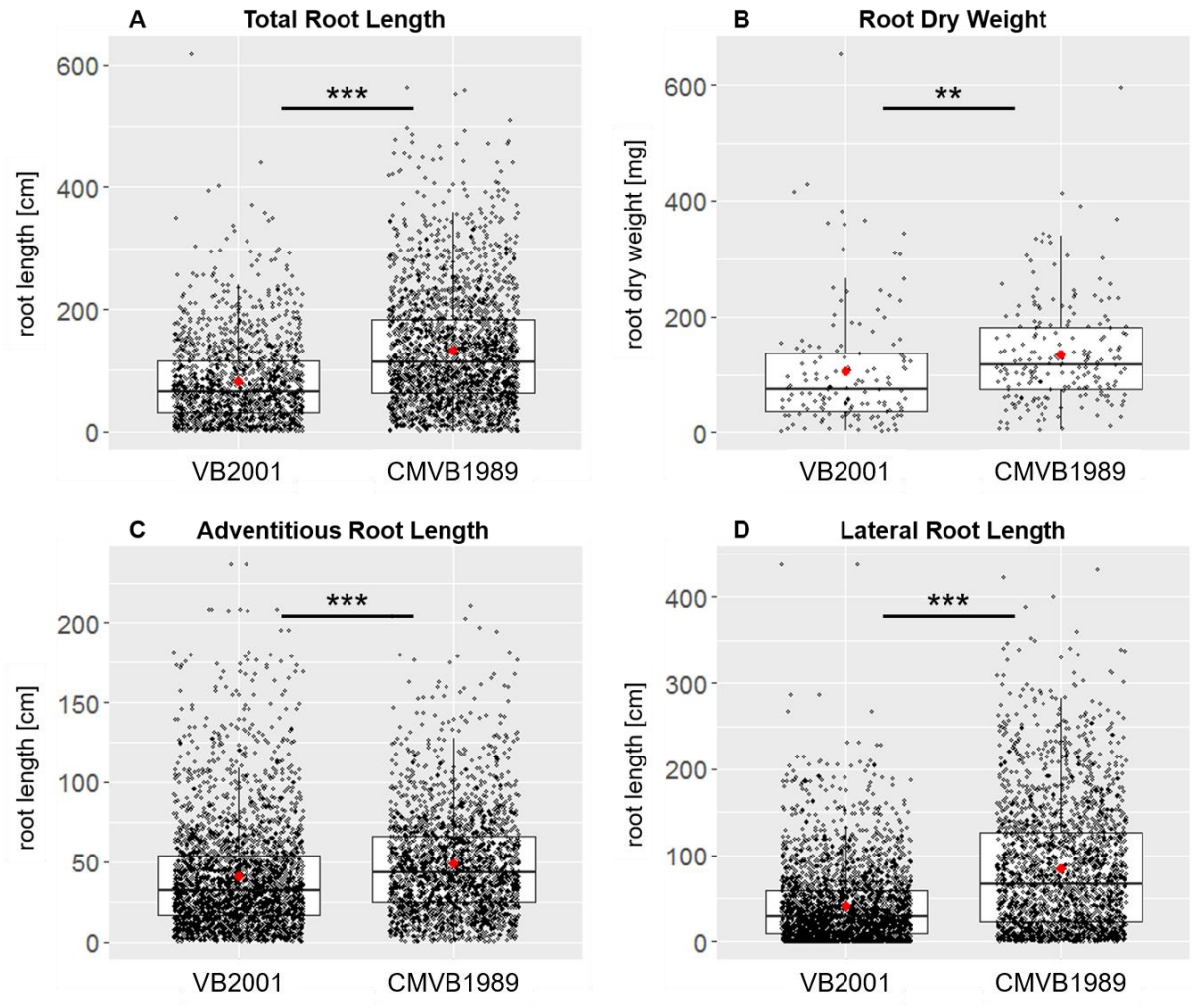

*Figure 20: Comparison of measured root-related phenotypic traits between both mapping populations 'VB2001' and 'CMVB1989'. **A**: Total root length ('VB2001', n=1441; 'CMVB1989', n=2276); **B**: Root dry weight ('VB2001': n=142; 'CMVB1989': n=200); **C**: Adventitious root length ('VB2001': n=1441; 'CMVB1989': n=2262); **D**: Lateral root length ('VB2001': n=1428; 'CMVB1989': n=2276). Mean values are indicated as red point. Significance levels are shown as asterisks: * < 0.05; ** < 0.01; *** < 0.001.*

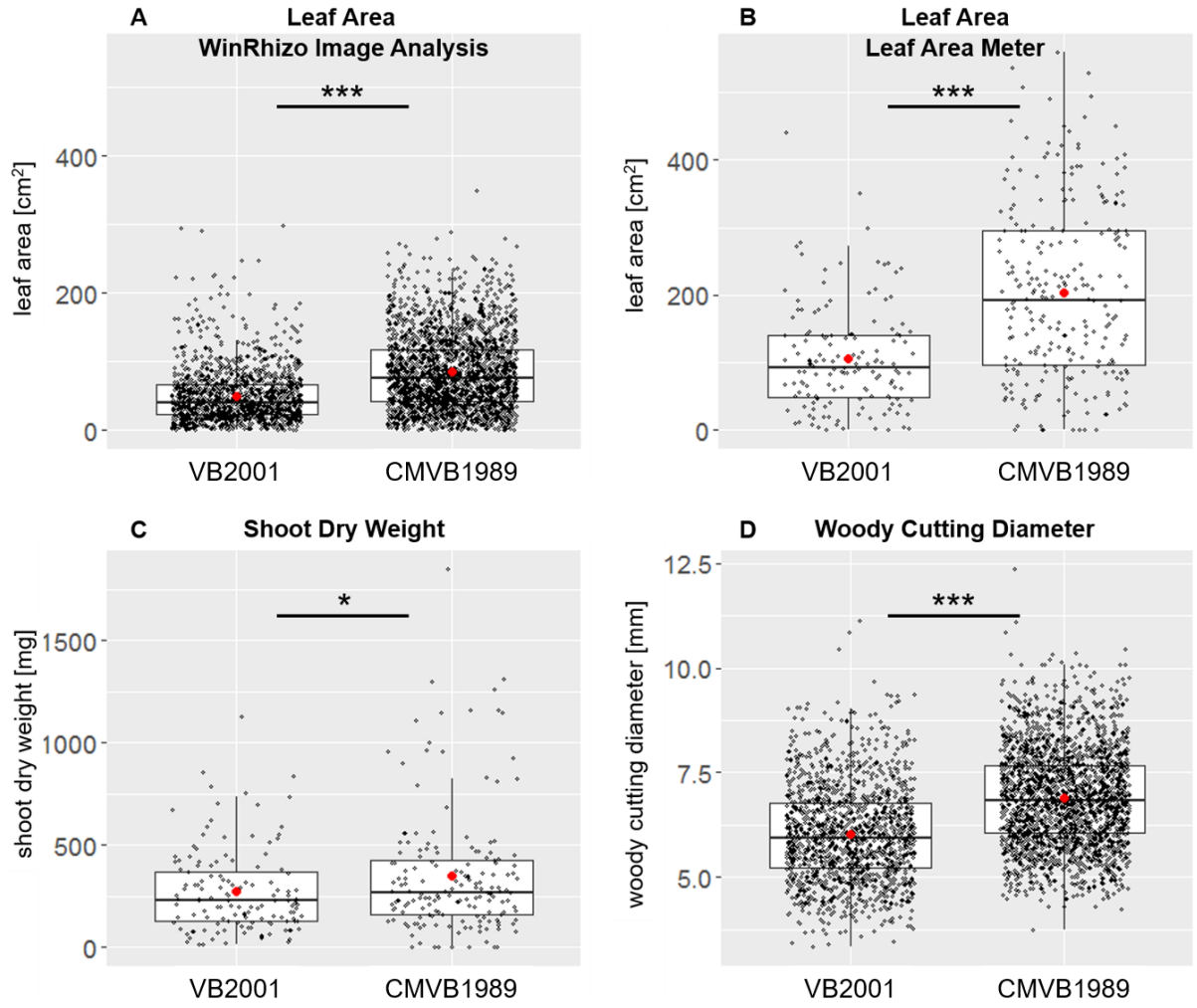

*Figure 21: Comparison of measured aboveground plant traits between both mapping populations 'VB2001' and 'CMVB1989'. **A**: Leaf area from automated image analysis (WinRHIZO) ('VB2001': n=1355; 'CMVB1989': n=2235); **B**: Leaf area measured manually with leaf area meter ('VB2001': n=146, 'CMVB1989': n=243); **C**: Shoot dry weight ('VB2001': n=136, 'CMVB1989': n=150); **D**: Woody cutting diameter ('VB2001': n=1441, 'CMVB1989': n=2276). Mean values are indicated as red point. Significance levels are shown as asterisks: * < 0.05; ** < 0.01; *** < 0.001.*

By statistical modelling woody cutting diameter and the experimental repetition were included as fixed effects. This revealed a positive effect of woody cutting diameter on all measured traits: total root length, adventitious root length, lateral root length and leaf area increased with a broader woody cutting diameter. Effects of woody cutting diameter on the measured parameters are illustrated in figure 22.

Effects of experimental repetition are presented in figure 23 and were not consistent along the measured traits. For genotypes of mapping population 'VB2001', mean values of total root length and lateral root length were highest during the second experiment in 2018. Adventitious root length decreased, and leaf area increased along the experimental repetitions. Individuals of 'CMVB1989' showed a consistent trend of lowest mean values in 2018, followed by constantly high mean values for both experiments in 2019 for total root length, lateral root

length and leaf area. Interestingly, mean values of adventitious root length were similar in first both experiments but decreased in the third experiment.

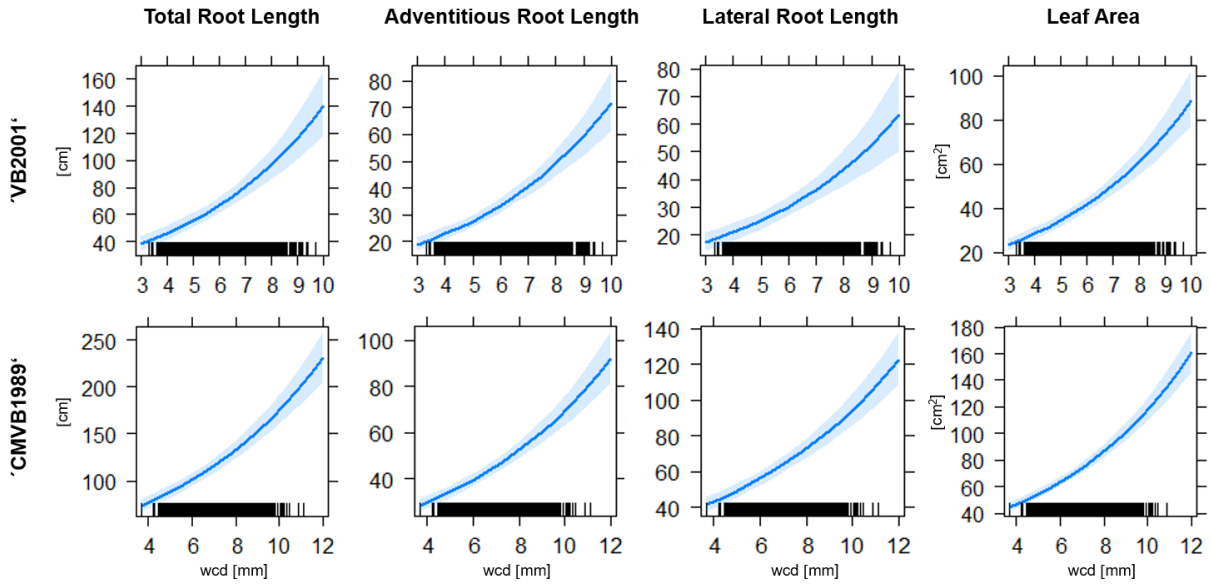

Figure 22: Effects of woody cutting diameter (WCD) on total root length, adventitious root length, lateral root length and leaf area in both mapping populations based on fitted generalized linear mixed models.

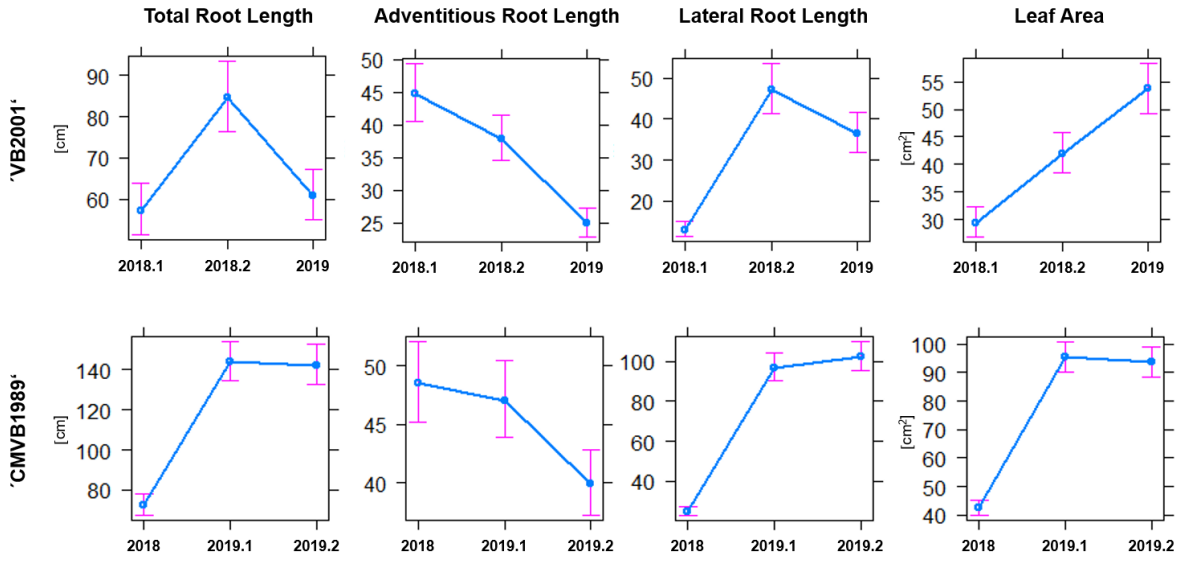

Figure 23: Effects of experimental repetition on total root length, adventitious root length, lateral root length and leaf area in both mapping populations based on fitted generalized linear mixed models.

Both, woody cutting diameter and experimental repetition, were included into statistical modelling as fixed effects. Genotype was included as random effect. Best linear unbiased prediction (BLUP) values were used for the estimation of random effects and display how much

each genotype differs from the average population level. Figure 24 shows the genotype ranking for total root length, adventitious root length, lateral root length and leaf area in both mapping populations including the parental genotypes highlighted by arrows. All traits were measured by automated WinRHIZO image analysis. Regarding root traits (TRL, ARL, and LRL), the parental genotypes ‘V3125’ and ‘Börner’ showed similar rankings under (TRL, ARL) or at (LRL) population average level. In contrast, the parental genotypes ‘Calardis Musqué’ and ‘Villard Blanc’ were greatly divergent: ‘Calardis Musqué’ was over (TRL, LRL) or at (ARL) the population average, whereas ‘Villard Blanc’ was ranked under average (TRL, ARL and LRL). Interestingly, this trend was not shown for leaf area as ‘V3125’ and ‘Börner’ showed a wider distance in the ranking with ‘Börner’ placed on and ‘V3125’ placed under population average and ‘Calardis Musqué’ and ‘Villard Blanc’ were both ranked as under population average in the lower third of the ranking. The rankings of all individual F1 genotypes of the populations are given in figures S8-S11.

‘VB2001‘ - ‘V3125‘ × ‘Börner‘

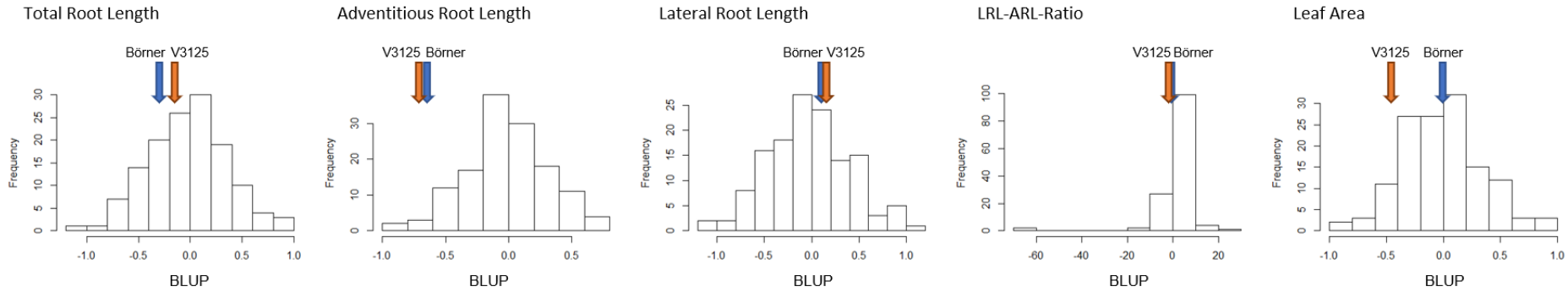

‘CMVB1989‘ - ‘Calardis Musqué‘ × ‘Villard Blanc‘

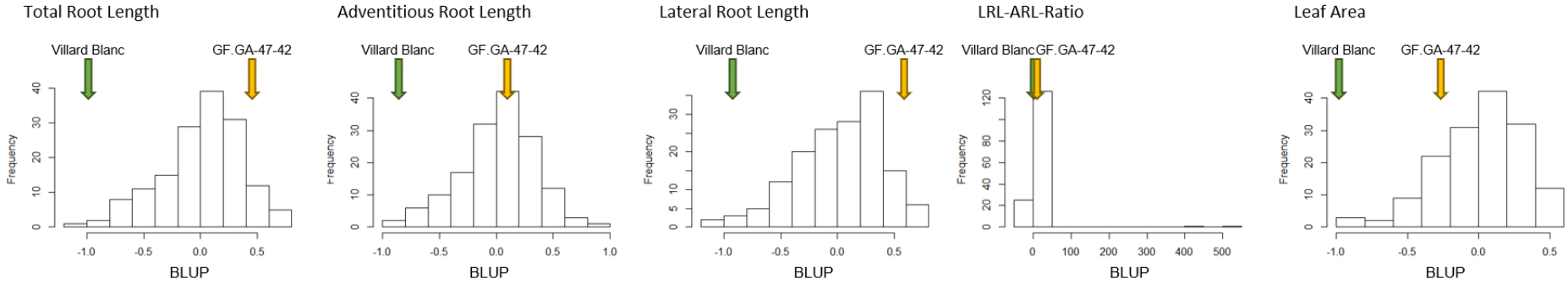

Figure 24: Distribution of root parameters and leaf area in both mapping populations ‘VB2001’ and ‘CMVB1989’: Total root length, adventitious root length, lateral root length, ratio between lateral and adventitious root length, and leaf area. Parental genotypes are indicated by arrows. Phenotypic data is given as best linear unbiased prediction estimates (BLUP) derived from the respective statistical model. Frequency is the number of genotypes.

3.4.5. QTL Mapping

QTL mapping was performed with best linear unbiased prediction values extracted from the respective statistical model. In both mapping populations, a total of 22 QTLs for root parameter and leaf area were identified. Results of QTL mapping are shown in table 8, representing the phenotypic trait, the population and the linkage group (chromosome) where the QTL was identified on. The QTL position (cM) was derived from the corresponding LOD_{max} value. Permutation test reveals the given LOD thresholds of the individual linkage groups and genome wide. The confidence interval (cM) was given as the interval of $LOD_{max} \pm 1$. Linked markers revealed by interval mapping are presented as well as marker and positions confirmed by Kruskal-Wallis mapping. In case a linked marker was confirmed, the significance level of Kruskal-Wallis mapping is given as asterisks. When a neighbouring marker was found by Kruskal-Wallis mapping, marker name and significance level are presented. Otherwise, in case Kruskal-Wallis mapping did not confirm the linked marker previously found by interval mapping, positions are indicated as "-". The last column of table 8 represents the explained phenotypic variance (%).

Figure 25 shows a schematic illustration of the physical positions (PN40024 12X v.2) of all QTLs identified by QTL mapping in both mapping populations based on confidence interval LOD max. ± 1. Out of 22 QTLs identified via interval mapping; 19 QTLs were confirmed by Kruskal-Wallis mapping. QTLs for total root length were identified by interval mapping on linkage groups 1, 13, and 15 for mapping population 'VB2001' and on linkage groups 7, 9, and 17 for mapping population 'CMVB1989'. For adventitious root length, QTLs were identified on linkage groups 1 and 15 for mapping population 'VB2001' as well as on linkage groups 3, 7, 9, and 17 for mapping population 'CMVB1989'. Interval mapping revealed only one QTL for lateral root length in 'VB2001' on linkage group 15, whereas two QTLs on linkage group 7 and 17 were found in 'CMVB1989' for lateral root length. Two QTLs for the ratio between lateral and adventitious root length could be identified for population 'VB2001' on linkage groups 12 and 13, whereas no QTL was discovered for population 'CMVB1989' for this trait. Two QTLs for leaf area were identified in 'VB2001' on linkage groups 1 and 13 and in 'CMVB1989' on linkage groups 2 and 13. The QTL for leaf area on chromosome 13 was the only overlapping QTL region between both mapping populations

*Table 8: Results of QTL mapping with QTLs identified by interval mapping for root traits and leaf area from both mapping populations 'VB2001' and 'CMVB1989'. Kruskal-Wallis significance levels are given as asterisks *** < 0.01; **** < 0.005; ***** < 0.001.*

trait	population	LG	QTL position (cM)	Confidence Interval ± 1 LOD in cM	LOD max	LOD threshold (LG)	LOD threshold genome	linked marker Interval Mapping	Kruskal-Wallis test	explained phenotypic variance (%)
total root length	'VB2001'	01	13.0	8.5 - 14.6	3.24	2.9	4.5	VMC4f9.2	VMC4f9.2 ****	10.6
		13	79.2	0 - 6.7	3.23	2.9		UDV_088_181	VVIN62_356 ***	10.6
		15	25.4	19.6 – 29.3	3.18	2.7		-	GF15-07 ****	10.4
	'CMVB1989'	17	16.6	8.0 - 21.8	3.71	2.8	4.3	UDV-072_126	VMC2H3 ***	10.7
		07	166.6	160.6 - x	3.19	3.0		GF07-08	GF07-08 ***	9.3
		09	8.0	0 - 18.2	3.01	2.8		VMC1C10	VMC1C10 ***	8.8
adventitious root length	'VB2001'	01	13.0	8.5 - 14.6	3.44	3.1	4.4	VMC4f9.2	VMC4f9.2 ****	11.2
		15	26.4	20.6 – 29.3	3.31	2.6		-	GF15-07 ****	10.8
	'CMVB1989'	09	8.6	2.0 – 15.6	3.95	2.8	4.3	VMC1C10	VMC1C10 *****	11.3
		07	166.6	160.6 - x	3.51	2.8		GF07-08	GF07-08 ****	10.1
		03	52.1	35.9 – 61.0	3.44	2.7		GF03-07_273	GF03-07_273 ****	10.0
		14	30.1	23.9 - 36.3	3.27	2.9		VVIP22	VVIP22 ****	9.5
		17	16.6	8.0 - 20.6	3.03	2.6		UDV-072_126	-	8.8
lateral root length	'VB2001'	13	78.5	0 - 11.3	3.83	3	4.5	UDV_088_181	VVIN62_356 ****	12.4
		15	25.4	19.6 - 30.3	3.18	2.5		UDV_116	UDV_116 ***	10.4
	'CMVB1989'	17	16.6	8.0 - 29.2	4.04	2.7	4.4	UDV-072_126	VMC2H3 ****	11.6
		07	166.6	160.6 - x	2.94	3.9		GF07-08	-	8.6
lateral-adventitious root length ratio	'VB2001'	12	37.8	27.8 - 66.7	2.91	2.4	4.0	-	VMC4f3.1 ****	9.6
	'CMVB1989'	-	-	-	-	-	-	-	-	-
leaf area	'VB2001'	13	79.2	0 - 4.7	3.65	2.8	4.4	UDV_088_181	-	11.9
		01	13.3	10.0 - 18.6	3.13	3.1		VMC4f9.2	VMC4f9.2 ***	10.3
	'CMVB1989'	13	6.5	0 - 26.5	3.39	2.8	4.4	-	VVIH54 ****	9.8
		02	16.7	1.7 - 33.2	2.84	2.4		GF02-42_167	GF02-39 ****	8.3

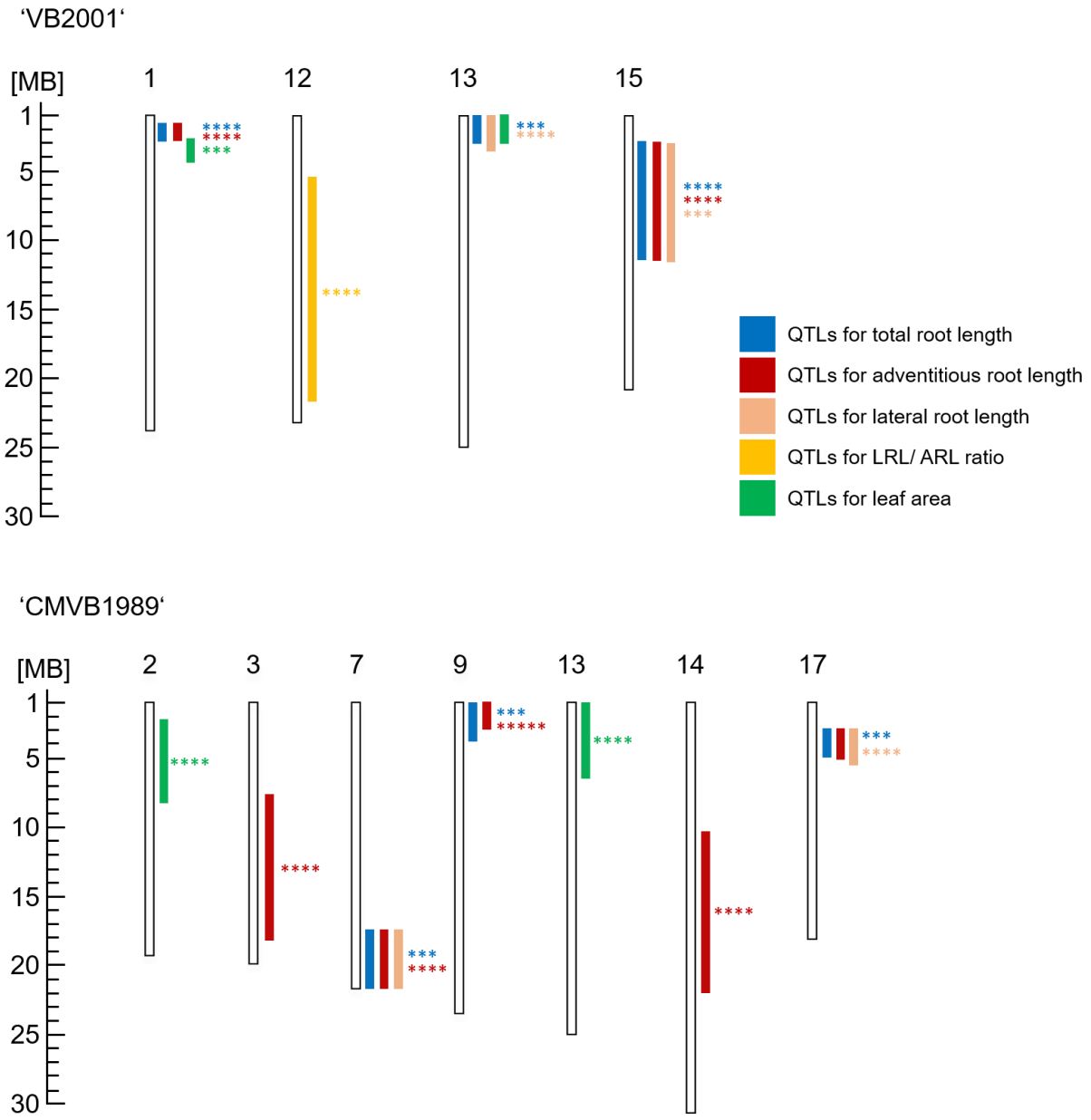

Figure 25: Schematic illustration of physical QTL positions (in PN40024 12X v.2) identified via interval mapping by use of rhizotrons and automated image analysis for total root length, adventitious root length, lateral root length, ratio between lateral and adventitious root length, and leaf area of mapping populations 'VB2001' and 'CMVB1989'. Significant confirmation by Kruskal-Wallis mapping are indicated with asterisks.

3.4.6. *In silico* Candidate Gene Analysis

Candidate gene analysis was conducted for the genomic regions on chromosome 9 (32.080 - 3.854.406 Mb, given by LOD_{max}±1 confidence interval between marker 'GF09-09' and 'GF09-48') and chromosome 13 (3.024.838 - 3.333.487 Mb, given by LOD_{max}±1 confidence interval between marker 'UDV-088' and 'VVIH54'). The QTL region identified on linkage group 9 was considered for *in silico* candidate gene analysis because a recent study analysing grapevine root development from woody cuttings grown in perlite substrate identified QTLs in the same

genomic region for total root length and root diameter (Alahakoon, 2020). In addition, the QTL region on linkage group 13 was selected for *in silico* candidate gene analysis as this region was revealed in both mapping populations of this study for growth related traits of roots and leaf area. Both genomic regions on chromosome 9 and chromosome 13 were examined for putative candidate genes using the *V. vinifera* reference genome sequence PN40024 12X v.2 (GENOSCOPE, CRIBI Consortium VIGNA and IGA; Jaillon et al. 2007; Goremykin et al. 2008). In total, 14 selected putative candidate genes were found for linkage group 9 and are listed in table 9, presenting the gene names, physical positions, and their putative function or homologs indicating their potential role in root growth and development. One candidate gene was found on the corresponding genomic region of linkage group 13 see table 10).

Table 9: List of putative candidate genes found within the identified QTL region on linkage group 9 (EnsemblPlants, UniProtKB)

Gene	Gene location	Protein / Homologs / Functions
VIT_09s0002g00890	647.306 - 649.289 Mb	Regulation of defense response, regulation of jasmonic acid mediated signaling pathway, response to wounding
VIT_09s0002g01370	1.150.521 - 1.153.564 Mb	AP2 / ERF domain containing protein, transcription factor in Vitis. Homolog (WGA Coverage 71.40) in A. thaliana: At1G72570: AP2-linke ethylene-responsive transcription factor AIL1. Probably acts as a transcriptional activator. Binds to the GCC-box pathogenesis-related promoter element. May be involved in the regulation of gene expression by stress factors and by components of stress signal transduction pathways (By similarity). Ethylene-activated signaling pathway.
VIT_09s0002g01420	1.193.649 - 1.203.172 Mb	Uncharacterized Protein in Vitis. Homolog (WGA Coverage 64.31) in A. thaliana: At1G17440: TAF12B, Transcription initiation factor: TAFs are components of the transcription factor IID (TFIID) complex that is essential for mediating regulation of RNA polymerase transcription. Required for the expression of a subset of ethylene-responsive genes. Probably involved in the negative regulation of cytokinin sensitivity. Cytokinin-activated signaling pathway, JA-mediated signaling pathway, regulation of ethylene-activated signaling pathway.
VIT_09s0002g01520	1.296.073 - 1.297.748 Mb	Uncharacterized Protein in Vitis. ARBA annotation (UniProtKB): Protein involved in auxin transport. Regulator of the auxin signaling pathway
VIT_09s0002g01850	1.638.319 - 1.614.659 Mb	Protein-serine / threonine phosphatase in Vitis. Homologs (WGA Coverages of 99.80) in A. thaliana: HAB1 (At1G72770), HAB2 (At1G17550): Key component and repressor of the abscisic acid (ABA) signaling pathway that regulates numerous ABA responses, such as stomatal closure, seed germination and inhibition of vegetative growth. Confers enhanced sensitivity to drought. (Saez et al. 2006)
VIT_09s0002g03410	3.075.730 - 3.079.091 Mb	Auxin-responsive protein. Aux/IAA proteins are short-lived transcriptional factors that function as repressors of early auxin response genes at low auxin concentrations. Homologs (WGA Coverage 80.70 and 72.61) in A. thaliana: IAA18 (At1G51950), IAA26 (At3G16500): Formation of heterodimers with ARF (auxin response factor) proteins may alter their ability to modulate early auxin response genes expression.
VIT_09s0002g03540	3.223.163 - 3.224.630 Mb	HTH myb-type domain containing protein; response to auxin, ethylene, and gibberellin
VIT_09s0002g03550	3.229.012 - 3.242.582 Mb	ABC transporter domain-containing protein
VIT_09s0002g03610	3.279.559 - 3.283.962 Mb	HTH myb-type domain containing protein; response to auxin, ethylene, and gibberellin
VIT_09s0002g03640	3.328.212 - 3.336.626 Mb	Uncharacterized Protein in Vitis. Homologs (WGA Coverage 93.47) in A. thaliana: ABCG36 (At1G59870): Together with ABCG37, regulates auxin homeostasis and responses by playing a dual role in coumarin (e.g., esculin) and in the auxin precursor indole 3-butyric acid (IBA) efflux transport, thus influencing cotyledons, roots and root hairs development (Ruzicka et al. 2010). Promotes resistance to abiotic stresses (e.g. drought and salt stress) and favors general growth by preventing sodium accumulation in plants (Borghi et al. 2015).
VIT_09s0002g03940	3.665.089 - 3.665.967 Mb	AP2 / ERF domain containing protein
VIT_09s0002g04080	3.749.950 - 3.753.753 Mb	Auxin-responsive protein Aux/IAA proteins are short-lived transcriptional factors that function as repressors of early auxin response genes at low auxin concentrations.

Table 10: Putative candidate gene found within the identified QTL region on linkage group 13 (EnsemblPlants, UniProtKB)

Gene	Gene location	Protein / Homologs / Functions
VIT_13s0019g01650	3.120.580 - 3.122.163 Mb	Expansin: Involved in cell wall organization
VIT_13s0019g01890	3.227.777 - 3.228.605 Mb	Uncharacterized Protein in Vitis. Homolog (WGA Coverage 77.72) in A. thaliana: DVL8 (At2G39705): Involved in the biological process of shoot system development (Wen et al. 2004).

3.5. Discussion

3.5.1. Phenotyping of Grapevine Roots in Rhizotron System

In the past, grapevine phenotyping was mostly determined by manual, destructive and visual scoring. Phenotyping based on non-destructive sensors offers advantages like potential automation, objectivity, high-precision and high-throughput. Recently, the utilization of scanners and automated image analysis has found its entry into grapevine research (Rist et al. 2018, Bendel et al. 2020). However, objective, high-throughput phenotyping methods for grapevine root phenotyping are still scarce and urgently needed. In this study, a rhizotron system was developed and tested with two different mapping populations in order to provide phenotypic root related data for identification of QTL regions and contribution to grapevine breeding research for rootstocks best adapted to future climates and environments.

Rhizotron Setup and Experimental Design

The developed rhizotron system of this study delivers quantitative phenotypic data about root length and root branching in terms of differentiation between adventitious and lateral roots at high-throughput level. Regarding throughput potential, another root phenotyping platform based on rhizotrons and image-based analysis developed by Nagel et al. (2012) enables scans of 60 root systems per hour followed by image analysis attaining five root systems per hour. Simultaneous phenotyping of whole plants can also be done by magnetic resonance imaging with a throughput of 14 small plants per hour (Jansen et al. 2014). For grapevine, only few rhizotron studies have been conducted so far with relatively low throughput (Fortea et al. 2009, de Herralde et al. 2010, Dumont et al. 2016, and Fort and Fraga, 2017).

The rhizotron system developed and tested in this study reached performance of four samples per hour including material preparation, rhizotron setup (with three persons), image acquisition (with three persons), and image analysis. It should be noted that this throughput was reached during rhizotron experiments including time-consuming acquisition of the reference data required for method validation like leaf area meter measurements and root washing for the determination of root dry weight. Without these steps, throughput might be accelerated significantly. In addition, reuse of trays, foils, floral foam stripes and sieved soil can further reduce the preparation time of subsequent experiments. Therefore, the system allows non-invasive root phenotyping of whole grapevine mapping populations and with sufficiently high number of replicates to provide an extensive basis of phenotypic data for subsequent QTL analysis.

Besides high throughput, another advantage of the rhizotron system is the monitoring of roots and shoot simultaneously in order to correlate root traits to whole-plant development. This is achieved by use of two cameras which are triggered simultaneously within the photo box.

Selection of shoot and root traits simultaneously, accelerates genetic gain within the whole plant compared to selection on shoot or root traits alone. Observation of shoot and root traits might increase the ability to link roots to their functional attributes and contribute to the understanding of whole-plant function (Tracy et al. 2020).

Validation of Automated Image Analysis

Comparison of manual (ImageJ) and automated (WinRHIZO) image analysis revealed no significant differences in root related parameters: total root length, adventitious root length, and lateral root length. Regression analysis resulted in coefficients of determination ranging from 0.86 (adventitious root length) to 0.99 (total root length). These results are comparable to experiments with durum wheat. Bodner et al. (2018) described the development and validation of soil-filled rhizoboxes in combination with hyperspectral imaging and subsequent image segmentation. Both, spectral and colour-based image segmentation was compared with manual image analysis and resulted in $R^2 = 0.81$, and $R^2 = 0.87$, respectively.

Regarding leaf area, regression coefficient was $R^2 = 0.74$, describing a positive correlation. Although, leaf area was significantly underestimated by automated image analysis by WinRHIZO. This effect was predominantly observed in population genotypes with many leaves and probably caused by overlapping leaf structure at the shoot. The effect even intensified with increasing leaf area produced by the shoot, particularly when a high number of leaves is overlapping each other. Therefore, automated image analysis and observation of aerial plant parts should take place in early developmental stages, especially for observation of fast-growing genotypes.

Correlation Between Image Analysis and Plant Biomass

Based on the linear regression model, correlation between root dry weight and total root length resulted in a moderate correlation of $R^2 = 0.59$. In a rhizotron study by Nagel et al. (2012), coefficients of determination amounted 0.92 - 0.97 for the tested plants rice, barley, Arabidopsis, rapeseed, and Brachypodium. Interestingly, in the same study, correlation for maize resulted in correlation of only $R^2 = 0.35$. Only a part of the whole root system is visible via rhizotrons and it is known that this proportion varies between plant species and seems to depend on the specific root weight and root diameter of the certain species. Root systems of thinner roots exhibit a higher proportion of visible roots in rhizotrons, e.g., proportion of visible roots in Arabidopsis is approx. 77%, while only approximately 17% of maize roots are visible in rhizotrons. In a preliminary experiment conducted at Research Centre Jülich (unpublished data), 15 grapevine cultivars were investigated in rhizotrons. The proportion of visible root length ranged between 9.2% and 21.8% depending on the variety. On average, 12.5% of the total root length was visible at the rhizotron surface (n = 135). Thicker roots and a stronger

three-dimensional root growth could contribute to the lower correlations of root length and root biomass of maize or grapevines. Nevertheless, Nagel et al. (2012) concluded that the visible part of the root system in rhizotrons might be utilized as measure for root system growth when differences between plant species are considered.

Correlation between shoot dry weight and leaf area measured with WinRHIZO was relatively low (R^2 = 0.36) but reasonable due to the significant underestimation of leaf area with automated image analysis as discussed before. However, a moderate correlation was shown between shoot dry weight and leaf area measured with leaf area meter (R^2 = 0.55). Interestingly, this correlation is comparable to the observed correlation between root dry weight and total root length (R^2 = 0.59), providing a potential first scale for correlations between biomass and area measurements for grapevines grown in rhizotrons. However, since further comparable data for grapevine is lacking, future experiments are necessary to form a stable data basis to confirm these first indications.

Correlation Between Belowground and Aboveground Plant Parts

Highest correlation between belowground and aboveground plant parts was R^2 = 0.69 for correlation between total root length and leaf area measured with leaf area meter. The same correlation was found for these traits in maize (Nagel et al. 2012), besides considerably higher correlations in rice (R^2 = 0.99), rapeseed (R^2 = 0.98), Arabidopsis (R^2 = 0.98), Brachypodium (R^2 = 0.94), and barley (R^2 = 0.89). This discrepancy might also relate to the exhibition of lower proportion of visible roots due to higher root diameter in maize and grapevine.

Correlation between root dry weight and shoot dry weight was described with R^2 = 0.52. Jeudy et al. (2016) found a shoot/root dry biomass ratio of 0.57 for grapevine plants growing in RhizoTubes similar compared to shoot/root dry biomass ratio calculated for pot-grown plantlets, indicating that overall plant development was not modified in RhizoTubes. Investigation of adventitious root formation of poplar woody cuttings showed correlation coefficients of 0.69 between root dry weight and shoot dry weight, and 0.58 between root number and leaf number on shoots (Sun et al. 2019). Correlations and results repeatability indicated that genotypes with more adventitious roots tended to have larger aboveground shoot biomass. The rhizotron derived data confirmed this trend of a positive correlation between root traits and aerial plant parts in grapevine. In addition, it could be shown that root and shoot related traits were under strongly coordinated genetic regulation in *A. thaliana* (Rauh et al. 2002), maize (Hund et al. 2004), and wheat (Laperche et al. 2006) indicating a strong relation between belowground and aboveground plant parts. Interestingly, the genetic architecture of aerial and roots traits in field-grown grafted grapevines was largely independent as shown in a segregating F1 mapping population (Tandonnet et al. 2018). Notably, the suggestion of independent genomic control of biomass allocation, root biomass, and aerial

biomass was based on grafted grapevines in contrast to the current rhizotron study with ungrafted cuttings. Regulatory rootstock-scion interactions might be considered in future rhizotron experiments by studying the genetic architecture of rootstock traits for a wide range of scions.

3.5.2. QTL Mapping and *in silico* Candidate Gene Analysis

As shown in previous studies, investigating genetic diversity and control of morphological root traits suggested the genetic control of root system architecture in grapevine (Yildirim et al. 2018, Peiró et al. 2020). In this study, interval mapping with data of both mapping populations resulted in the identification of 22 QTLs in total. Not all QTLs identified in 'VB2001' were also found in 'CMVB1989'. Differences might be attributed to the use of populations with distinct genetic backgrounds (Ribeiro et al. 2016). In general, different markers used for genetic map construction or contrast map distance among different maps can lead to identification of different QTL regions. In addition, a different number of identified QTLs might be due to population parents exhibiting greater difference in root growth and therefore, contributing to distinct separation in the F_1 population (Sun et al. 2019). In total, 10 QTLs could be identified in mapping population 'VB2001', while 12 QTLs were identified in mapping population 'CMVB1989'. However, QTLs of 'VB2001' were distributed over only four linkage groups, whereas QTLs of 'CMVB1989' were identified on seven linkage groups.

A recent study by Alahakoon (2020) examined root system architecture of grapevine cuttings grown in perlite substrate and identified a total of 42 QTLs associated with 11 root system architecture related phenotypic traits in a grapevine F2 population. One QTL hotspot has been identified on linkage group 9 associated with five phenotypic traits including total root length and average diameter. Interestingly, two QTLs in these regions were found in our experiment in mapping population 'CMVB1989' for total root length and adventitious root length. In addition, Alahakoon (2020) identified another QTL hotspot on linkage group 13 for seven root related traits including total root length, root volume, and root fresh weight. Our study revealed three QTLs in this genomic region in mapping population 'VB2001' for the traits total root length, lateral root length, and leaf area, and additionally one QTL in mapping population 'CMVB1989' for leaf area.

Regarding plant hormones, auxin is the major promoting hormone for initiation of adventitious rooting (Li et al. 2009). Within the QTL region on chromosome 9, several candidate genes putatively linked to auxin signaling could be found. Two genes VIT_09s0002g03410 (3.075.730 - 3 079.091 Mb) and VIT_09s0002g04080 (3.749.950 - 3.753.753 Mb) are encoding auxin-responsive proteins which act as transcriptional factors and are involved in auxin-activated signaling pathway. A homolog of VIT_09s0002g03410 in *A. thaliana* (At1G51950, Whole Genome Alignment coverage of 80.70) is called IAA18 and known to be

involved in positive regulation of lateral root formation and shoot development (Uehara et al. 2008). VIT_09s0002g01520 (1.296.073 - 1.297.748 Mb) encodes for an unknown protein in *Vitis* but is suggested to be involved in auxin transport and in regulation of auxin signaling pathway based on ARBA (Association Rule Based Annotator) annotation (https://www.uniprot.org/help/arba). Additional, two genes namely VIT_09s0002g03550 (3.229.012 - 3.242.582 Mb) and VIT_09s0002g03640 (3.328.212 - 3.336.626 Mb) encode ABC transporter domain-containing proteins. The homologs in *A. thaliana*, ABCG35 (At1G15210, WGA coverage of 92.31), ABCG36 (At1G59870, WGA coverage of 93.47), and ABCG29 (At3G16340, WGA coverage of 92.58) belong to the subfamily of so-called ABCG active membrane transport proteins localized within the plasma membrane and cell compartment membranes (Dhara and Raichaudhuri, 2021). Expression sites of ABCG35, ABCG36, and ABCG29 include root tissue as well as other plant organs. Besides enhancement towards drought and salt stress in plants overexpressing ABCG36, the transporter seems to contribute to heavy metal resistance and detoxification (Kim et al. 2010, Dhara and Raichaudhuri, 2021). In addition, ABCG36 is suggested to be an efflux transporter of IBA (Indole-3-butyric acid of the auxin plant hormone family) from root cells, catalyzing the transport of IBA and therefore, possibly being related to auxin homeostasis (Borghi et al. 2015, Gräfe and Schmitt, 2020). Interestingly, exogenous IBA promoted the formation of adventitious roots in blueberry green cuttings by initiation of adventitious root primordia right after induction of IBA (An et al. 2020). Additionally, ABCG35 expression is known to improve resistance to cadmium (Cd^{2+}) and lead (Pb^{2+}) (Kim et al. 2007) and ABCG29 was shown to play important role in lignin biosynthesis (Takeuchi et al. 2018). Therefore, the latter two ABCG transporters seem to improve root growth under toxic soil conditions and probably contribute to root growth and elongation by detoxification and increased adaptability to critical locations. Besides that, *in silico* candidate gene analysis revealed two genes encoding for HTH myb-type domain-containing proteins which are involved in response to auxin, ethylene, and gibberellin: VIT_09s0002g03540 (3.223.163 - 3.224.630 Mb) and VIT_09s0002g03610 (3.279.559 - 3.283.962 Mb). MYB transcription factors are widely common in plants and play important roles in plant growth and development among other functions in morphology or stress response (reviewed in Cao et al. 2020). In *A. thaliana*, MYB77 interacts with auxin responsive factors in auxin signaling transduction and lateral root growth and root number (Shin et al. 2007).

Next to auxin, ethylene and jasmonic acid stimulate the formation of adventitious roots (Druege et al. 2016). Candidate gene analysis revealed two genes VIT_09s0002g01370 (1.150.521 - 1.153.564 Mb) and VIT_09s0002g03940 (3.665.089 - 3.665.967 Mb) encoding a AP2/ERF (APETALA2/Ethylene Responsive Factor) domain-containing protein. The corresponding *A. thaliana* homolog (At1G72570, WGA coverage of 71.40) is an AP2-like ethylene-responsive transcription factor called AIL1 (AINTEGUMENTA LIKE1). Interestingly, AIL1 is involved in

formation of adventitious roots in poplar. Transcriptome analysis revealed specific temporal induction of AIL1 during adventitious root formation. Moreover, Rigal et al. (2012) demonstrated that transgenic poplar lines overexpressing PtAIL1 exhibited an increased number of adventitious roots. In addition, AIL genes are known to be expressed in dividing tissues and necessary for the formation of adventitious root primordia in *A. thaliana* (Galinha et al. 2007). Further, two genes within QTL region of chromosome 9 might be involved in jasmonic acid signaling: VIT_09s0002g01420 (1.193.649 - 1.203.172 Mb) and VIT_09s0002g00890 (647.306 - 649.289 Mb). The *A. thaliana* homolog of VIT_09s0002g01420 TAF12B (TATA BOX BINDING PROTEIN ASSOCIATED FACTOR12) (At1G17440, WGA coverage of 64.31) is a component of transcription factor IID (TFIID) complex, required for the expression of a subset of ethylene-responsive genes and probably involved in the negative regulation of cytokinin sensitivity (Kubo et al. 2011). The corresponding protein of VIT_09s0002g00890 contains a Tify domain and is known to be involved in the regulation of defense response, jasmonic acid mediated signaling pathway, and response to wounding. Wounding can induce the adventitious root formation as survival strategy in case the cutting site leads to isolation from the resource and signal network of the whole plant (Druege et al. 2016). In petunia cuttings, jasmonic acid was accumulated during adventitious root induction phase (Ahkami et al. 2009) and a significant positive and accelerating role of jasmonic acid was documented for formation of root primordia (Lischewski et al. 2015). Even though this positive effect of JA in induction of adventitious root formation has also been observes in other crops like pea (Rasmussen et al. 2015). In *A. thaliana*, jasmonic acid seems to inhibit adventitious rooting (Gutierrez et al. 2012).

Besides chromosome 9, QTL region on chromosome 13 was investigated regarding putative candidate genes resulting in the gene VIT_13s0002g01650 encoding expansin, a protein involved in catalyzation of cell wall expansion in plants. In soybean, a root-specific expansin gene was suggested to be responsible for root elongation and accelerating root growth (Lee et al. 2003). In addition, Cheng et al. (2016) found evidence for multiple expansin genes probably regulating root growth of tomato at different developmental stages. Next, VIT_13s0002g01890 encodes an unknown protein in *Vitis*, but the homolog in *A. thaliana* (At1G72790, WGA coverage of 77.69) seems to belong to the RTFL peptides DEVIL (DVL1) and ROTUNDIFOLIA4 (ROT4) which are involved in regulation of leaf and fruit development (Wen et al. 2004). Interestingly, both mapping populations in our grapevine rhizotron study revealed a QTL for leaf area within the same region of chromosome 13.

The developed rhizotron phenotyping system considerably contributed to the identification of root trait related QTLs. All in all, *in silico* candidate gene analysis resulted in 14 genes potentially involved in the regulation of adventitious root growth. However, the regulation of

root development by plant hormones and signaling pathways is poorly understood yet, especially in woody species like grapevine. Root phenotyping methods like the use of rhizotrons could potentially provide the basis for further transcriptomic studies and contribute to the exploration of the underlying processes. This will promote the adaptation of grapevine rootstocks to climate change and provide possible future perspectives for grapevine breeding and breeding research of rootstock varieties.

3.5.3. Future Perspectives

The developed rhizotron system utilized for QTL mapping of root related traits in general might be further modified in future experiments in order to enhance the variety of application methods e.g., comparison of drought, salinity or nutrient supply treatments to target functional traits like nitrogen and water use efficiency. In addition, use of the rhizotron system could be extended aiming at root trait measurements at different time points. Growth rates and root elongation rates could be involved, and experimental design could include phases of treatment and subsequent recovery phases. All in all, this study proved that the developed rhizotron system and the associated workflow provide a promising basis of high throughput grapevine root phenotyping, possessing enormous potential for a variety of upcoming studies.

3.6. References

Adeleke, E.; Millas, R.; McNeal, W.; Faris, J.; Taheri, A. (2020): Variation Analysis of Root System Development in Wheat Seedlings Using Root Phenotyping System. Agronomy 10, 206

Ahkami, A.H.; Lischewski, S.; Haensch, K.-T.; Porfirova, S.; Hofmann, J.; Rolletschek, H. (2009): Molecular physiology of adventitious root formation in Petunia hybrida cuttings: involvement of wound response and primary metabolism. New Phytol. 181,613-625

Alahakoon, D. (2020): Exploiring Phenotypic Diversity and Quantitative Trait Loci Mapping for Root Architecture, Freezing Tolerance, Chilling Fulfillment, and Photoperiod Traits in Grapevine Populations. Electronic Theses and Dissertations. 4855

An, H.; Zhang, J.; Xu, F.; Jiang, S.; Zhang, X. (2020): Transcriptomic profiling and discovery of key genes involved in adventitious root formation from green cuttings of highbush blueberry (*Vaccinium corymbosum* L). BMC Plant Biology. 20:182

Bendel, N.; Kicherer, A.; Backhaus, A.; Köckerling, J.; Maixner, M.; Bleser, E.; Klück, H.-C.; Seiffert, U.; Voegele, R.T.; Töpfer, R. (2020): Detection of Grapevine Leafroll-Associated Virus 1 and 3 in White and Red Grapevine Cultivars Using Hyperspectral Imaging. Remote Sens. 12(10), 1693

Bodner, G.; Nakhforoosh, A.; Arnold, T.; Leitner, D. (2018): Hyperspectral imaging: a novel approach for plant phenotyping. Plant Methods 14, 84

Borghi, L.; Kang, J.; Ko, D.; Lee, Y.; Martinoia, E. (2015): The role of ABCG-type ABC transporters in phytohormone transport. Biochem. Soc. Trans. 43(5):924-30

Cheng, F.; Cheng, Z.; Meng, H.; Tang, X. (2016): The Garlic Allelochemical Diallyl Disulfide Affects Tomato Root Growth by Influencing Cell Division, Phytohormone Balance and Expansin Gene Expression. Front. Plant Sci. Vol. 7, 1199

Cao, Y.; Li, K.; Li, Y.; Zhao, X.; Wang, L. (2020): MYB Transcription Factors as Regulators of Secondary Metabolism in Plants. Biology 9, no. 3: 61

De Herralde, F.; Savé, R.; Aranda, X.; Biel, C. (2010): Grapevine Roots and Soil Environment: Growth, Distribution and Function. In: Delrot et al. (2010): Methodologies and Results in Grapevine Research. Springer Science and Business, Media B.V.

Dhara, A. and Raichaudhuri, A. (2021): ABCG transporter proteins with beneficial activity on plants. Phytochemistry. Vol. 184, 112663

Delrot, S.; Grimplet, J.; Carbonell-Bejerano, P. et al. (2020): Genetic and Genomic Approaches for Adaptation of Grapevine to Climate Change. In: Genomic Designing of Climate-Smart Fruit Crops. Edited by Kole, C. Springer

Druege, U.; Franken, P.; Hajirezaei, M.R. (2016): Plant Hormone Homeostasis, Signaling, and Function during Adventitious Root Formation in Cuttings. Front. Plant. Sci. 7, 381

Dumont, C.; Cochetel, N.; Lauvergeat, V.; Cookson, S.J.; Ollat, N.; Vivin, P. (2016): Screening root morphology in grafted grapevine using 2D digital images from rhizotrons. Acta Hortic. 1136. ISHS 2016, Proc. I Int. Symp. On Grapevine Roots. Eds.: F. Gaiotti et al.

Fechter, I.; Hausmann, L.; Zyprian, E.; Daum, M.; Holtgräve, D.; Weisshaar, B.; Töpfer, R. (2014): QTL analysis of flowering time and ripening traits suggests an impact of a genomic region on linkage group 1 in Vitis. Theor. Appl. Genet. 127, 1857-1872

Fort, B. and Fraga, B. (2017): Early Measures of Drought Tolerance in four Grapevine Rootstocks. J. Amer. Soc. Hort. Sci. 142(2):36-46

Fortea, G.; Savé, R. Biel, C.; de Herralde, F.; Aranda, X. (2009): Late season root profile development of two contrasting vine rootstocks. In: Proc. 7th ISRR Symp. Root Res. Appl. (RootRAP). Vienna

Galinha, C.; Hofhuis, H.; Luijten, M.; Willemsen, V.; Blilou, I.; Heidstra, R. (2007): PLETHORA proteins as dose-dependent master regulators of Arabidopsis root development. Nature 449, 1053-1057

Goremykin, V.V.; Salamini, F.; Velasco, R.; Viola, R. (2008): Mitochondrial DNA of Vitis vinifera and the issue of rampant horizontal gene transfer. Molecular Biology and Evolution, 26(1):99-110

Gräfe, K.; Schmitt, L. (2020): The ABC transporter G subfamily in Arabidopsis thaliana. Journal of Experimental Botany. Vol. 72:1, 92-106

Gray, S.B.; Brady, S.M. (2016): Plant developmental responses to climate change. Developmental Biology 419, 64-77

Gutierrez, L.; Mongelard, G.; Floková, K.; Pacurar, D.I.; Novák, O.; Staswick, P.; Kowalczyk, M.; Pacurar, M.; Demailly, H.; Geiss, G. (2012): Auxin Controls Arabidopsis Adventitious Root Initiation by Regulating Jasmonic Acid Homeostasis. Plant Cell 24, 2515-2527

Houle, D.; Govindaraju, D.R.; Omholt, S. (2010): Phenomics: The next challenge. Nat. Rev. Genet. 11:855-866

Hund, A.; Fracheboud, Y.; Soldati, A.; Frascaroli, E.; Salvi, S.; Stamp, P. (2004): QTL controlling root and shoot traits of maize seedlings under cold stress. Theor. Appl. Genet. 3, 618-629

Jaillon, O.; Aury, J.M.; Noel, B. et al. (2007): The grapevine genome sequence suggests ancestral hexaploidization in major angiosperm phyla. Nature, 449(7161):463-467

Jansen, M.; Pinto, F.; Nagel, K.A.; van Dusschoten, D.; Fiorani, F.; Rascher, U.; Schneider, U.; Walter, A.; Schurr, U. (2014): Non-invasive phenotyping methodologies enable the accurate characterization of growth and performance of shoots and roots. In Genomics of Plant Genetic Resources (Tuberosa et al. eds.), pp. 173-206, Springer

Jeudy, C.; Adrian, M.; Baussard, C. et al. (2016): RhizoTubes as a new tool for high throughput imaging of plant root development and architecture: test, comparison with pot grown plants and validation. Plant Methods 12, 31.

Khan, M.A.; Gemenet, D.C.; Villordon, A. (2016): Root system architecture and Abiotic Stress Tolerance: Current Knowledge in Root and Tuber Crops. Front Plant Sci. 7, 1584

Kim, D.-Y.; Bovet, L.; Maeshima, M.; Martinoia, E.; Lee, Y. (2007): The ABC transporter AtPCR8 is a cadmium extrusion pump conferring heavy metal resistance. The Plant Journal. 50, 207-218

Kim, D.-Y.; Jin, J.-Y.; Alejandro, S.; Martinoia, E.; Lee, Y. (2010): Overexpression of AtABCG36 improves drought and salt stress resistance in *Arabidopsis*. Physiologia Plantarum. Vol. 139(2), 170-180

Kubo, M.; Furuta, K.; Demura, T.; Fukunda, H.; Liu, Y.-G.; Shibata, D.; Kakimoto, T. (2011): The CKH1/EER4 Gene Encoding a TAF12-Like Protein Negatively Regulates Cytokinin Sensitivity in *Arabidopsis thaliana*. Plant and Cell Physiology. Vol. 52:4, 629-637.

Laperche, A.; Devienne-Barret, F.; Maury, O.; le Gouis, J.; Ney, B. (2006): A simplified conceptual model of carbon/nitrogen functioning for QTL analysis of winter wheat adaptation to nitrogen deficiency. Theor. Appl. Genet. 113, 1131-1146

Lee, D.-K.; Ahn, J.H.; Song, S.-K.; Choi, Y.D.; Lee, J.S. (2003): Expression of a Expansin Gene is Correlated with Root Elongation in Soybean. Plant Physiology. Vol 131, 985-997

Li, S.W.; Xue, L.; Xu, S.; Feng, H.; An, L. (2009): Mediators, Genes and Signaling in Adventitious Rooting. The Botanical Review. 75, 230-247

Lischewski, S.; Muchow, A.; Guthörl, D.; Hause, B. (2015): Jasmonates act positively in adventitious root formation in petunia cuttings. BMC Plant Biol. 15:229

Nagek, K.A.; Kastenholz, B.; Jahnke, S.; van Dusschoten, D.; Aach, T.; Mühlich, M.; Truhn, D.; Scharr, H.; Terjung, S.; Walter, A.; Schurr, U. (2009): Temperature response of roots: impact on growth, root system architecture and implications for phenotyping. Functional Plant Biology, 36(11):947-959

Nagel, K.A.; Putz, A.; Gilmer, F.; Heinz, K.; Fischbach, A.; Pfeifer, J.; Faget, M.; Bloßfeld, S.; Ernst, M.; Dimaki, C.; Kastenholz, B.; Kleinert, A.-K.; Galinski, A.; Scharr, H.; Fiorani, F.; Schurr, U. (2012): GROWSCREEN-Rhizo is a novel phenotpying robot enabling simultaneous measurements of root and shoot growth for plants grown in soil-filled rhizotrons. Funct. Plant Biol. 39, 891-904

Peiró, R.; Jiménez, C.; Perpiñà, G.; Soler, J.X.; Gisbert, C. (2020): Evaluation of the genetic diversity and root architecture under osmotic stress of common grapevine rootstocks and clones. Scientia Horticulturae, Vol. 226, 109283

Rae, A.M.; Tricker, P.; Bunn, S.; Taylor, G. (2007): Adaptation of tree growth to elevated CO2: quantitative trait loci for biomass in Populus. New Phytol. 175, 59-69.

Rasmussen, A.; Hosseini, S.A.; Hajirezaei, M.-R.; Druege, U.; Geelen, D. (2015): Adventitious rooting declines with the vegetative to reproductive switch and involves a changed auxin homeostasis. J. Exp. Bot. 66, 1437–1452

Rauh, B.L.; Basten, C.; Buckler, E.S. (2002): Quantitative trait loci analysis of growth response to varying nitrogen sources in Arabidopsis thaliana. Theor. Appl. Genet. 104, 743-750

Ray, D.K.; West, P.C.; Clark, M.; Gerber, J.S.; Prishchepov, A.V.; Chatterjee, S. (2019): Climate change has likely already affected global food production. PLoS ONE 14(5): e0217148

Ribeiro, C.L.; Silva, C.M.; Drost, D.R.; Novaes, E.; Novaes, C.R.; Dervinis, C.; Kirst, M. (2016): Integration of genetic, genomic, and transcriptomic information identifies putative regulators of adventitious root formation in Populus. BMC Plant Biol. 16:66.

Rigal, A.; Yordanov, Y.S.; Perrone, I.; Karlberg, A.; Tisserant, E.; Bellini, C.; Busov, V.B.; Martin, F.; Kohler, A.; Bhalerao, R.; Legué, V. (2012): The AINTEGUMENTA LIKE1 Homeotic Transcription Factor PtAIL1 Controls the Formation of Adventitious Root Primordia in Poplar. Plant Physiology. Vol. 160, 1996-2006

Rist, F.; Herzog, K.; Mack, J.; Richter, R.; Steinhage, V.; Töpfer, R. (2018): High-precision Phenotyping of Grape Bunch Architecture Using Fast 3D Sensor and Automation. Sensors. 18, 763

Ruzicka, K.; Strader, L.C.; Bailly, A.; Yang, H.; Blakeslee, J.; Langowski, L.; Nejedlá, E.; Fujita, H.; Itoh, H.; Syono, K.; Hejátko, J.; Gray, W.M.; Martinoia, E.; Geisler, M.; Bartel, B.; Murphy, A.S.; Friml, J. (2010): Arabidopsis PIS1 encodes the ABCG37 transporter of auxinic compounds including the auxin precursor indole-3-butyric acid. Proc. Natl. Acad. Sci. 107(23):10749-53

Saez, A.; Robert, N.; Maktabi, M.H.; Schroeder, J.I.; Serrano, R.; Rodriguez, P.L. (2006): Enhancement of abscisic acid sensitivity and reduction of water consumption in Arabidopsis by combined inactivation of the protein phosphatases type 2C ABI1 and HAB1. Plant Physiol. 141(4):1389-99

Shin, R.; Burch, A.Y.; Huppert, K.A.; Tiwari, S.B.; Murphy, A.S.; Guilfoyle, T.J.; Schachtman, D.P (2007): The Arabidopsis transcription factor MYB77 modulates auxin signal transduction. Plant Cell. 19(8):2440-53

Smith, S.; De Smet, I. (2012): Root system architecture: Insights from Arabidopsis and cereal crops. Philos. Trans R. Soc. B Biol. Sci. 367, 1441-1452

Sun, J.; Sun, Y.; Imtiaz Ahmed, R.; Ren, A.; Xie, M. (2019): Research Progress on Plant RING Finger Proteins. Genes, 10(12), 973

Takeuchi, M.; Kegasa, T.; Watanabe, A.; Tamura, M.; Tsutsumi, Y. (2018): Expression analysis of transporter genes for screening candidate monolignol transporters using Arabidopsis thaliana cell suspensions during tracheary element differentiation. Journal of Plant Research 131, 297-305

Tandonnet, J.P.; Marguerit, E.; Cookson, S.J.; Ollat, N. (2018): Genetic architecture of aerial root traits in field-grown grafted grapevines is largely independent. Theor. Appl. Genet. 131:903-915

Tracy, S.R.; Nagel, K.A.; Postma, J.A.; Fassbender, H.; Wasson, A.; Watt, M. (2020): Crop Improvement from Phenotyping Roots: Highlights Reveal Expanding Opportunities. Trends in Plant Science. Vol. 25, No. 1

Uehara, T.; Okushima, Y.; Mimura, T.; Tasaka, M.; Fukaki, H. (2008): Domain II Mutations in CRANE/IAA18 Suppress Lateral Root Formation and Affect Shoot Development in Arabidopsis thaliana. Plant and Cell Physiol. Vol. 49:7, 1025-1038

Wen, J.; Lease, K.A.; Walker, J.C. (2004): DVL, a novel class of small polypeptides: overexpression alters Arabidopsis development. Plant J. 37(5):668-77

Yates, A.D.; Achuthan, P.; Akanni, W.; Allen, J.; Allen, J.; Alvarez-Jarreta, J.; Ridwan Amode, M.; Armean, I.M.; Azov, A.G.; Bennett, R. et al. (2020): Ensembl 2020. Nucleic Acids Research. Vol. 48:1, 682-688

Yildirim, K.; Yagci, A.; Sucu, S.; Tunc, S. (2018): Response of grapevine rootstocks to drought through altered root system architecture and root transcriptomic regulations. Plant Physiology and Biochemistry 256-268

Zang, U.; Goisser, M.; Häberle, K.-H.; Matyssek, R.; Matzner, E.; Borken, W. (2014): Effects of drought stress on photosynthesis, rhizosphere respiration, and fine-root characteristics of beech saplings: A rhizotron field study. J. Plant Nutr. Soil Sci. 177, 168-177

Software

Bardecode: Softek Software, Sheffield, UK

ImageJ:

ImageJ 1.5r, Wayne Rasband, National Institutes of Health, USA. http://imagej.nih.gov/ij

MapQTL6:

Van Ooijen, J.W. (2009): MapQTL 6, Software for the mapping of quantitative trait loci in experimental populations of diploid species. Kyazma BV; Wageningen, Netherlands

R Studio:

R Core Team (2020): R: A language and environment for statistical computing. R Foundation for Statistical Computing, Vienna, Austria. URL https://www.R-project.org/

- **Brooks, M.E.; Kristensen, K.; van Benthem, K.J.; Magnusson, A.; Berg, C.W.; Nielsen, A.; Skaug, H.J.; Maechler, M.; Bolker, B.M. (2017):** glmmTMB Balances Speed and Flexibility Among Packages for Zero-inflated Generalized Linear Mixed Modeling. The R Journal. 9(2), 378-400.
- **Fox, J.; Weisberg, S. (2019):** An R Companion to Applied Regression, Third edition. Sage, Thousand Oaks CA.
- **Kassambara, A. (2020):** ggpubr: 'ggplot2' Based Publication Ready Plots. R package version 0.4.0
- **Wickham, H. (2016):** *ggplot2:* Elegant Graphics for Data Analysis. Springer-Verlag, New York. ISBN 978-3-319-24277-4, https://ggplot2.tidyverse.org.
- **Zeileis, A.; Hothorn, T. (2002):** Diagnostics Checking in Regression Relationships. R News, 2(3), 7-10

WinRHIZO:

WinRHIZO Pro Regent Instruments Inc., 146 QC, Canada

Internet Sources:

Datenbank EnsemblPlants: http://plants.ensembl.org/index.html

4. Chapter 4: Grapevine Root Development in Field Trial

4.1. Introduction

Most phenotyping studies considering grapevine root systems were conducted under controlled environmental conditions e.g. in pot experiments (Vršič et al. 2016), with help of RhizoTubes (Jeudy et al. 2016), rhizotrons (Fort and Fraga, 2017), or X-ray µCT scanners (Schmitz et al. 2021). A controlled environment provides higher probabilities to obtain reproducible phenotypes and data than field phenotyping. However, phenotypic performance needs to meet the demands of agricultural field practices, especially for root related traits exhibited in later developmental stages and under real environmental conditions (Watt et al. 2013).

In general, traditional methods for root phenotyping under field conditions are excavations, soil coring, and minirhizotron tubes. To investigate grapevine roots, several approaches have been made regarding root phenotyping. In the field and with help of a mini excavator, Soar and Loveys (2007) extracted soil cores with roots at various sites and distances from the grapevine trunk to observe vertical distribution of roots in the soil. Besides the use of excavators, trenching is another field approach used for observation of grapevine root systems. A one-meter-deep trench at one side of the vine row enabled counting of roots and determination of root distribution (Battista et al. 2016). Minirhizotrons were utilized for observation of spatial root distribution in field as well as in pots demonstrating the difficult nature of root measurements due to high variation (Linsenmeier et al. 2010). First QTLs related to grapevine root systems in the field were identified by Tandonnet et al. (2018) by investigation of field-grown grafted grapevines. Besides correlations between the measured root traits, several QTLs could be revealed explaining approximately 20% of the phenotypic variance.

All field phenotyping methods are highly time-consuming and require material costs for equipment as well as manpower. Accessing root systems is even more difficult for perennial species like grapevines. As greenhouse experiments might be poor predictors for crops' field performance and yield, shifting to reliable methods in field trialing will be a future opportunity for crop breeding. Therefore, the aim of this study was to set up a pilot field trial for observation of root systems of grapevine woody cuttings grown in the field in a preferably non-destructive manner. In addition, phenotypic measurements of individuals of a grapevine mapping population should be used for QTL mapping and identification of genomic regions related to root system growth and development in field-grown plants.

4.2. Material and Methods

4.2.1. Plant Material

136 genotypes of the F1 progeny descending from a cross between ‘V3125’ (‘Schiava Grossa’ × ‘Riesling’) and rootstock cultivar ‘Börner’ (*V. riparia* Gm183 × *V. cinerea* Arnold) (‘VB2001’) were analysed in this field trial together with the parental genotypes ‘V3125’ and ‘Börner’ and six reference genotypes regarding their root system development. Therefore, dormant, two-bud woody cuttings were collected during winter prune and subsequently sterilized with a 0.5% solution of Chinosol® (Riede de Haen AG, Seelze, Germany). Afterwards cuttings were stored at 5°C until they were utilized for experiments. Table S2 gives a list of genotypes and number of replicates planted in experimental years 2018 and 2019 including genotypes of the mapping population ‘VB2001’, the parental genotypes ‘V3125’ and ‘Börner’, rootstock cultivars ‘5C Geisenheim’, ‘1103 Paulsen’, ‘Couderc 3309’, ‘Kober 125 AA’ and ‘Ramsey’ as well as the scion cultivar ‘Calardis Musqué’.

4.2.2. Experimental Set Up

The field trial was located in Weisenheim am Sand (see figure 26). This location is known for sandy soil conditions and previous utilization for vine nursery purposes demonstrated that grapevine root systems could be removed from this soil relatively easy, with low disturbance and nearly no root loss.

Figure 26: Location of the field trail in Weisenheim am Sand. Field area for the experiment is indicated as red triangle (Google Maps, 05.03.2020)

In order to facilitate root system excavation, the field was prepared by building up three dams. The dams were 80 cm (2018) or 60 cm (2019) high and 50 cm wide (see figure 27A) and were covered with foil. In addition, dams were equipped with irrigation tubes at the soil surface (see figure 27C). Dams were watered for 6 hours immediately after being formed and subsequently covered with foil for sun protection. One day before planting, dams were again irrigated for 6 hours.

*Figure 27: Setup of dams in the field, **A**: Section scheme of the soil dam with dimensions, irrigation tube, and planted woody cutting; **B**: Soil dams with grapevines four weeks before excavation; **C**: Irrigation tubes on the dam.*

Woody cuttings of the mapping population 'VB2001' were pre-planted into Jiffy pellets (Jiffy-7 Peat Pellets, Jiffy Products International BV, Zwijndrecht, Netherlands) in the green house for eight weeks until the shoots were at least 10 cm long. Afterwards, they were planted randomized into the field. With help of a bulb planter for digging planting holes along the dams, woody cuttings could be placed into the soil dams. Within the field growing period (five months in 2018 and four months in 2019), plants were watered five times for 6 hours each time. Foil was removed from the dams 20 days (2018) and one day (2019) before excavation.

Leaves were removed and leafless shoots were collected within two days before excavation (see figure 28A). For excavation of the root systems, a mini-excavator (Kubota, Zweibrücken, Germany) dug out the six months old plant samples exposing their root systems. The excavator was digging from the long and short side of the dams and shaking of the shovel promoted loosening of the soil from the root systems (see figure 28B and C). Root system samples were collected and cart off for phenotypic measurements.

*Figure 28: Excavation of grapevine root systems, **A**: Soil dams with leafless shoots one day before excavation; **B**: Mini-excavator digging underneath the dam and loosen the soil; **C**: root systems can be pulled out of the soil.*

Collected root samples were brought to Hochschule Geisenheim University for image acquisition and phenotypic measurements. Whole root systems were photographed with a single-lens reflex camera. Afterwards, the following traits were measured manually: Diameter of the woody cutting (WCD), diameter of the thickest root (RD), length of the longest root (RL), considered as maximal rooting depth, and number of adventitious roots with a diameter > 1 mm (RN). Shoots and roots were subsequently dried in a drying chamber at 60°C to a constant weight to determine shoot dry weight (SDW) and root dry weight (RDW) with a fine balance (Sartorius 9391/l).

Images of root systems of year 2019 were divided into 10 cm depth sections and each section was analysed with WinRHIZO software (Pro 2019, Regent Instruments Inc., Canada) in order to measure the root area per depth section (RA) based on pixel colour. WinRHIZO settings including defined colour classes are given in table S3.

Table 11: List of traits obtained in field trial with abbreviations and descriptions.

Trait	Abbreviation	Unit	Description
Root dry weight	RDW	g	Roots were dried and weighted with a fine scale
Maximal root length	RL	cm	Length of the longest root indicating the maximal rooting depth
Root Number	RN		Number of adventitious roots with a diameter > 1 mm
Maximal root diameter	RD	mm	Diameter of the thickest root measured with a caliper
Shoot dry weight	SDW	g	Leafless shoots were dried and weighted with a fine scale
Woody cutting diameter	WCD	mm	Woody cutting diameter measured with a caliper
Root area	RA	cm^2	Area of the root system was measured with WinRHIZO based on images and pixel colour and for each depth section

4.2.3. Statistical Analysis

All measured root and shoot related traits were statistically analysed with R Studio (Version 3.5.1; R Core Team 2020). Differences between genotypes were analysed by use of package ‘stats’ and applying non-parametric Kruskal-Wallis test or ANOVA was performed in case assumptions of variance homogeneity and normal distribution were met. Variance homogeneity was verified with Levene’s test using ‘car’ package (Fox and Weisberg, 2019). Normal distribution of residuals was confirmed by Shapiro-Wilk test. Tukey HSD post-hoc test was used with significance level set at 0.05 ($p < 0.05$) by utilizing packages ‘emmeans’ (Lenth, 2020) and ‘multcomp’ (Hothorn et al. 2008), followed by visualization using ‘ggplot2’ package (Wickham, 2016).

Population data was analysed by statistical modelling. Generalized linear mixed effect models were fitted for all measured root traits and shoot dry weight with 'glmmTMB' package (Brooks et al. 2017). In all models, genotype was included as random effect, while woody cutting diameter and experimental year were included as fixed effects. Model diagnostics for generalized linear mixed effect models were performed by plotting Pearson residuals versus fitted values to inspect variance homogeneity (see figure S14).

Principal component analysis was performed with extracted best linear unbiased prediction values (BLUP) by using R packages 'FactoMineR' (Lê et al. 2008) and 'factoextra' (Kassambara and Mundt, 2020). Pearson correlation coefficients between measured traits were calculated with 'Hmics' package (Harrell, 2020) on individual values of 'VB2001' F1 genotypes, parental genotypes 'V3125' and 'Börner' and cultivars '5C Geisenheim', 'Gloire de Montpellier', 'Villard Blanc', '1103 Paulsen', 'Couderc 3309', 'Calardis Musqué', 'Kober 125 AA', and 'Ramsey'.

4.2.4. QTL Mapping and *in silico* Candidate Gene Analysis

Package 'lme4' (Bates et al. 2015) was utilized to extract best linear unbiased prediction estimates (BLUP) for each genotype. QTL mapping was carried out with BLUP values and the consensus map of the population 'VB2001' by Fechter et al. (2014) based on 195 F1 individuals. The genetic map is illustrated in figure S12. QTL detection was performed with MapQTL 6 (MapQTL 6.0; Van Ooijen 2009) using interval mapping. The significant LOD threshold was calculated with α = 0.05 (5 %) for each linkage group through 1000 permutations. Additionally, Kruskal-Wallis test was performed to further verify significance of genomic regions detected by interval mapping.

For *in silico* candidate gene analysis, the Ensembl online platform (Yates et al. 2020, http://plants.ensembl.org/index.html) was utilized by searching for putative candidate genes involved in processes of root growth and development within the identified QTL region with the sequence of Pinot Noir PN40024 12X v.2 (GENOSCOPE, CRIBI Consortium VIGNA and IGA; Jaillon et al. 2007; Goremykin et al. 2008). Candidate gene analysis was conducted on the genomic region on chromosome 1 between 632.258 - 4.630.078 Mb, given by LOD_{max}±1 confidence interval between SSR marker 'VMC4f8' and 'UDV_055b'.

4.3. Results

4.3.1. Comparison of cultivars

Measured plant traits of analysed cultivars in experimental year 2019 are presented in figure 29. Comparing all cultivars with each other, revealed significant differences in root dry weight (Kruskal-Wallis: H(7) = 27.31; p = 0.00029), maximal root length (Kruskal-Wallis: H(7) = 32.07; p = 3.935 e^{-5}), adventitious root number (ANOVA: F(7, 68) = 10.82; p = 4.39 e^{-9}), maximal root

diameter (ANOVA: F(7, 68) = 1.91; p = 0.08), shoot dry weight (Kruskal-Wallis: H(7) = 28.22; p = 0.00021), and woody cutting diameter (Kruskal-Wallis: H(7) = 20.75; p = 0.0042). No significant difference was observed between the population parents ‘V3125’ and ‘Börner’ in any trait.

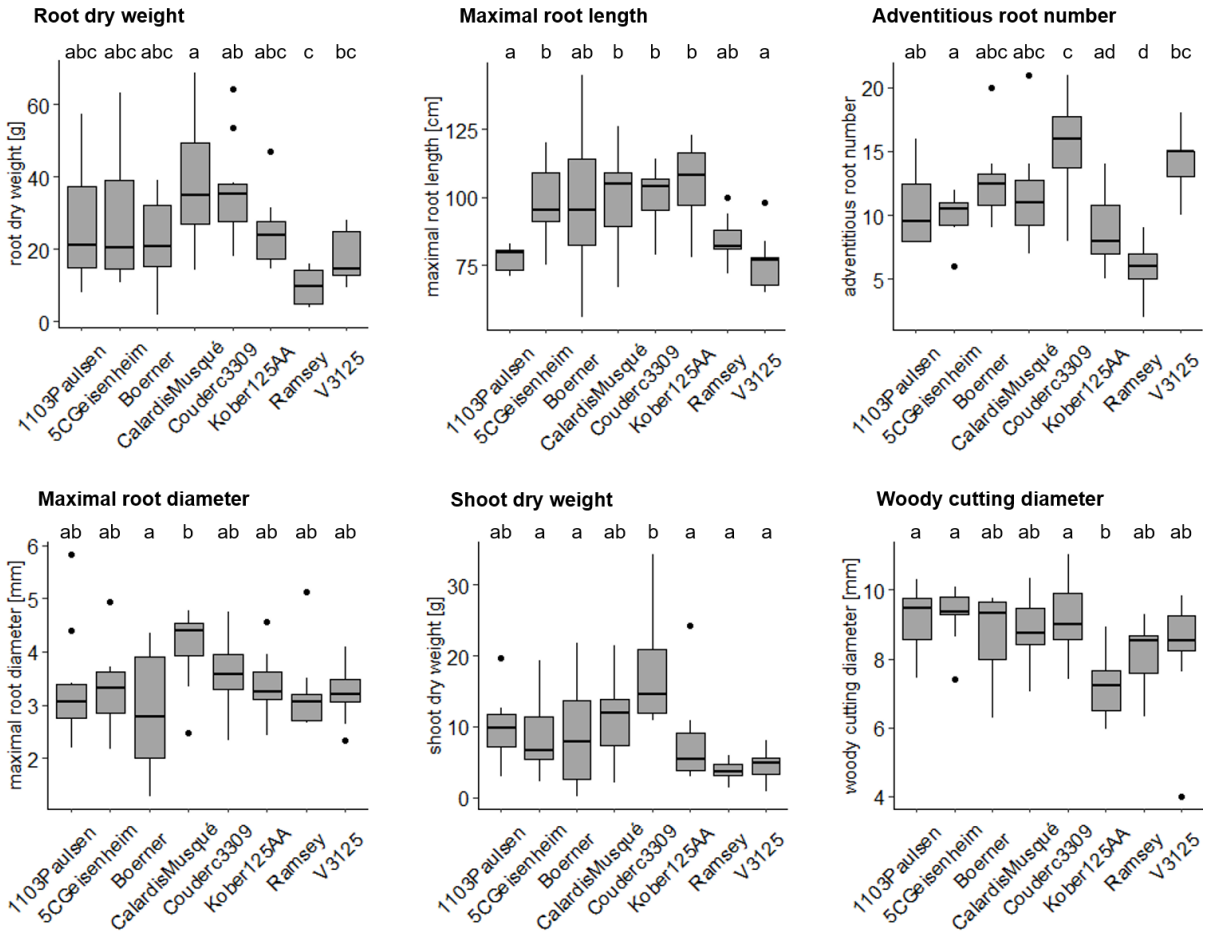

Figure 29: Boxplots indicate the median and quartiles for every measured trait of cultivars ‘1103 Paulsen’ (n = 10), ‘5C Geisenheim’ (n = 10), ‘Börner’ (n = 8), ‘Calardis Musqué’ (n = 10), ‘Couderc 3309’ (n = 10), ‘Kober 125AA’ (n = 10), ‘Ramsey’ (n = 9), and ‘V3125’ (n = 9). Different letters indicate significant differences at p < 0.05 by Tukey HSD post-hoc test.

To further investigate phenotypic differences between the cultivars, root growth was analyzed per depth section (figure 30 A). Therefore, root area was calculated based on images every 10 cm in order to map root growth patterns and compare the cultivars (see example in figure 30 A). Figure 30 B shows the resulting depth diagram of the analyzed cultivars including the population parents ‘V3125’ and ‘Börner’. Root areas of all cultivars were compared on each depth section and results are presented in table 12. ‘V3125’ showed a significantly greater root area compared to ‘Börner’ in the first two depth sections in 17 and 27 cm soil depth. Both cultivars did not differ significantly in deeper soil sections. ‘Couderc 3309’ and ‘Calardis

Musqué' showed the highest root area, especially from a soil depth of 70 cm and deeper. Smallest root area in the first 70 cm was measured for 'Ramsey' even though 'V3125' showed the least rooting depth.

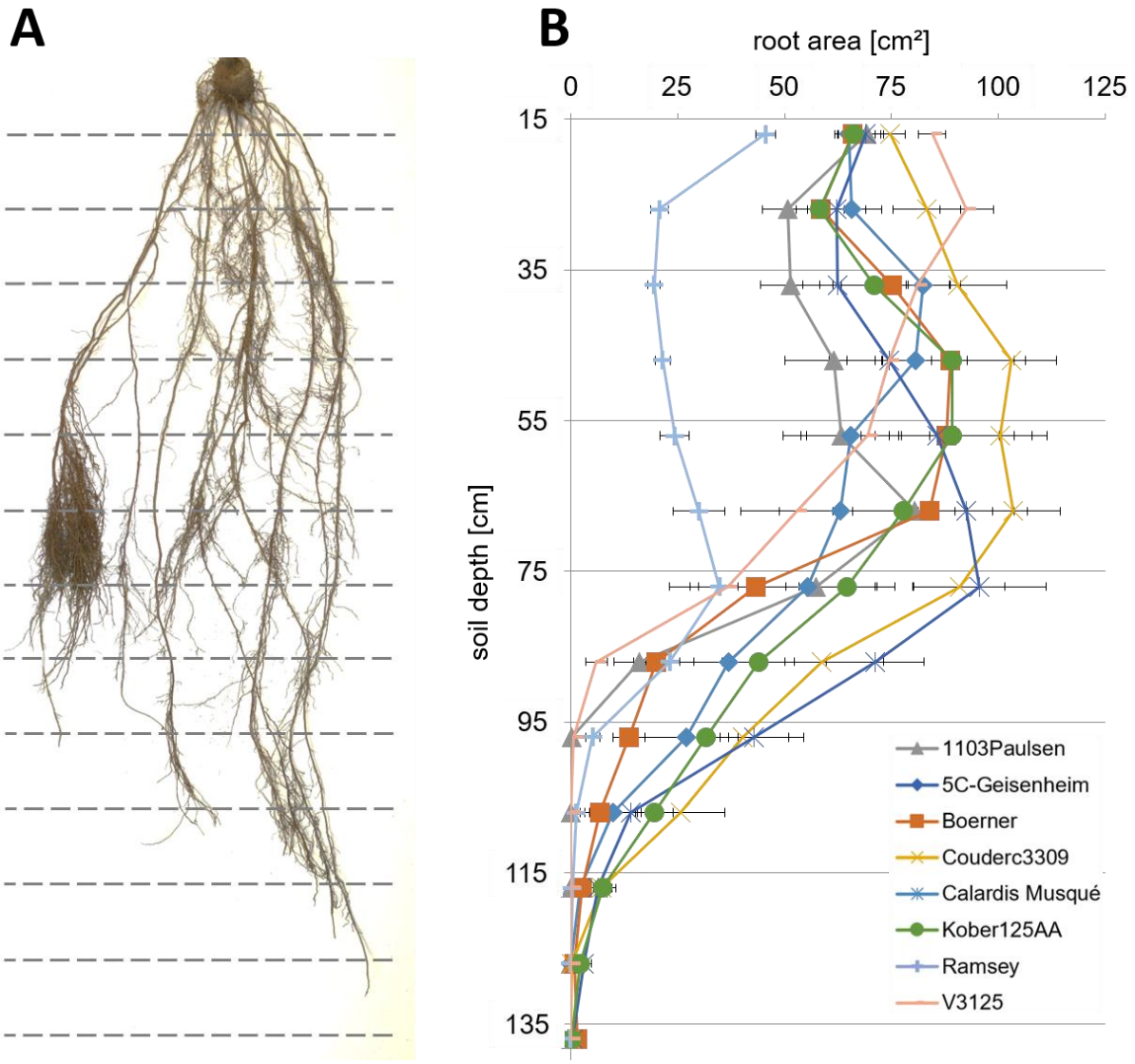

*Figure 30: **A**: Root system images were divided into depth sections every 10 cm of soil depth. **B**: Root depth profile showing root area means of every section and each cultivar: '1103 Paulsen' (n = 10), '5C Geisenheim' (n = 10), 'Börner' (n = 8), 'Calardis Musqué' (n = 10), 'Couderc 3309' (n = 10), 'Kober 125AA' (n = 10), 'Ramsey' (n = 9), and 'V3125' (n = 9). Standard errors are given as error bars.*

Table 12: Root area comparison between all cultivars at the soil depth sections. Different letters indicate significant differences at significance level α = 0.05 (Tukey HSD).

Soil depth [cm]	1103 Paulsen	5C Geisenheim	Börner	Calardis Musqué	Couderc 3309	Kober 125AA	Ramsey	V3125	Statistical test ANOVA / Kruskal-Wallis
17	a	a	a	a	ab	a	c	b	H(7) = 35.46; p = 9.164e^{-06}
27	a	abc	ab	ab	bc	ab	d	c	H(7) = 39.62; p = 1.489e^{-06}
37	ab	ac	ac	ac	c	ac	b	ac	H(7) = 32.98; p = 2.675^{e-05}
47	ab	a	a	a	a	a	b	a	H(7) = 26.86; p = 0.0004
57	ab	ab	a	a	a	a	b	ab	F(7,69) = 3.00; p = 0.0083
67	ab	ab	ab	a	a	ab	b	ab	H(7) = 19.57; p = 0.0066
77	ab	ab	ab	a	ab	ab	b	b	H(7) = 18.53; p = 0.0098
87	a	abc	ab	c	bc	abc	ab	a	H(7) = 34.91; p = 1.165e^{-05}
97	a	ab	ab	b	b	ab	a	a	H(7) = 41.22; p = 7.355e^{-07}
107	a	ab	ab	ab	b	ab	a	a	H(7) = 37.17; p = 4.358e^{-06}
117	a	a	a	a	a	a	a	a	H(7) = 28.54; p = 0.0002
127	a	a	a	a	a	a	a	a	H(7) = 19.04; p = 0.0081
137	a	a	a	a	a	a	a	a	H(7) = 11.42; p = 0.1214

4.3.2. Root System Determination of Mapping Population 'VB2001'

A Principal component analysis (PCA) was performed with BLUP values for all traits measured during the field trial of mapping population 'VB2001' and results are shown in figure 31. Variation was explained by five principal components. The first principal component (Dimension 1) explained 45.3%, the second 19%, and the third 16.8% of the variation (Figure 31 A). The first dimension was mostly explained by root dry weight (33.7%) and shoot dry weight (27.5%) (Figure 31 C). The second dimension is mostly defined by root number (59.9%) and root diameter (35.2%). Contributions to all dimensions are given in figure S3.

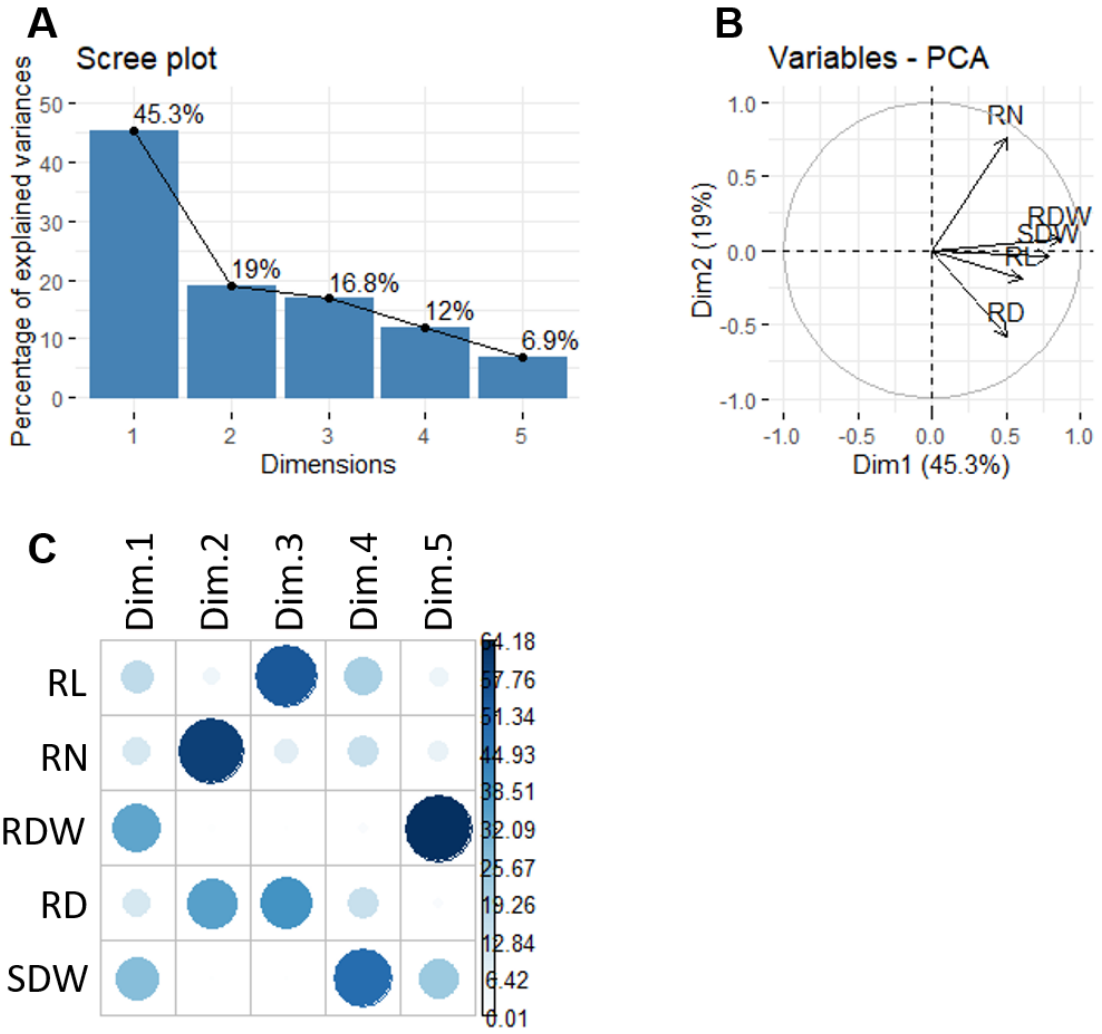

*Figure 31: Principal component analysis (PCA) of field study traits of mapping population 'VB2001'. **A**: Proportion of variance explained by each eigenvalue; **B**: Distribution of the phenotypic traits on the plan defined by the two first components PC1 (Dimension 1) and PC2 (Dimension 2); **C**: Contributions of variables accounting for the variability in the principal components (dimensions) expressed in percentage*

Table 13 presents Pearson correlation coefficients between measured phenotypic traits based on individual values of all analyzed genotypes (n = 767). Significant correlations ($p < 0.05$) are

highlighted in bold. Highest correlations were found between root and shoot dry weight (r = 0.84), woody cutting diameter and shoot dry weight (r = 0.73), root dry weight and maximal root diameter (r = 0.72), root dry weight and woody cutting diameter (r = 0.72), and maximal root diameter and shoot dry weight (r = 0.72).

Table 13: Pearson correlation coefficients among measured phenotypic traits root dry weight (RDW), maximal root length (RL), number of adventitious roots with diameter > 1 mm (RN), maximal root diameter (RD), shoot dry weight (SDW), and woody cutting diameter (WCD). Significant correlations are highlighted in bold.

Traits	RDW	RL	RN	RD	SDW	WCD
RDW	1					
RL	**0.67**	1				
RN	**0.16**	0.003	1			
RD	**0.72**	**0.67**	**-0.11**	1		
SDW	**0.84**	**0.62**	**0.08**	**0.72**	1	
WCD	**0.72**	**0.57**	**0.14**	**0.65**	**0.73**	1

Generalized linear mixed models showed a significant positive effect of woody cutting diameter on all measured traits as visualized in figure 32. Effects of the experimental year on phenotypic traits are shown in figure 33. Root dry weight, maximal root length, maximal root diameter and shoot dry weight were significantly higher in 2018 compared to 2019. Only the number of adventitious roots with diameter > 1 mm was significantly higher in 2019.

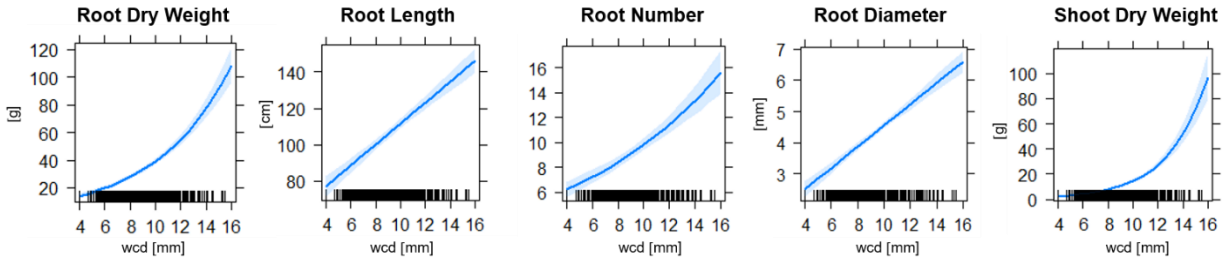

Figure 32: Effect of woody cutting diameter (wcd) on root dry weight, maximal root length, number of adventitious roots with diameter > 1 mm, maximal root diameter and shoot dry weight in mapping population 'VB2001'.

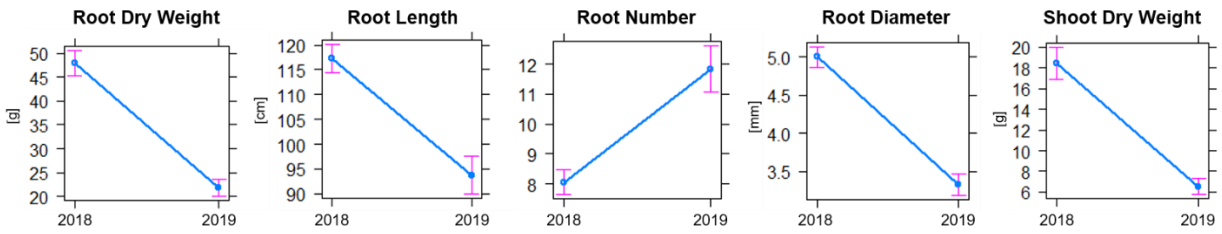

Figure 33: Effect of experimental year on root dry weight, maximal root length, number of adventitious roots with diameter > 1 mm, maximal root diameter and shoot dry weight in mapping population 'VB2001'.

Both, woody cutting diameter and experimental year, were included into statistical modelling as fixed effects. Genotype was included as random effect. By extracting the BLUP (best linear unbiased prediction) value, the best predictive value for each genotype was generated and variance resulting from woody cutting diameter and experimental year was reduced. Histograms in figure 34 show the distribution of phenotypic traits of mapping population 'VB2001'. The parental genotypes 'V3125' and 'Börner' exhibit similar rankings within the F1 population genotypes for adventitious root number and maximal root diameter. A greater distance was observed between the parental genotypes for maximal root length, root dry weight and shoot dry weight. The rankings of all individual F1 genotypes of the population are given in figure S16-18.

QTL mapping with BLUP values identified four QTLs for three traits on two linkage groups as presented in table 14. The QTL position (cM) derived from the corresponding LOD_{max} (logarithm of the odds) value. The confidence interval (cM) is given as the interval of LOD_{max} ± 1. The permutation test produced the given LOD thresholds of linkage group and genome wide. Interval mapping revealed three QTLs on linkage group 1 for root dry weight, maximal root length and shoot dry weight with one linked marker for shoot dry weight but all three QTL positions confirmed by Kruskal-Wallis mapping. Explained variance ranged between 13 % and 15.2 %. Another QTL for root dry weight was identified on linkage group 14 confirmed by Kruskal-Wallis mapping and explained variance of 13.9%. No QTLs could be identified for adventitious root number and maximal root diameter. Figure 35 gives a schematic figure of physical positions of QTLs identified my interval mapping.

As three QTLs were found on linkage group 1 around the same genomic region, this region was considered for *in silico* candidate gene analysis. Twelve selected putative candidate genes are listed in table 15, presenting the gene names, physical positions, and their function or homologs indicating potential functions involved in root growth and development.

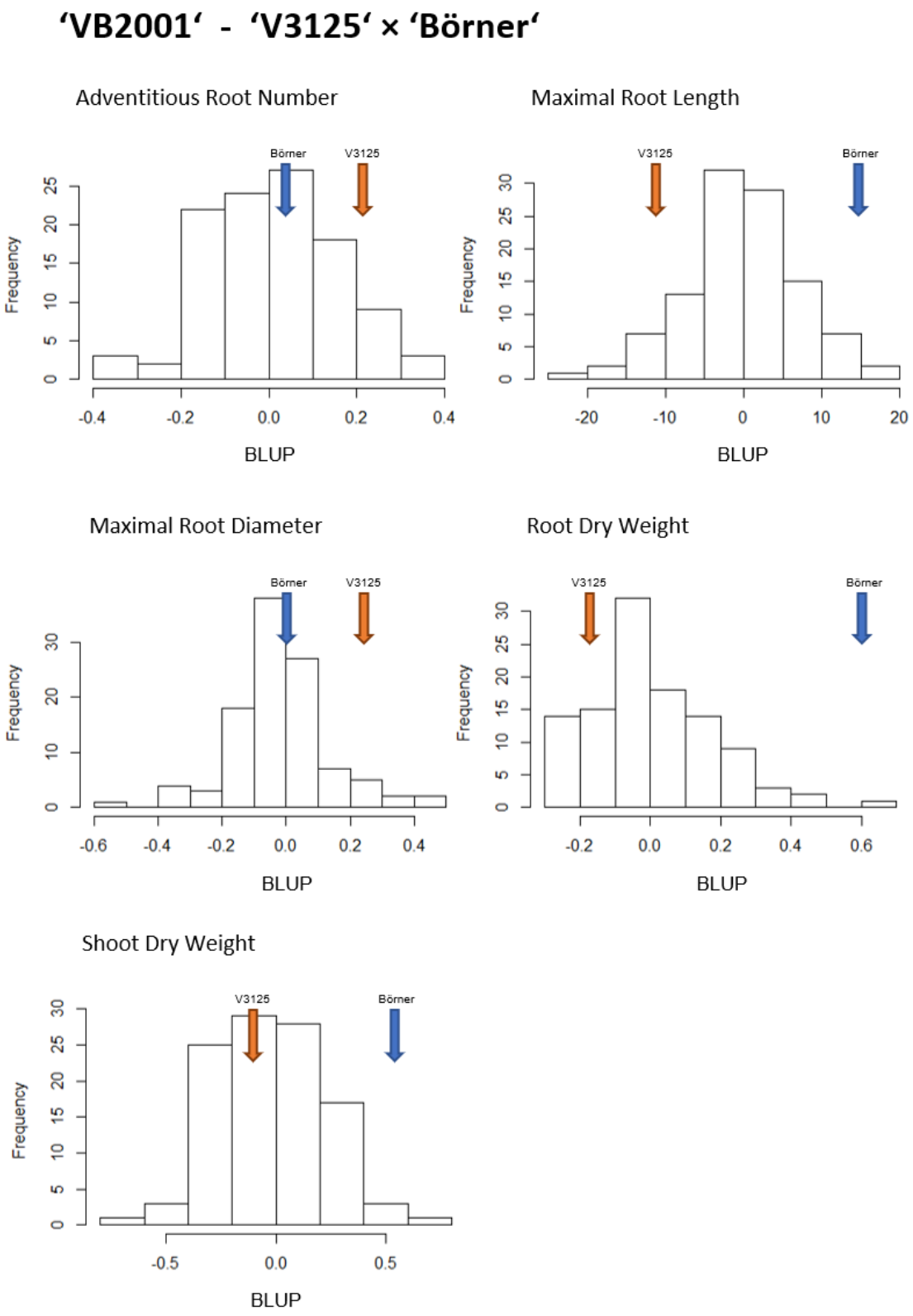

Figure 34: Distribution of measured traits in mapping population 'VB2001': Adventitious root number, maximal root length, maximal root diameter, root dry weight, and shoot dry weight. Parental values are indicated by arrows. Phenotypic data is given as best linear unbiased prediction estimates (BLUP) derived from the respective statistical model. Frequency is the number of genotypes.

*Table 14: Results of QTL mapping with QTLs identified by interval mapping for root traits and leaf area from mapping population 'VB2001'. Kruskal-Wallis significance levels are given as asterisks *** < 0.01; **** < 0.005; ***** < 0.001.*

Trait	LG	QTL position (cM)	Confidence Interval ± 1 LOD in cM	LOD max	LOD threshold (LG)	LOD threshold genome wide	linked marker Interval Mapping	Kruskal-Wallis Test	explained phenotypic variance (%)
root dry weight	01	11.0	7.5 - 14.6	3.8	3.2	4.3	-	VMC4f9.2 ***	15.2
	14	4.0	0 - 10.1	3.44	3.0		-	GF14-05_97 ****	13.9
maximal root length	01	8.5	0 - 17.4	3.21	3.0	4.4	-	VCHr01a_224 ***	13.0
adventitious root number	-	-	-	-	-	-	-	-	-
maximal root diameter	-	-	-	-	-	-	-	-	-
shoot dry weight	01	13.3	10.2 - 17.4	3.45	3.0	4.4	VMC4f9.2	VMC4f9.2 ***	14.0

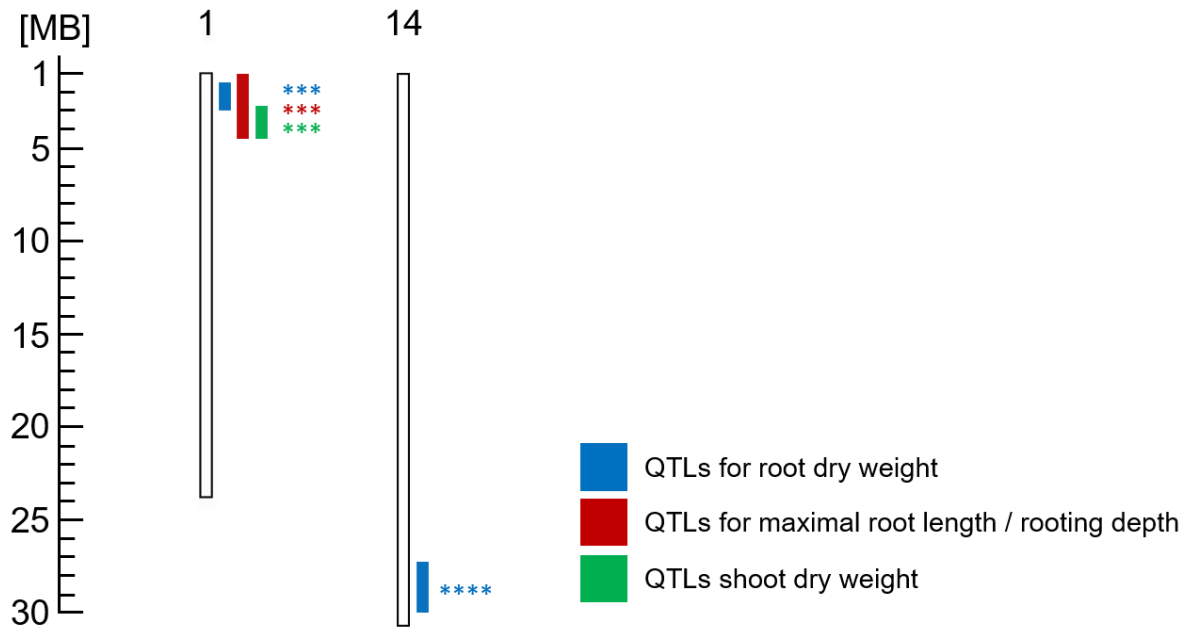

Figure 35: Schematic illustration of physical QTL positions based on LOD max. ±1 (in PN40024 12X v.2) identified via interval mapping of field trial phenotypic data of mapping population 'VB2001': root dry weight, maximal root length, and shoot dry weight. Significance confirmation by Kruskal-Wallis mapping are indicated with asterisks.

Table 15: List of putative candidate genes found within the identified QTL region on linkage group 1 (EnsemblPlants, UniProtKB) based on sequences from PN40024 12X v.2

Gene	Gene location	Protein / Homologs / Function
VIT_01s0011g01050	924.701 - 929.880 Mb	Peroxidase enzyme
VIT_01s0011g01650	1.495.867 - 1.499.101 Mb	Peptidylprolyl isomerase Homolog (WGA Coverage 98.95) in *A. thaliana:* Peptidyl-prolyl cis/trans isomerase Pin1At regulates root gravitropism
VIT_01s0011g02160	839.802 - 883.645 Mb	Uncharacterized Protein in Vitis. Homolog (WGA Coverage 99.90) in *A. thaliana*: Zinc finger C3HC4 type RING finger family protein (At5G23110): Involved in root growth and development.
VIT_01s0011g02990	2.677.653 - 2.684.941 Mb	Uncharacterized Protein in Vitis. Homolog (WGA Coverage 86.75) in *A. thaliana*: SOG1 (At1G25580): SUPRESSOR OF GAMMA RESPONSE 1 maintains genome integrity for proper cell division during the development of lateral root primordium
VIT_01s0011g03070	2.751.566 - 2.753.036 Mb	Uncharacterized Protein in Vitis. Homolog (WGA Coverage 90.94) in *A. thaliana:* AP2/ERF and B3 domain-containing transcription factor ARF14. Probably acts as a transcriptional activator. Binds to the GCC-box pathogenesis-related promoter element. May be involved in the regulation of gene expression by stress factors and by components of stress signal transduction pathways
VIT_01s0011g03110	2.781.518 - 2.783.517 Mb	MYB-like putative GARP-type transcription factor. Homologs (WGA Coverage 81.38, 96.13) in *A. thaliana*: HHO3 (At1G25550), HHO2 (At1G68670), transcription factors involved in phosphate signaling in roots
VIT_01s0011g03470	3.142.869 - 3.144.296 Mb	AP2/ERF domain-containing protein Homologs (WGA Coverage 60.26, 60.56) in *A. thaliana*: Ethylene-responsive transcription factors: ERF116 (At1G25470), ERF118 (At1G68550)
VIT_01s0011g03730	3.375.041 - 3.376.409 Mb	Uncharacterized Protein in Vitis. Homolog (WGA Coverage 64.31) in *A. thaliana*: Transcription factor MYB62: Involved in gibberellic acid (GA) biosynthesis and signaling. Modulates root architecture and phosphatase activity
VIT_01s0011g04070	3.720.067 - 3.721.588 Mb	Auxin responsive protein. Aux/IAA proteins are short-lived transcriptional factors that function as repressors of early auxin response genes at low auxin concentrations. Involved in auxin-activated signaling pathway and regulation of transcription. Homolog (WGA Coverage 80.19, 76.37) in *A. thaliana*: IAA34, IAA32; Aux/IAA proteins interacting with auxin response factors (ARFs) and bind to the auxin-responsive promoter element (AuxRE).

Gene	Gene location	Protein / Homologs / Function
VIT_01s0011g04760	4.330.010 - 4.331.639 Mb	MYBC2-L1 protein
VIT_01s0011g04860	4.474.942 - 4.478.329 Mb	Auxin efflux carrier component, transmembrane transporter activity. Homologs (GOC-Score 100) in *A. thaliana*: PIN7 (At1G23080), PIN3 (At1G70940), PIN4 (At2g01420): auxin-activated signaling pathway

4.4. Discussion

4.4.1. Root Phenotyping of Field Grown Root Systems

An excavation experiment following this concept was performed at this location for the first time. Based on our observations, approximately 90 - 95 % of the root system could be extracted in that way without demolishing. This was mostly due to the sandy soil conditions allowing the extraction of whole root system without disturbance. However, some individuals in experiment of 2018 rooted too deep to be reached at their maximum depth with the excavator shovel. Therefore, plants of 2019 were excavated one month earlier. As the duration of the experiment was 4 weeks longer in 2018, it might be reasonable why measured phenotypic traits are increased compared to experimental year 2019. Interestingly, this is not applicable to the number of adventitious roots. This indicates a higher number of adventitious roots in earlier developmental stages and decline of adventitious root number, when root growth is further advanced. Whereas young roots absorb most of the water, primarily through root hairs and other epidermal (outer layer) cells, suberized ("woody") roots take up water at lower but constant rate (Hellman, 2003).

Comparing the reference cultivars revealed several significant differences in the measured root traits. 'Ramsey' showing the lowest number of roots was in accordance with earlier observations (Southey, 1992). The lowest root length and therefore shallow root systems were exhibited by '1103 Paulsen' and 'V3125'. Interestingly, '1103 Paulsen' was described as drought tolerant rootstocks in several earlier studies (Sommer, 2009; Ramteke and Karibasappa 2005). Regarding the mapping population parents, no significant differences were found between 'V3125' and 'Börner' when comparing their mean values. But using their depth profiles detected a significantly higher root area of 'V3125' within the first 27 cm of soil. The utilization of depth profiles enlarged the opportunities to identify root growth differences between genotypes. In addition, it has been documented in other crops that depth specific root development influences the whole crop. For instance, root length density in the upper active root zone area enhanced the uptake of water and nutrients of chickpea plants grown under water deficit conditions (Varshney et al. 2011).

Highest correlation between phenotypic traits was observed between root and shoot dry weight ($r = 0.84$), whereas correlation between aerial and root biomass in earlier studies was $r = 0.41$ in grafted soil-grown grapevines (Tandonnet et al. 2018) and $r = 0.66$ in poplar woody cuttings (Sun et al. 2019). Number of adventitious roots was not strongly correlated to the other measured traits exhibiting values of $r = 0.003$ to 0.16. Interestingly, these findings confirm lower correlations between adventitious root number and aerial biomass ($r = 0.11$) as well as root biomass ($r = 0.30$) revealed by Tandonnet et al. (2018). Similarly, the distribution of the

phenotypic traits defined by the first two dimensions also indicates a rather independent role of adventitious root number from root biomass.

4.4.2. QTL Mapping and *in silico* Candidate Gene Analysis

In general, root formation and root system development are influenced by several environmental factors as well as endogenous factors. At the genetic level, root system development is believed to be under the regulation of several genes and different genomic loci. In poplar, another woody species, a moderate inheritability of adventitious root traits has been suggested by Ribeiro et al. (2016). Broad-sense heritability of a grapevine mapping population analyzed regarding root system related phenotypic traits was calculated in a study by Tandonnet et al. (2018) and resulted in H^2 between 0.52 and 0.70.

By Alahakoon (2020), one QTL hotspot has been identified on linkage group 1 associated with four phenotypic traits including the average root diameter. In our study, QTL Mapping revealed a region on chromosome 1 between 0 and 17.4 cM (0 - 5.089 Mb) linked to root dry weight, maximal root length and shoot dry weight. As root dry weight was positively correlated with maximal root diameter (r = 0.72), an *in silico* analysis of putative candidate genes was performed on http://plants.ensembl.org/index.html with the sequence of Pinot Noir PN40024 12X v.2 (GENOSCOPE, CRIBI Consortium VIGNA and IGA; Jaillon et al. 2007; Goremykin et al. 2008).

As root development in plants is largely regulated by the phytohormone auxin, genes involved in auxin signaling could be promising putative candidates for root growth and development. Auxin is regulated by signaling genes including *Aux/IAA* (Indole-3-acetic acid), *LAX* (auxin influx carrier) and *PIN* (auxin efflux carrier) (Carraro et al. 2012, Vandenbussche et al. 2010, Forestan and Varotto 2012). Within the QTL region identified on linkage group 1, three genes potentially related to the auxin signaling pathway were found: VIT_01s0011g04860 (4.475 - 4.478 Mb) is known as auxin efflux carrier, VIT_01s0011g04640 (4.175 - 4.176 Mb) encoding a protein comparable of PIN-LIKEs 2 of *Arabidopsis thaliana*, and VIT_01s0011g04070 (3.720 - 3.722 Mb) whose expression leads to an auxin-responsive protein. The auxin efflux carrier protein PIN is known to conduct auxin flow and regulate root development (Drdová et al. 2013) with their membrane spanning transmembrane domain to direct the intercellular flow of auxin molecules (Petrásek and Friml 2009). In Eucalyptus and Arabidopsis, a low auxin content was found to be directly correlated to poor rooting ability (Negishi et al. 2014; Gonin et al. 2019).

Another putative candidate gene is VIT_01s0011g01650 (1.496 - 1.499 Mb) encoding a peptidyl-prolyl isomerase. It was previously shown that the peptidyl-prolyl cis/trans isomerase Pin1At regulates root gravitropism in *Arabidopsis thaliana* (Xi et al. 2016). As key regulators of root gravitropism, peptidyl-prolyl isomerase might enhance rooting depth and root elongation.

Moreover, the modification of the developmental program of target cells in initiation of adventitious root formation is driven by the differential auxin distribution between the cells that will become root initials. Therefore, auxin transport proteins like PIN and AUX might play a significant role in this process (Druege et al. 2019). In addition, tomato mutants with substantially reduced peptidyl-propyl isomerase activity showed slow gravitropic response indicating important function of peptidyl-propyl isomerase in auxin regulation of plant growth and development (Oh et al. 2006). Interestingly, mutations in LATERAL ROOTLESS2 (LRT2, OsCYP2), a gene encoding for cyclophilin-type peptidyl-proplyl cis/trans isomerase, cause phenotypes with defective lateral root development in rice (Zheng et al. 2013).

VIT_01s0011g02990 encodes for a protein which remains uncharacterized in *V. vinifera*, but the homolog AT1G25580 (1:8.997 - 8.999 Mb) with whole genome alignment coverage score (WGA coverage) of 86.75 encodes SUPRESSOR OF GAMMA RESPONSE 1 (SOG1) in *A. thaliana*. SOG1 was shown to maintain genome integrity for proper cell division during the development of lateral root primordia. However, these findings were gained by inspecting mutants derived by DNA damaging zeocin treatment concluding that SOG1 regulated DNA repair and therefore plays a key role in controlling lateral root formation under genotoxic stress and not necessarily under non-stress conditions (Davis et al. 2016).

VIT_01s0011g02160 encodes for an uncharacterized protein in *V. vinifera*, but the homolog AT5G23110 (5:7.758 - 7.776 Mb) encodes a zinc finger, C3HC4 type RING finger family protein in *A. thaliana*. RING finger proteins are E3 ubiquitin ligases characterized by their RING domain of 40-60 residues. They were also shown to be involved in root growth and development of *A. thaliana* (histone monoubiquitination1, HUB1), *M. sativa* (RING-H2 zinc finger protein, MsRH2-1), and *C. annuum* (RING zinc finger protein 1, CaRZFP1) (Sun et al. 2019). The RING E3 ligase HUB1 regulates root growth rate and mutants of the HUB1 gene showed a slower growth of primary roots in *A. thaliana* (Fleury et al. 2007). Interestingly, MsRH2-1 participates in the development of lateral roots in Alfalfa within the auxin signaling pathway (Karlowsi and Hirsch 2003). Transgenic lines of tobacco overexpressing CaRZFP1 exhibited larger primary roots and a higher number of lateral roots (Zeba et al. 2009).

Two further uncharacterized proteins in *V. vinifera* are encoded by VIT_01s0011g03470 (3.143 - 3.144 Mb) and VIT_01s0011g03070 (2.752 - 2.753 Mb). They contain an AP2/ERF (APETALA2/ethylene responsive factor) domain. The family of AP2/ERF transcriptional regulators plays important roles in plant growth and development and response to environmental factors (Nakano et al. 2006). During adventitious root formation of poplar, a highly specific temporal induction of the AINTEGUMENTA LIKE1 (PtAIL1) transcription factor of the AP2 family was found in transcriptome analysis and PtAIL1 was suggested as positive regulator of early adventitious root development (Rigal et al. 2012). In rice, the gene CROWN

ROOT LESS1 (CRL1) encodes an AP2/ERF family transcription factor, which is induced by auxin and positively regulates an inhibitor gene of the cytokinin pathway (Kitomi et al. 2011).

Furthermore, three genes were found with MYB transcription factor protein motifs: VIT_01s0011g04760 (4.330 - 4.332 Mb), VIT_01s0011g03110 (2.782 - 2.784 Mb), and VIT_01s0011g03730 (3.375 - 3.376 Mb). Two homologs in *A. thaliana* HHO2 and HHO3 are probably involved in the regulation of developmental response of lateral roots, acquisition and mobilization of phosphate and expression of a subset of genes involved in phosphate sensing and signaling pathway. Transcription factor HHO2 is known to be a target of transcription factor PHR1 (Nagarajan et al. 2016). Additionally, MYB61 genes have been suggested to be involved in the modulation of root system architecture because they can affect gibberellins activity in Arabidopsis (Matías-Hernández et al. 2017). In addition, R2R3-MYB genes were shown to play important roles as transcription factors during adventitious root formation in mulberry with different functions in corresponding signaling pathways (Du et al. 2017).

Another interesting gene VIT_01s0011g01050 encodes for a peroxidase enzyme. Peroxidases are known to play a role in auxin level regulation during rooting of cuttings, e.g., in avocado (García-Gómez et al. 1995) and mung bean cuttings (Nag et al. 2013).

Taken together, the identified region on chromosome 1 is a promising genomic region for further fine mapping and future marker development for root growth related traits in grapevine as it was recently supposed by Tandonnet et al. (2018). These findings can provide a proper basis for the next steps in the complex process up to marker-assisted selection in prospective rootstock breeding purposes.

4.5. References

Alahakoon, D. (2020): Exploiring Phenotypic Diversity and Quantitative Trait Loci Mapping for Root Architecture, Freezing Tolerance, Chilling Fulfillment, and Photoperiod Traits in Grapevine Populations. Electronic Theses and Dissertations. 4855

Battista, F.; Gaiotti, F.; Bragato, G.; Tomasi, D. (2016): Root system distribution and density of 'Pinot Gris': effect on yield and grape quality. Acta Hortic. 1136, Proc. I Int. Symp. On Grapevine Roots.

Carraro, N.; Tisdale-Orr, T.E.; Clouse, R.M. (2012): Diversification and expression of the PIN, AUX/LAX, and ABCB families of putative auxin transporters in Populus. Front Plant Sci. 3:17

Davis, O.M.; Ogita, N.; Inagaki, S.; Takahashi, N.; Umeda, M. (2016): DNA damage inhibits lateral root formation by up-regulating cytokinin biosynthesis genes in Arabidopsis thaliana. Genes Cells. 21(11):1195-1208

Drdová, E.J.; Synek, L.; Pečenková, T. (2013): The exocyst complex contributes to PIN auxin efflux carrier recycling and polar auxin transport in Arabidopsis. Plant J. 73:709-719

Druege, U.; Hilo, A.; Pérez-Pérez, J.M.; Klopotek, Y.; Acosta, M.; Shahinnia, F.; Zerche, S.; Franken, P.; Hajirezaei, M.R. (2019): Molecular and physiological control of adventitious rooting in cuttings: phytohormone action meets resource allocation. Annals of Botany, 123:929-949

Du, X.L.; Cao, X.; Yin, C.R.; Tang, Z.; Du, W.; Ban, Y.Y.; Cheng, J.L. (2017): Comprehensive Analysis of R2R3-MYB genes during adventitious root formation in cuttings of *Morus alba*. Journal of Plant Growth Regulation, 36:290-299

Fechter, I.; Hausmann, L.; Zyprian, E.; Daum, M.; Holtgräve, D.; Weisshaar, B.; Töpfer, R. (2014): QTL analysis of flowering time and ripening traits suggests an impact of a genomic region on linkage group 1 in Vitis. Theor. Appl. Genet. 127, 1857-1872

Fleury, D.; Himanen, K.; Cnops, G.; Nelissen, H.; Boccardi, T.M.; Maere, S.; Beemster, G.T.S.; Neyt, P.; Anami, S.; Robles, P.; Micol, J.L.; Inzé, D.; Van Lijsebettens, M. (2007): The *Arabidopsis thaliana* Homolog of Yeast *BRE1* Has a Function in Cell Cycle Regulation during Early Leaf and Root Growth. The Plant Cell, Vol. 19, 417-432

Forestan, C.; Varotto, S. (2012): The role of PIN auxin efflux carriers in polar auxin transport and accumulation and their effect on shaping maize development. Mol. Plant. 5:787-798

Fort, B. and Fraga, B. (2017): Early Measures of Drought Tolerance in four Grapevine Rootstocks. J. Amer. Soc. Hort. Sci. 142(2):36-46

García-Gómez, M.L.; Sánchez-Romero, C.; Barceló-Muñoz, A.; Heredia, A.; Pliego-Alfaro, F. (1995): Peroxidase activity during adventitious root formation in avocado microcuttings. Can. J. Bot. 73:1522-1526

Gonin, M.; Bergougnoux, V.; Nguyen, T.D.; Gantet, P.; Champion, A. (2019): What makes adventitious roots? Plants. 8:240

Goremykin, V.V.; Salamini, F.; Velasco, R.; Viola, R. (2008): Mitochondrial DNA of Vitis vinifera and the issue of rampant horizontal gene transfer. Molecular Biology and Evolution, 26(1):99-110

Hellmann, E.W. (2003): Grapevine Structure and Function. In: E.W. Hellman (editor). Oregon Viticulture. Oregon State University Press. Corvallis, Oregon

Jaillon, O.; Aury, J.M.; Noel, B. et al. (2007): The grapevine genome sequence suggests ancestral hexaploidization in major angiosperm phyla. Nature, 449(7161):463-467

Jeudy, C.; Adrian, M.; Baussard, C. et al. (2016): RhizoTubes as a new tool for high throughput imaging of plant root development and architecture: test, comparison with pot grown plants and validation. Plant Methods 12, 31.

Karlowski, W.M.; Hirsch, A.M. (2003): The over-expression of an alfalfa RING-H2 gene induces pleiotropic effects on plant growth and development. Plant Molecular Biology, 52:121-133

Kitomi, Y.; Ito, H.; Hobo, T.; Aya, K.; Kitano, H.; Inukai, Y. (2011): The auxin responsive AP2/ERF transcription factor CROWN ROOTLESS5 is involved in crown root initiation in rice through the induction of OsRR1, a type-A response regulator of cytokinin signaling. Plant J. 67:472–484.

Linsenmeier, A.; Lehnart, R.; Löhnertz, O.; Michel, H. (2010): Investigation of grapevine root distribution by in situ minirhizotron observation. VITIS 49, 1-6.

Matías-Hernández, L.; Jiang, W.; Yang, K.; Tang, K.; Brodelius, P.E.; Pelaz, S. (2017): AaMYB1 and its orthologue AtMYB61 a_ect terpene metabolism and trichome development in Artemisia annua and Arabidopsis thaliana. Plant J. 90:520–534.

Nag, S.; Paul, A.; Choudhuri, M.A. (2013): Changes in peroxidase activity during adventitious root formation at the base of mung bean cuttings. International Journal of Scientific & Technology Research, 2(5):171-177

Nagarajan, V.K.; Satheesh, V.; Poling, M.D.; Raghothama, K.G.; Jain, A. (2016): Arabidopsis MYB-related HHO2 exerts a regulatory influence on a subset of root traits and genes governing phosphate homeostasis. Plant Cell Physiol. 57:1142-1152

Nakano, T.; Suzuki, K.; Fujimura, T.; Shinshi, H. (2006): Genome-wide analysis of the ERF gene family in *Arabidopsis* and rice. Plant Physiol. 140:411-432.

Negishi, N.; Nakahama, K.; Urata, N.; Kojima, M.; Sakakibara, H.; Kawaoka, A. (2014): Hormone level analysis on adventitious root formation in Eucalyptus globulus. New Forest 45:577–587.

Oh, K.; Ivanchenko, M.G.; White, T.J.; Lomax, T.L. (2006): The diageotropica gene of tomato encodes a cyclophilin: a novel player in auxin signaling. Planta. 224(1):133-44

Petrásek, J. Friml, J. (2009): Auxin transport routes in plant development. Development 136:2675-2688

Ramteke, S.D.; Karibasappa, G.S. (2005): Screening of grape (*Vitis vinifera*) genotypes for drought tolerance. Ind. J. Agric. Sci. 75, 355-357

Ribeiro, C.L.; Silva, C.M.; Drost, D.R.; Novaes, E.; Novaes, C.R.; Dervinis, C.; Kirst, M. (2016): Integration of genetic, genomic and transcriptomic information identifies putative regulators of adventitious root formation in Populus. BMC Plant Biol. 16:66.

Rigal, A.; Yordannov, Y.S.; Perrone, I.; Karlberg, A.; Tisserant, E.; Bellini, C.; Busov, V.B.; Martin, F.; Kohler, A.; Bhalerao, R.; Legué, V. (2012): The AINTEGUMENTA LIKE1 Homeotic Transcription Factor PtAIL1 Controls the Formation of Adventitious Root Primordia in Poplar. Plant Physiol. 160:1996-2006

Schmitz, R.; Atkinson, B.S.; Sturrock, C.J.; Hausmann, L.; Töpfer, R.; Herzog, K. (2021): High-resolution 3D phenotyping of the grapevine root system using X-ray Computed Tomography. VITIS, Vol. 60, no 1

Soar, C.J.; Loveys, B.R. (2007): The effect of changing patterns in soil-moisture availability on grapevine root distribution, and viticultural implications for converting full-cover irrigation into a pointsource irrigation system. Aust. J. Grape Wine Res. 13, 2-13

Sommer, K. (2009): Spring recovery-resilience of Sultana to drought. The Vine, 5, 32-34

Southey, J.M. (1992): Root distribution of different grapevine rootstocks on a relatively saline soil. S. Afr. J. Enol. Vitic., Vol. 13, No. 1

Sun, P.; Jia, H.; Zhang, Y.; Li, J.; Lu, M.; Hu, J. (2019): Deciphering Genetic Architecture of Adventitious Root and Related Shoot Traits in *Populus* Using QTL Mapping and RNA-Seq Data. Int. J. Mol. Sci. 20, 6114

Tandonnet, J.P.; Marguerit, E.; Cookson, S.J.; Ollat, N. (2018): Genetic architecture of aerial root traits in field-grown grafted grapevines is largely independent. Theor. Appl. Genet. 131:903-915

Vandenbussche, F.; Petrásek, J.; Zádníková, P. (2010): The auxin influx carriers AUX1 and LAX3 are involved in auxin-ethylene interactions during apical hook development in *Arabidopsis thaliana* seedlings. Development 127:5157-5165

Varshney, R.K.; Pazhamala, L.; Kashiwagi, J.; Gaur, P.M.; Krishnamurthy, L.; Hoisington, D. (2011): Genomics and physiological approaches for root trait breeding to improve drought tolerance in chickpea (*Cicer arietinum* L.). Root Genomics, Springer. Berlin, Heidelberg, 2011; 233-250

Vršič, S.; Kocsis, L.; Pulko, B. (2016): Influence of Substrate pH on Root Growth, Biomass and Leaf Mineral Contents of Grapevine Rootstocks Grown in Pots. J. Agr. Sci. Tech. Vol. 18:483-490

Watt, M.; Moosavi, S.; Cunningham, S.C.; Kirkegaard, J.A.; Rebetzke, G.J.; Richards, R.A. (2013): A rapid, controlled-environment seedling root screen for wheat correlates well with rooting depths at vegetative, but not reproductive, stages at two field sites. Ann. Bot. 112, 447-455

Xi, W.; Gong, X.; Yang, Q.; Yu, H.; Liou, Y.-C. (2016): Pin1At regulates PIN1 polar localization and root gravitropism. Nat. Commun. 21;7:10430

Yates, A.D.; Achuthan, P.; Akanni, W.; Allen, J.; Allen, J.; Alvarez-Jarreta, J.; Ridwan Amode, M.; Armean, I.M.; Azov, A.G.; Bennett, R.; et al. (2020): Ensembl 2020. Nucleic Acids Research. Vol. 48:1, 682-688

Zeba, N.; Isbat, M.; Kwon, N.J.; Lee, M.O.; Kim, S.R.; Hong, C.B. (2009): Heat-inducible C3HC4 type RING zinc finger protein gene from Capsicum annuum enhances growth of transgenic tobacco. Planta, 229:861-871

Zheng, H.; Li, S.; Ren, B.; Zhang, J.; Ichii, M.; Taketa, S.; Tao, Y.; Zuo, J.; Wang, H. (2013): LATERAL ROOTLESS2, a cyclophilin protein, regulates lateral root initiation and auxin signaling pathway in rice. Molecular Plant, 6:1719-1721

Software:

MapQTL6:

Van Ooijen, J.W. (2009): MapQTL 6, Software for the mapping of quantitative trait loci in experimental populations of diploid species. Kyazma BV; Wageningen, Netherlands

R Studio:

R Core Team (2020): R: A language and environment for statistical computing. R Foundation for Statistical Computing, Vienna, Austria. URL https://www.R-project.org/

- **Brooks, M.E.; Kristensen, K.; van Benthem, K.J.; Magnusson, A.; Berg, C.W.; Nielsen, A.; Skaug, H.J.; Maechler, M.; Bolker, B.M. (2017):** glmmTMB Balances Speed and Flexibility Among Packages for Zero-inflated Generalized Linear Mixed Modeling. The R Journal. 9(2), 378-400.
- **Bates, D.; Maechler, M.; Bolker, B.; Walker, S. (2015):** Fitting Linear Mixed-Effects Models Using lme4. Journal of Statistical Software, 67(1), 1-48.
- **Fox, J.; Weisberg, S. (2019):** An R Companion to Applied Regression, Third edition. Sage, Thousand Oaks CA.
- **Harrell, F.E. Jr., Dupont, C. et al. (2020).** Hmisc: Harrell Miscellaneous. R package version 4.4-2.
- **Hothorn, T.; Bretz, F.; Westfall, P. (2008):** Simultaneous Inference in General Parametric Models. *Biometrical Journal*, 50(3), 346-363.
- **Kassambara, A. and Mundt, F. (2020):** factoextra: Extract and Visualize the Results of Multivariate Data Analyses. R package version 1.0.7.
- **Lê, S.; Josse, J.; Husson, F. (2008):** FactoMineR: A Package for Multivariate Analysis. *Journal of Statistical Software*, 25(1), 1–18.
- **Lenth, R. (2020):** emmeans: Estimated Marginal Means, aka Least-Squares Means. R package version 1.4.7.
- **Wickham, H. (2016):** *ggplot2:* Elegant Graphics for Data Analysis. Springer-Verlag, New York. ISBN 978-3-319-24277-4, https://ggplot2.tidyverse.org.

WinRHIZO:

WinRHIZO Pro Regent Instruments Inc., 146 QC, Canada

Internet Sources:

Google maps (05.03.2020) location of field trail:

https://www.google.com/maps/place/Weisenheim+am+Sand/@49.4922721,8.0242748,4904 9m/data=!3m2!1e3!4b1!4m5!3m4!1s0x479631098738b1ed:0xe213bc572cabaa6d!8m2!3d49. 5175634!4d8.2470219

Datenbank EnsemblPlants: http://plants.ensembl.org/index.html

5. Chapter 5: General Discussion

In the past decades, opportunities in plant genomics have enhanced enormously reaching high-throughput levels. On the other hand, acquisition of phenotypic data in the same amount has become a major bottleneck in functional studies (Yang et al. 2020). Therefore, sensor and data technology has been involved into developmental processes of appropriate phenotyping techniques, mostly aiming at the aerial plant parts. Due to the hidden nature of plant roots in soil, development of high-throughput phenotyping methods for root systems has been rare. In addition, the physiological and molecular basis of adventitious root growth of woody species compared to model species is not fully understood due to the lack of mutant phenotypes for practical studies (Pizarro and Díaz-Sala, 2019). Therefore, sufficient phenotyping platforms need to be developed and utilized facilitating accurate prediction of genomic regions underlying these processes (Valliyodan et al. 2016). Contrary to grapevine aerial crop characteristics, investigation of grapevine roots has been scarce in the past years and the development of grapevine root phenotyping platforms is highly needed to aim the possibilities of root system related genetic improvement.

Table 16 presents all three implemented grapevine root phenotyping methods of this study to compare their performance regarding throughput, automation, outcome as well as costs and effort. Grapevines grown in perlite and rhizotrons were placed in the greenhouse whereas plant samples in the field trial were exposed to many environmental factors. Besides the genotype, soil properties, climatic conditions and in some case vineyard management techniques may strongly impact the development of grapevine root systems in general (Ollat et al. 2015). This influence complicates the unambiguous identification of genetically determined root system characteristics and clearly shows the challenging nature of root studies under field conditions. In addition, perlite grown and rhizotron grown plant roots were determined at relatively early developmental stages being four and six weeks old, respectively. It remains uncertain whether root architecture and root growth assayed in a greenhouse on young vines could be related to the performance of mature vines in the field (James et al. 1985; Fort and Fraga, 2017). Therefore, comparative studies consisting of different methods could bring new insights into correlations between green house and field experiments.

Within the field trial, five phenotypic traits were measured, whereas three and four phenotypic characteristics could be measured within the perlite experiment and the rhizotron experiment, respectively. Notably all four traits gathered in the rhizotron study were acquired through automated image analysis, whereas perlite experiment phenotyping required manual image analysis and field trial phenotyping was exclusively done by manual measurements. However, it could be shown that additional image analysis of field grown root systems provides promising depth profile information for further approaches. As shown in Chapter 4, genotypes exhibiting

no significant differences when comparing traits of their whole root system, determination of depth segments resulted in significant differences at single soil depth levels.

Only phenotypic data from rhizotron experiments provided information of adventitious and lateral root length. Distinguishing between main roots and secondary roots might contribute to the exploitation of root system related processes occurring during root development as they have different functions. De Harralde et al. (2010) stated that coarse roots (Ø > 2 mm) are main roots holding water and nutrient transport as well as storage functions while fine roots (Ø < 2 mm) contribute to water and nutrient foraging and mycorrhization of grapevines.

Perlite substrate experiments needed less time and labour effort to get set up and conducted. In addition, root growth assessment based on the classification scheme was quite fast, even though the manual image analysis took more time than automated image analysis of rhizotron and field grown root systems. Throughput was highest and material costs were lowest in perlite experiments due to the simple experimental setup. However, compared to classification schemes or manual measurements, automated application of sensors improves speed and objectivity of quantitative data collection and offers opportunities for machine learning and cloud-system approaches in the future (Koh et al. 2021). Therefore, upcoming approaches should be made to encourage sensors applications.

Potential influences of experimental year and woody cutting diameter were considered as fixed effects in statistical modeling. Whereas the woody cutting diameter had no effects on root growth in the perlite experiments, root development was positively affected by woody cutting diameter in rhizotron and field experiments. Interestingly, Alahakoon (2020) found no effect of cutting size for adventitious root growth, when conducting experiments with cuttings grown in perlite substrate, either. Effects of the cane's state on adventitious rooting behavior has been documented in the past: Nicholas et al. (1992) reported a poorer rooting ability of thinner cuttings from the distal ends of the cane compared to thicker cuttings from the basal ends. It was assumed that a reduced photosynthesis of the younger distal ends of the canes resulted in lower carbohydrate stores and therefore, in poorer rooting behavior. In addition, a smaller woody cutting diameter might be also caused by incomplete secondary vascular development contributing to diminished rooting ability (Smart et al. 2002).

Table 16: Comparison of the three implemented grapevine root phenotyping methods. Evaluation for time effort, throughput and material costs is given as + = "minor", ++ = "medium", and +++ = "high"; Colours indicate positive (green), negative (red), or medium (yellow) appraisal of method performance.

		Perlite Substrate	Rhizotrons	Field Trial
Location		Green House	Green House	Field
Duration / age of plant samples		4 weeks	6 weeks	4 - 5 months
Measured phenotypic traits		- Formation of adventitious roots by classification scheme - Adventitious root length - Adventitious root number - (Woody cutting diameter)	- Total root length - Adventitious root length - Lateral root length - Leaf area - (Woody cutting diameter)	- Adventitious root number - Maximal root length - Maximal root diameter - Root dry weight - Shoot dry weight - (Woody cutting diameter)
Number of phenotypic traits		3	4	5
Trait measurements		Image-based, classification scheme	Image-based	Manual measurements
Time / effort per sample	**Exp. Setup**	+	+++	++
	Image Acquisition	+	++	+++
	Image Analysis	+++	+	++
Throughput		+++	++	+
Material Costs		+	++	++
QTLs identified in 'VB2001'		4	9	4

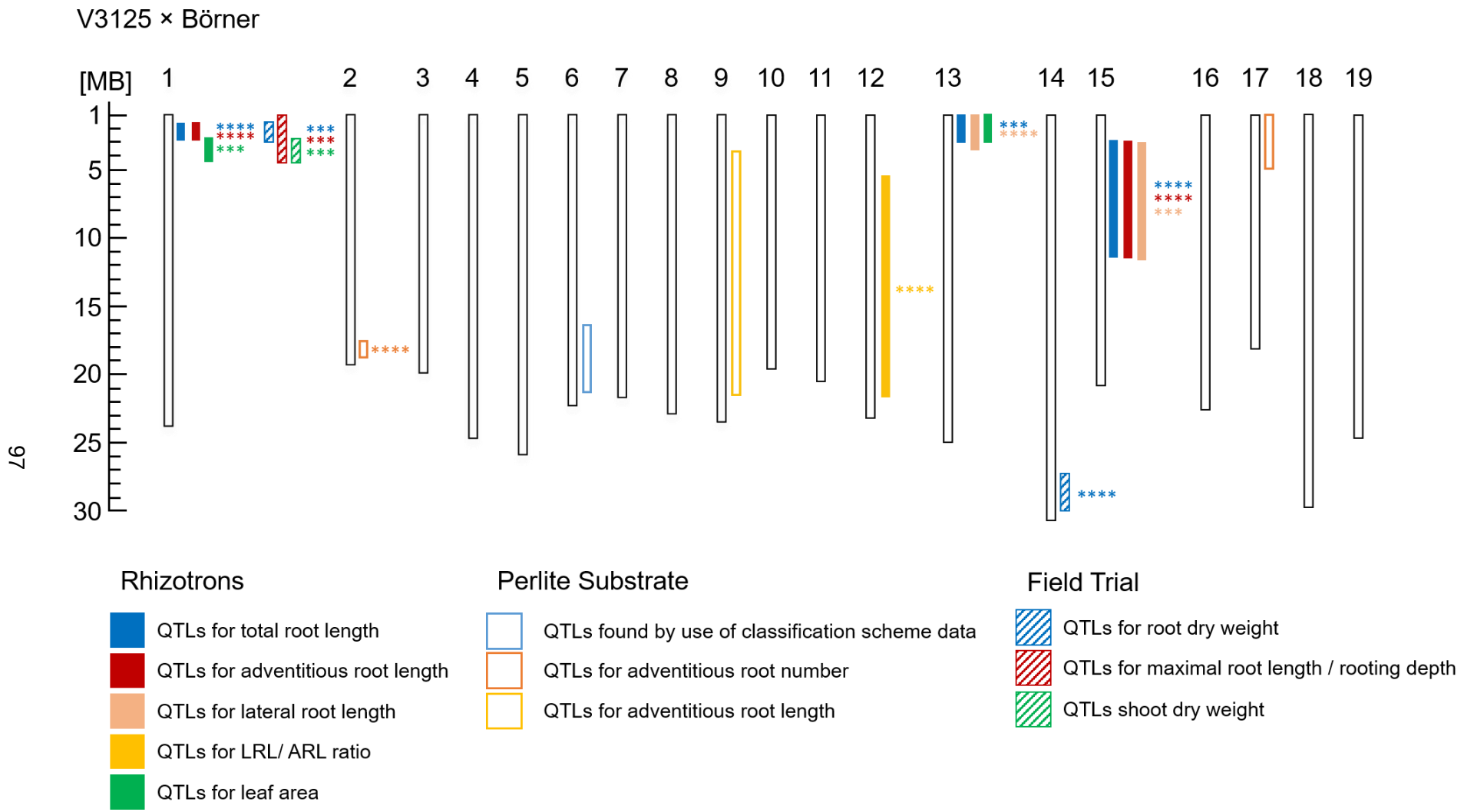

Figure 36: Schematic figure of physical positions (in PN40024 12X v.2) of QTLs identified via interval mapping of mapping population 'VB2001' grown in rhizotrons, perlite substrate and in the field. Significant correlations by Kruskal-Wallis mapping are indicated with asterisks.

Figure 36 shows a schematic illustration of physical positions of all QTLs identified via interval mapping of mapping population 'VB2001' grown in rhizotrons, perlite substrate and in the field. All in all, 9 QTLs were identified for mapping population 'VB2001' in rhizotron experiments whereas perlite and field grown root phenotyping reveled 4 QTLs, respectively. Notably, six QTLs were identified in the same genomic region on chromosome 1 in rhizotron and field experiments for total root length, adventitious root length and leaf area as well as for root dry weight, maximal root length and shoot dry weight. This region has been identified in previous QTL mapping studies of grapevine root related traits with QTLs found for root biomass and root number (> 4 mm) (Tandonnet et al. 2018) as well as root average diameter (Alahakoon, 2020). Interestingly, this QTL region was not identified in mapping population 'CMVB1989'. Comparing the determined populations and their origins revealed a common ancestry from *V.riparia* which is missing in 'CMVB1989' (see table 17). However, analyzing the segregating population 'CMVB1989' resulted in a total of 12 QTLs when grown in rhizotrons and could also be considered for future field experiments, especially because the differences in root growth between the parental genotypes 'Calardis Musqué' and 'Villard Blanc' might be a promising indicator for segregating root traits in the F1 population.

In both populations, a transgressive segregation could be observed with some F1 individuals showing even more extreme phenotypes than their parents (see figure S3, S8-11, and S16-S18). This phenomenon has been noticed before in different grapevine populations for several phenotypic characteristics e.g. flowering time (Schwandner, 2019). A transgressive segregation can be explained by polygenetic inheritance of a trait, which can lead to recombination of additive alleles at several genetic loci.

Table 17: Grapevine mapping populations utilized for QTL mapping of root related traits and their origin

	Population origin
Tandonnet et al. 2018	*V. vinifera* cv. Cabernet Sauvignon × *V. riparia* cv. Gloire de Montpellier
Alahakoon, 2020	*V. riparia* 'Manitoba 37' × 'Seyval' (Seibel 5656 Seibel × 4986)
'VB2001'	'V3125' (*V. vinifera* cv. Schiava Grossa' × *V. vinifera* Riesling) × 'Börner' (*V. riparia* Gm183 × *V. cinerea* Arnold)
'CMVB1989'	'Calardis Musqué' (*V. vinifera* 'Bacchus Weiß' × Seibel 'Seyval') × 'Villard Blanc' ('Seibel 6468' × Seibel 'Subéreux')

Regarding the explained phenotypic variance, values ranged between 9.1% for root classification of woody cuttings in perlite and 15.2% for root dry weight of plants in the field trial. Comparable values were reached in a field trial with grafted grapevines of Tandonnet et al. (2018) with explained phenotypic variance ranging from 6% (root number of roots with Ø > 4 mm) to 20.7% (root number). Most studies of parameters related to root initiation and root

system architecture resulted in polygenic determinism with each genetic region explaining only a low percentage of variability, e.g., root length (Dievart et al. 2013).

Phytohormones are substantial factors for adventitious root formation, affecting cell division and growth as well as led to interactions with other phytohormones and molecules (Da Costa et al. 2013). Most important phytohormones involved in adventitious root formation are auxin, ethylene, cytokinins, and gibberellins. The initial development of adventitious roots is primarily controlled by the availability of auxin and its proper localization, while most other hormones act as inhibitors or in combination with auxin (Ribeiro et al. 2016). Ethylene has promoting functions during first phase of de-differentiation in interaction with auxin, but can be inhibitory during induction phase (Klerk, 2002). Cytokinins seem to have inhibitory functions by interacting with auxin and have been shown to affect the quiescent center formation in Arabidopsis (Della Rovere et al. 2013). Gibberellins interfere with the polar transport of auxin and therefore, negatively impact initiation of adventitious root formation in Arabidopsis (Mauriat et al. 2014), but positively influence the emergence of adventitious roots and elongation as shown in Tobacco (Niu et al. 2013).

Even though propagation by cuttings is the common way of propagation and widely used in viticulture, the regulation by plant hormones and signaling pathways involved in adventitious root formation are poorly understood yet. The recently sequenced ‘Börner’ genome could hold opportunities to further investigate genomic origins of rooting behaviour and *in silico* candidate gene analysis (Frommer et al. 2020). Candidate genes could be selected by identification of genes with differential expression patterns between genotypes that possess extreme contrasts regarding different biological traits (Street et al. 2006). Future approaches might focus on QTL regions and underlying candidate genes identified in this study for transcriptome analysis.

In several studies, interactions between grapevine rootstock and scion varieties have been documented regarding berry quality, but also in terms of enhanced drought tolerance (Zombardo et al. 2020; Serra et al. 2013). Scion-rootstock interactions are important in regulating plant growth (Tandonnet et al. 2010) and identification of QTLs across a broader variability of different scion-rootstock combinations can reinforce the robustness of QTL regions and their potential interest for breeding (Tandonnet et al. 2018). Therefore, future studies will need to take these combinations into account when assessing grapevine root systems regarding resource use efficiency.

Grapevines are perennial crops with root systems developing for several years. In contrast, conclusions resulting from experiments like rhizotrons need to be considered critically regarding their validity for real viticultural conditions. Even though field trials can facilitate a better approximation, exceedingly few studies of grapevine roots determined fully grown root systems over years. However, the ability to form adventitious roots from woody cuttings can

be analysed and might support the improvement of varieties which are easy to propagate. In addition, studies of early adventitious root development provide new insights into the regulation and interaction between key components in the complex process of adventitious root formation from woody cuttings. Facing climate change and future extreme weather events, genetic improvements of crops are considered as major tool to stabilize and enhance crop yield and quality. Therefore, crop breeding programs need to focus on traits related to resource acquisition, coping stress conditions, and adaptation to changing environmental factors (De Dorlodot et al. 2007). This explicitly includes all traits related to root systems as key elements in drought adaptation and necessarily all phenotyping methods which enable the closer look on crop root system phenotypes.

5.1. References

Alahakoon, D. (2020): Exploiring Phenotypic Diversity and Quantitative Trait Loci Mapping for Root Architecture, Freezing Tolerance, Chilling Fulfillment, and Photoperiod Traits in Grapevine Populations. Electronic Theses and Dissertations. 4855

Da Costa, C.T.; de Almeida, M.R.; Ruedell, C.M.; Schwambach, J.; Maraschin, F.S.; Fett-Neto, A.G. (2013): When stress and development go hand in hand: Main hormonal controls of adventitious rooting in cuttings. Front. Plant Sci. 4:133.

De Harralde, F.; Savé, R.; Aranda, X.; Biel, C. (2010): Grapevine Roots and Soil Environment: Growth, Distribution and Function. In: Delrot et al. (eds.), Methodologies and Results in Grapevine Research. Springer Science + Business Media B.V. 2010

Della Rovere, F.; Fattorini, L.; D'Angeli, S.; Veloccia, A.; Falasca, G.; Altamura, M.M. (2013): Auxin and cytokinin control formation of the quiescent centre in the adventitious root apex of arabidopsis. Annals of Botany, 112(7), 1395-1407

Dievart, A.; Coudert, Y.; Gantet, P.; Pauluzzi, G.; Puig, J.; Fanchon, D.; Ahmadi, N.; Courtois, B.; Guiderdoni, E.; Périn, C. (2013): Dissection des bases biologiques de caractères d'intérêt chez le riz: architecture et development du système racinaire. Cah. Agric, 22:475-483

De Dorlodot, S.; Forster, B.; Pagès, L.; Price, A.; Tuberosa, R.; Draye, X. (2007): Root system architecture: Opportunities and constraints for genetic improvement of crops. Trends Plant Sci. 12, 474-481

Fort, B. and Fraga, B. (2017): Early Measures of Drought Tolerance in four Grapevine Rootstocks. J. Amer. Soc. Hort. Sci. 142(2):36-46

Frommer, B.; Holtgräve, D.; Hausmann, L.; Viehöver, P.; Huettel, B.; Töpfer, R.; Weisshaar, B. (2020): Genome Sequences of Both Organelles of the Grapevine Rootstock Cultivar 'Börner'. Microbiol. Resour. Announc. 9(15), e01471-19

James, B.; Bartlett, R.; Amadon, J. (1985): A root observation and sampling chamber (rhizotron) for pot studies. Plant Soil 85:291-293

Klerk, G.-J. (2002): Rooting of Microcuttings: Theory and Practice. In Vitro Cell. Dev. Biol.-Plant 38:415-422

Koh, J.C.O.; Spangenberg, G.; Kant, S. (2021): Automated Machine Learning for High-Throughput Image-based Plant Phenotyping. Sensors 13(5), 858

Mauriat, M.; Petterle, A.; Bellini, C.; Moritz, T. (2014): Gibberellins inhibit adventitious rooting in hybrid aspen and Arabidopsis by affecting auxin transport. Plant J. 78:382-384

Nicholas, P.R.; Chapman, A.P.; Cirami, R.M. (1992): Grapevine propagation, In: Coombe, B.G.; Dry, R.P. eds. Viticulture, Vol. 2, practices. Adelaide, Winetitles. p.1-22.

Niu, S.; Li, Z.; Yuan, H.; Fang, P.; Chen, X.; Li, W. (2013): Proper gibberellin localization in vascular tissue is required to regulate adventitious root development in tobacco. Journal of Experimental Botany. 64(11), 3411-3424

Ollat, N.; Peccoux, A.; Papura, D.; Esmenjaud, D.; Marguerit, E.; Tandonnet, J.-P. (2015): Rootstocks as a component of adaptation to environment. In Grapevine in a Changing Environment, a molecular and ecophysiological perspective. Eds. Geros, H.; Chaves, M.M.; Medrano Gil, H.; Delrot, S., Hoboken, N.J.; John Wiley & Sons, Inc., 68-108

Pizarro, A.; Díaz-Sala, C. (2019): Cellular dynamics during maturation-related decline of adventitious root formation in forest tree species. Physiologia Plantarum. 165(1), 73-80

Ribeiro, C.L.; Silva, C.M.; Drost, D.R.; Novaes, E.; Novaes, C.R.; Dervinis, C.; Kirst, M. (2016): Integration of genetic, genomic and transcriptomic information identifies putative regulators of adventitious root formation in Populus. BMC Plant Biol. 16:66.

Schwandner, A. (2019): Identifikation von Austriebs- und Blühloci im Genom der Weinrebe, zugrunde liegender Kandidatengene sowie genetischer Marker zur Marker-gestützten Selektion. Dissertation, 2019. https://doi.org/10.5073/dissjki.2019.005

Serra, I.; Strever, A.; Myburgh, P.A.; Deloire, A. (2013): Review: the interaction between rootstocks and cultivars (*Vitis vinifera* L.) to enhance drought tolerance in grapevine. Australien Journal of Grape and Wine Research. 20(1), 1-14

Smart, D.R.; Kocsis, L.; Walker, M.A.; Stockert, C. (2002): Dormant Buds and Adventitious Root Formation by *Vitis* and Other Woody Plants. J. Plant Growth Regul. 21:296-314

Street, N.R.; Skogström, O.; Sjödin, A.; Tucker, J.; Rodríguez-Acosta, M.; Nilsson, P.; Jansson, S.; Taylor, G. (2006): The genetics and genomics of drought response in *Populus*. The Plant Journal, 48:321-341

Tandonnet, J.P.; Cookson, S.J.; Vivin, P.; Ollat, N. (2010): Scion control biomass allocation and root development in grafted grapevines. Aust. J. Grape Wine Res, 16:290-300

Tandonnet, J.P.; Marguerit, E.; Cookson, S.J.; Ollat, N. (2018): Genetic architecture of aerial root traits in field-grown grafted grapevines is largely independent. Theor. Appl. Genet. 131:903-915

Valliyodan, B.; Ye, H.; Song, L.; Murphy, M.; Shannon, G.; Nguyen, H.T. (2016): Genetic diversity and genomic strategies for improving drought and waterlogging tolerance in soybeans. Journal of Experimental Botany, Vol. 68(8):1835-1849

Yang, W.; Feng, H.; Zhang, X.; Zhang, J.; Doonan, J.H.; Batchelor, W.D.; Xiong, L.; Yan, J. (2020): Crop Phenomics and High-Throughput Phenotyping: Past Decades, Current Challenges, and Future Perspectives. Molecular Plant, Vol. 13(2), 187-214

Zombardo, A.; Crosatti, C.; Bagnaresi, P.; Bassolino, L.; Reshef, N.; Puccioni, S.; Faccioli, P.; Tafuri, A.; Delledonne, M.; Fait, A.; Storchi, P.; Cattivelli, L.; Mica, E. (2020): Transcriptomic and biochemical investigations support the role of rootstock-scion interaction in grapevine berry quality. BMC Genomics 21, 468

6. Supplementary Material

6.1. Grapevine Root Development in Perlite Substrate

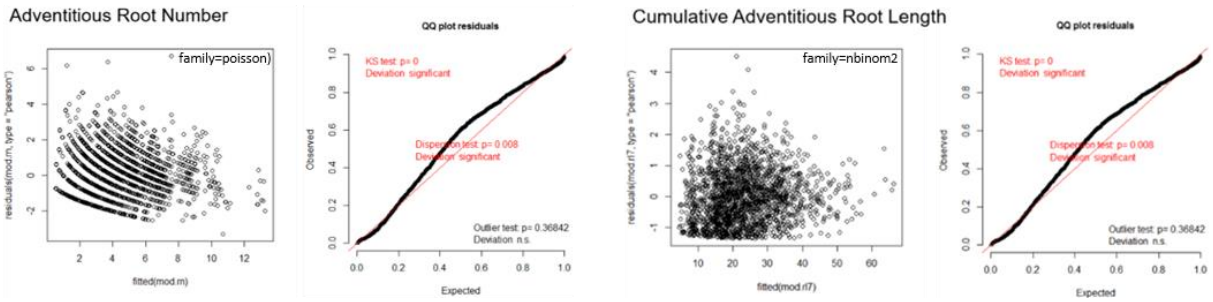

Figure S 1: Model diagnostics of mapping population 'VB2001' for statistic modeling of adventitious root formation of woody cuttings grown in perlite substrate

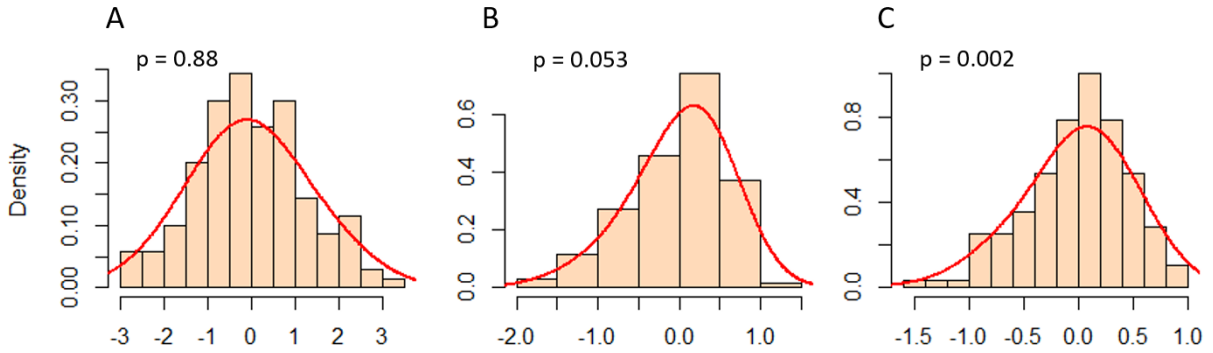

Figure S 2: Histograms of best linear unbiased prediction (BLUP) values of root classification scheme data (A), adventitious root number (B), and cumulative adventitious root length (C) of perlite experiment.

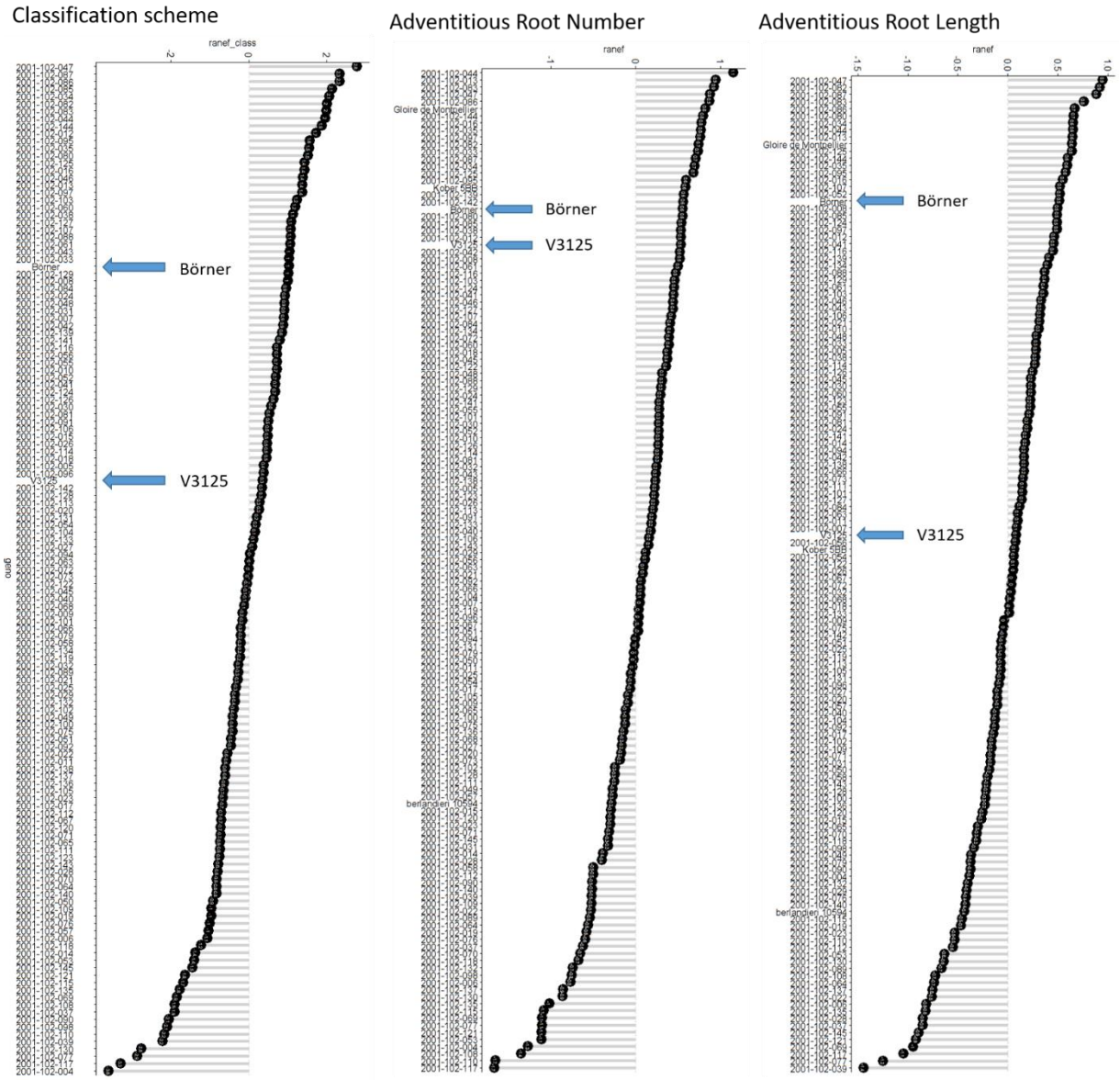

Figure S 3: BLUP values of population and parental genotypes of 'VB2001' grown in perlite substrate. Genotypes with measurements over population average are at the top of the plot. Genotypes with measurements under population average are at the bottom end of the plot.

6.2. Grapevine Root Development in Rhizotrons

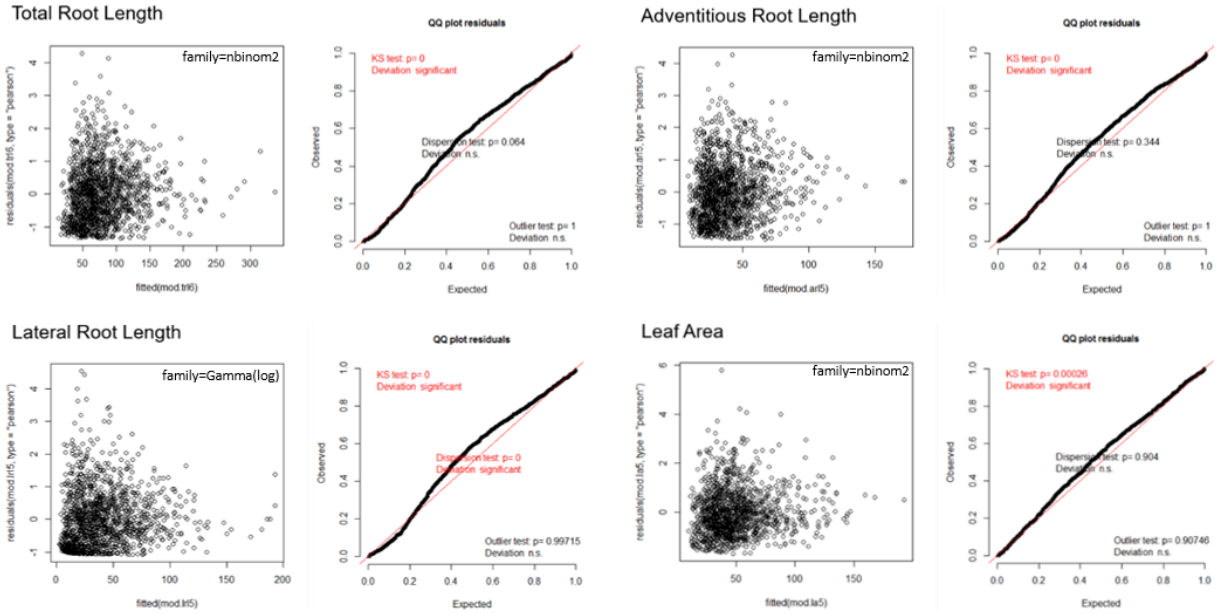

Figure S 4: Model diagnostics of mapping population 'VB2001' for statistic modeling of root systems grown in rhizotrons

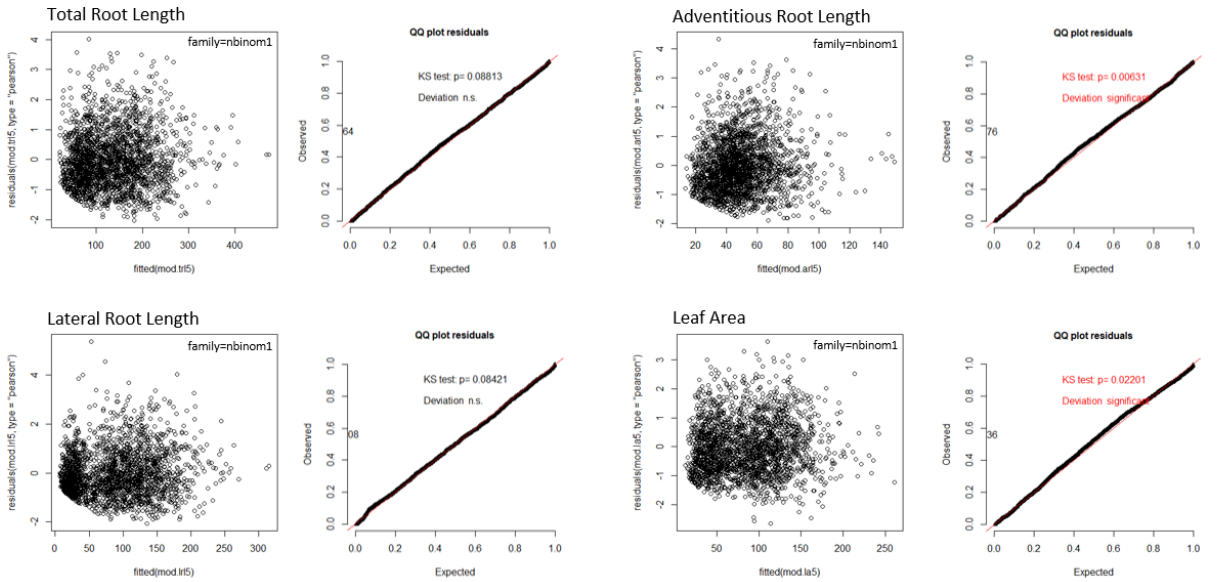

Figure S 5: Model diagnostics of mapping population 'CMVB1989' for statistic modeling of root systems grown in rhizotrons

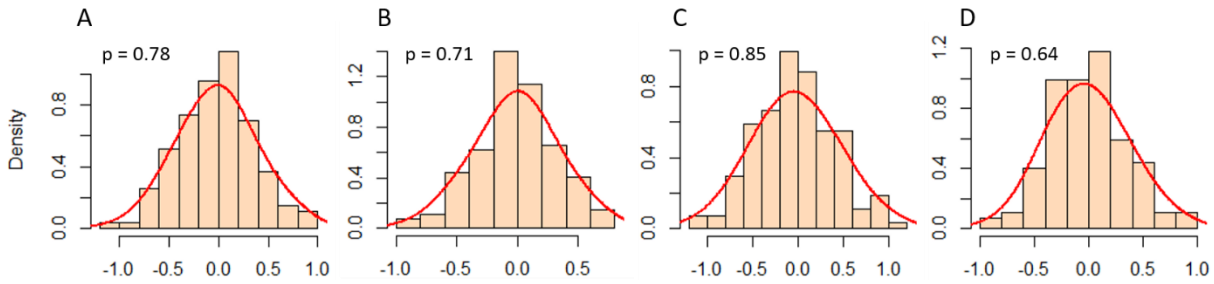

Figure S 6: Histograms of best linear unbiased prediction (BLUP) values of total root length (A), adventitious root length (B), lateral root length (C), and leaf area (D) of mapping population 'VB2001' grown in rhizotrons.

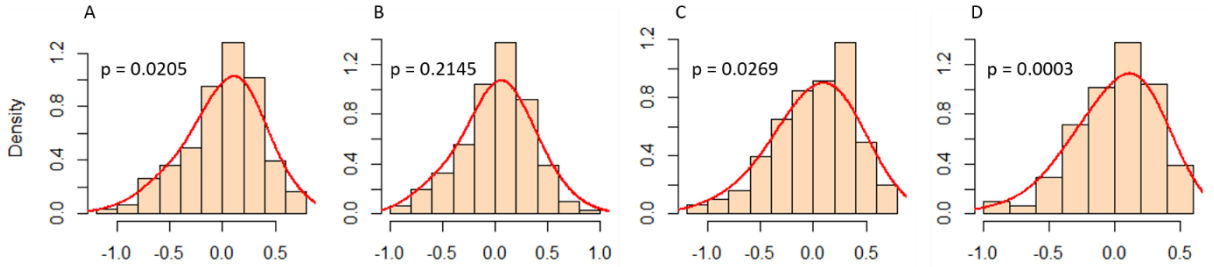

*Figure S 7: Histograms of best linear unbiased prediction (BLUP) values of total root length (A), adventitious root length (B), lateral root length (C), and leaf area (D) of mapping population 'CMVB1989'*grown in rhizotrons.

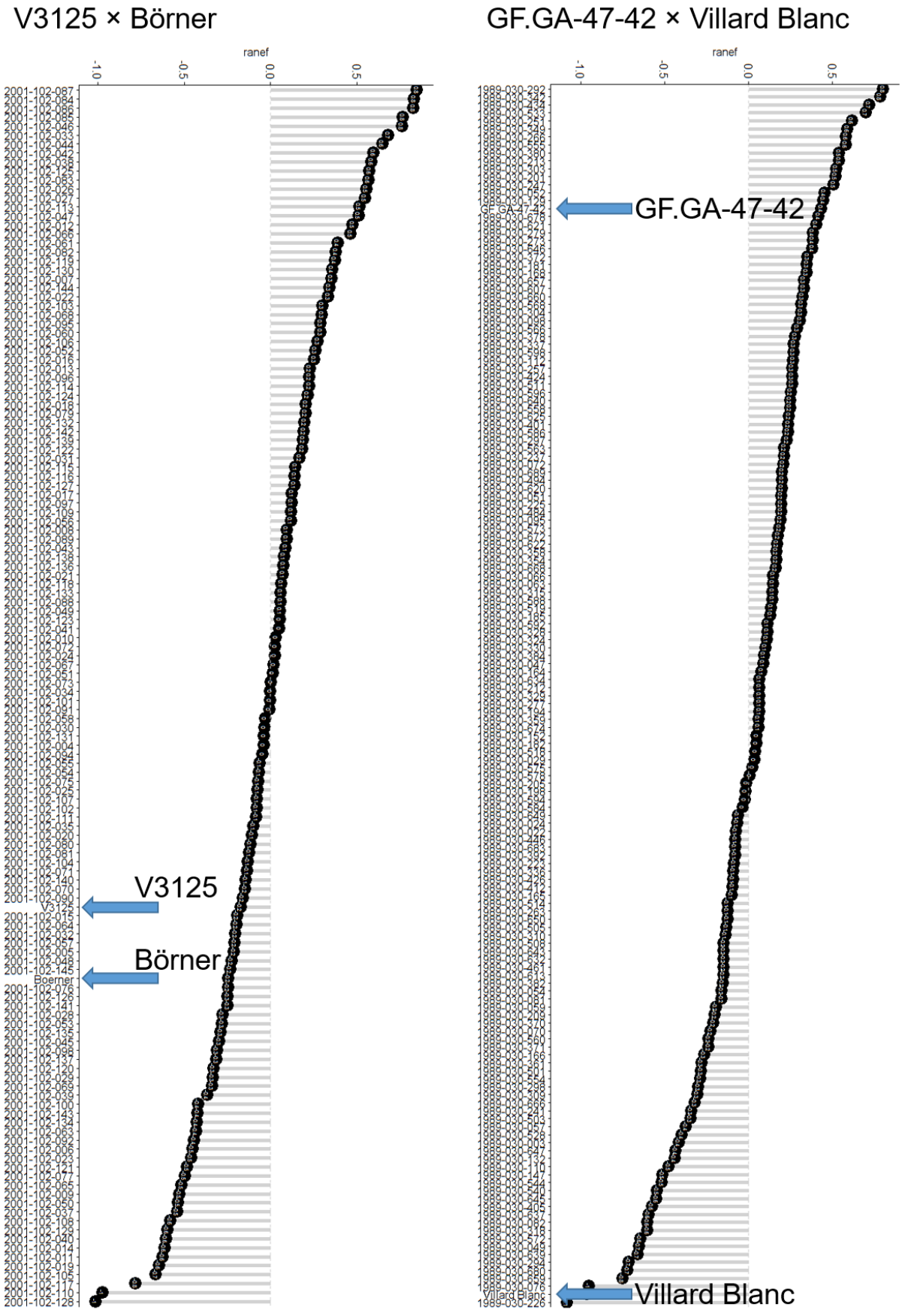

Figure S 8: BLUP values for total root length of population and parental genotypes of 'VB2001' and 'CMVB1989' grown in rhizotrons. Genotypes with measurements over population average are at the top of the plot. Genotypes with measurements under population average are at the bottom end of the plot.

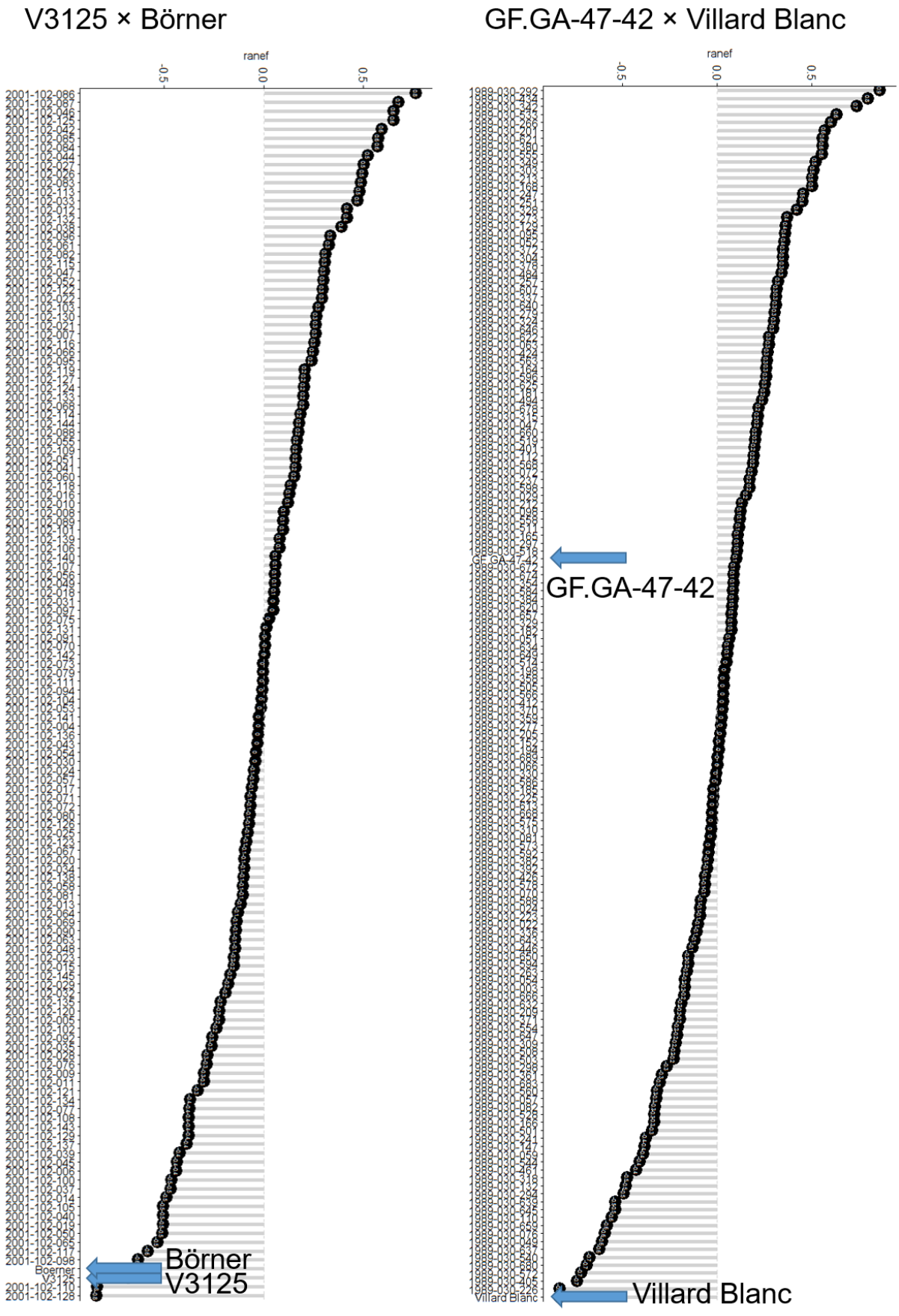

Figure S 9: BLUP values for adventitious root length of population and parental genotypes of 'VB2001' and 'CMVB1989' grown in rhizotrons. Genotypes with measurements over population average are at the top of the plot. Genotypes with measurements under population average are at the bottom end of the plot.

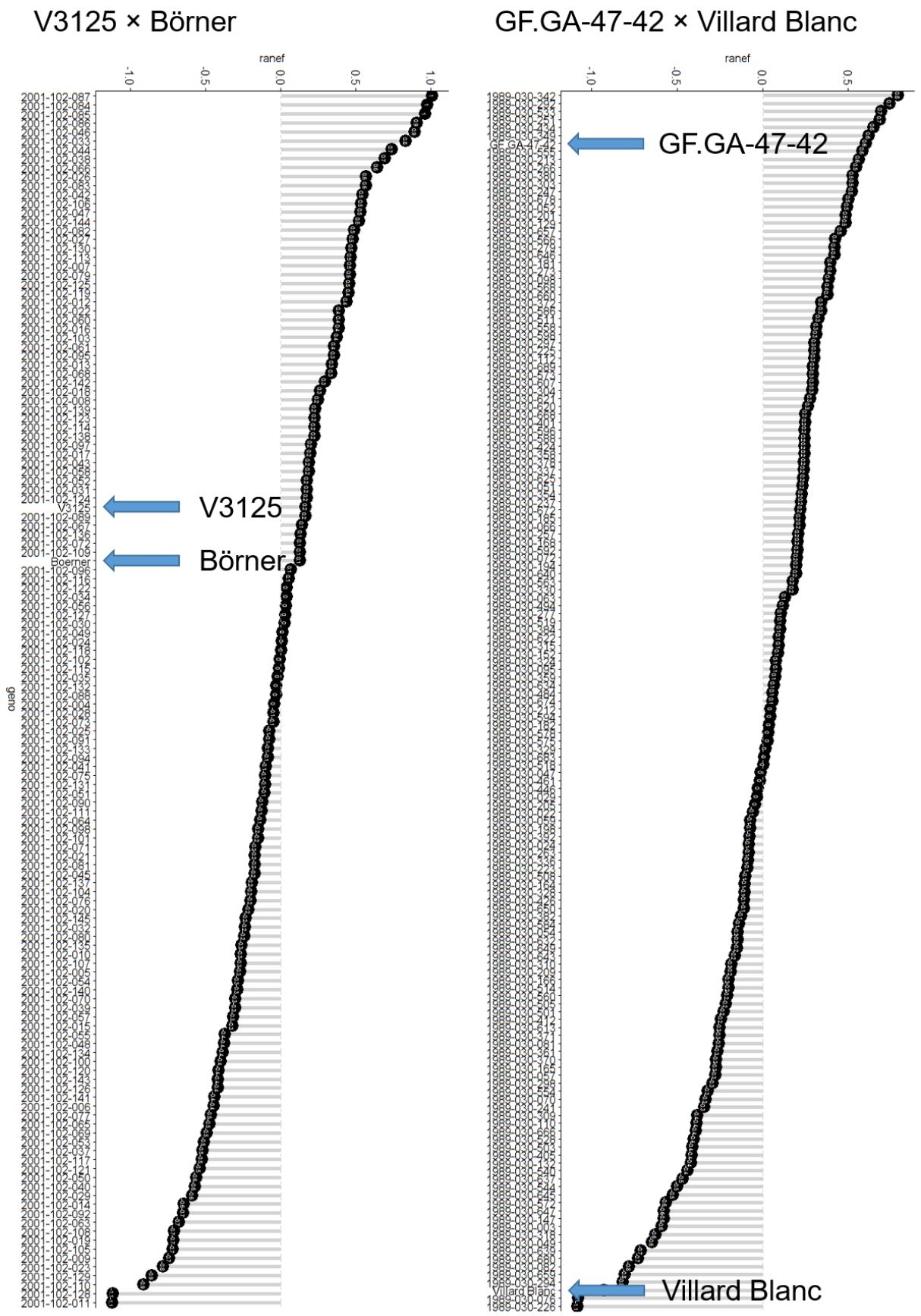

Figure S 10: BLUP values for lateral root length of population and parental genotypes of 'VB2001' and 'CMVB1989' grown in rhizotrons. Genotypes with measurements over population average are at the top of the plot. Genotypes with measurements under population average are at the bottom end of the plot.

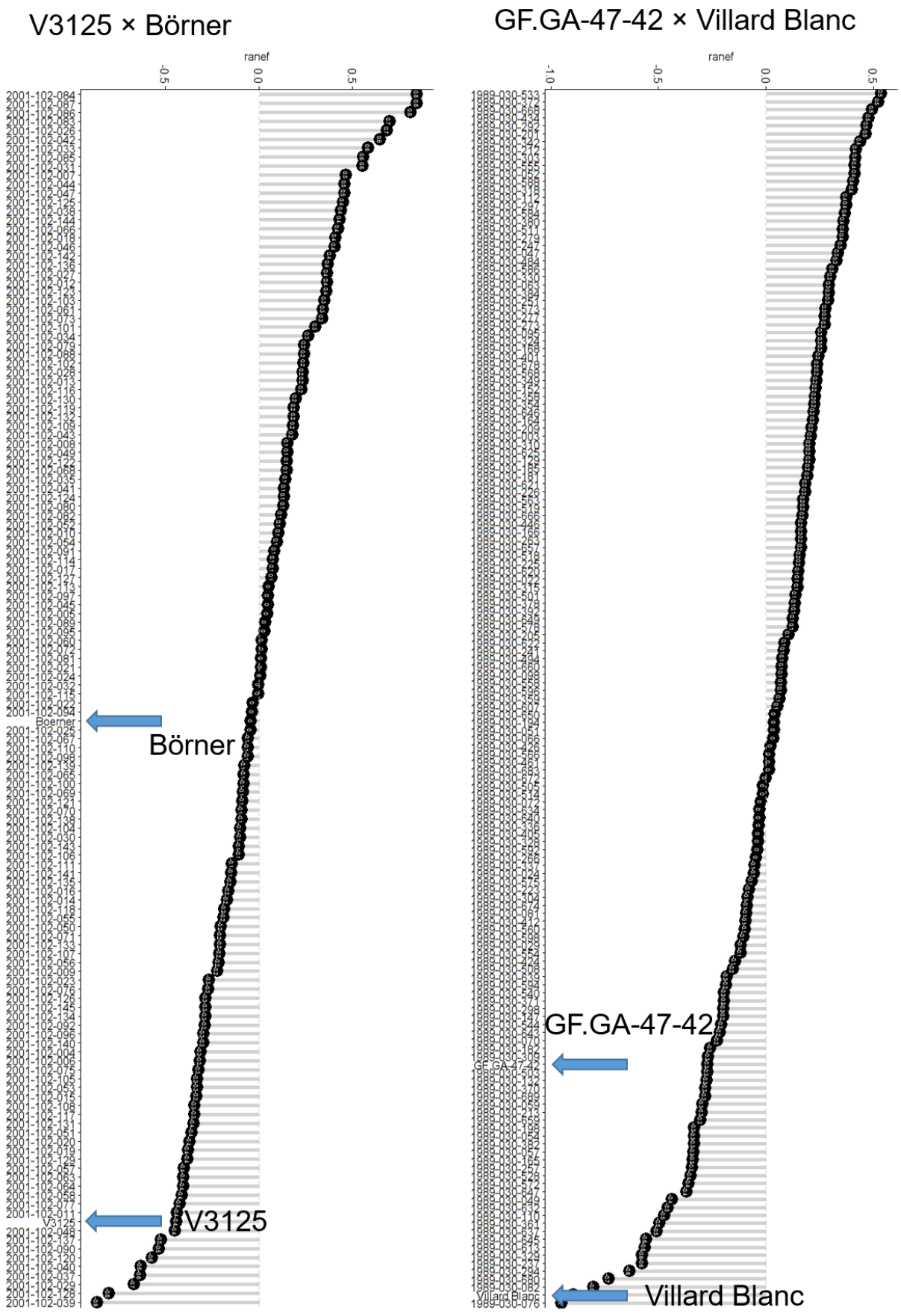

Figure S 11: BLUP values for leaf area of population and parental genotypes of 'VB2001' and 'CMVB1989' grown in rhizotrons. Genotypes with measurements over population average are at the top of the plot. Genotypes with measurements under population average are at the bottom end of the plot.

Table S 1: WinRHIZO settings for image analysis of root measurements and leaf area based on colour classes

Colour analysis	Pop	Year	Exp	Part	Filters			Colour Specification					
					Smoothing/ Noise Removal	Debris		Background			Root / Shoot		
						Area	LW Ratio	Hue	Saturation	Intensity/ Brightness	Hue	Saturation	Intensity/ Brightness
Colour analysis on with colour classes and groups defined in „Colour Class File“, classification based on colour	‚VB2001‘	2018	a	root	high	0.08	4.00	27	146	9	31 29	93 77	147 71
			b								27	78	120
		2019	c			0.10					14 23	62 9	185 128
		2018	a	shoot	off	off	off	4 47 29 29 13 30	243 91 252 138 229 64	141 12 231 171 55 113	49	105	86
			b										
		2019	c										
	‚CMVB1989‘	2018	d	root	medium	0.10	4.00	25 8 17 41 25 29 31 28 28 37 5 16	180 181 172 134 114 234 73 108 50 84 221 207	10 63 65 53 191 224 38 7 102 12 95 191	28 25 27 31 30 29 28 30 29 29 29 25	92 118 118 79 77 83 93 67 74 77 81 107	95 67 87 117 58 108 107 124 113 118 98 76
		2019	e					21	58	13	18 10	58 13	188 119
			f										
		2018	d	shoot	off	off	off	6 22 26 25 15 24	228 129 101 97 208 161	95 13 188 74 34 90	35 41	173 136	70 54
		2019	e					249 1 217 42 8	148 147 80 26 116	180 123 233 14 51	37 19	139 213	33 59
			f										

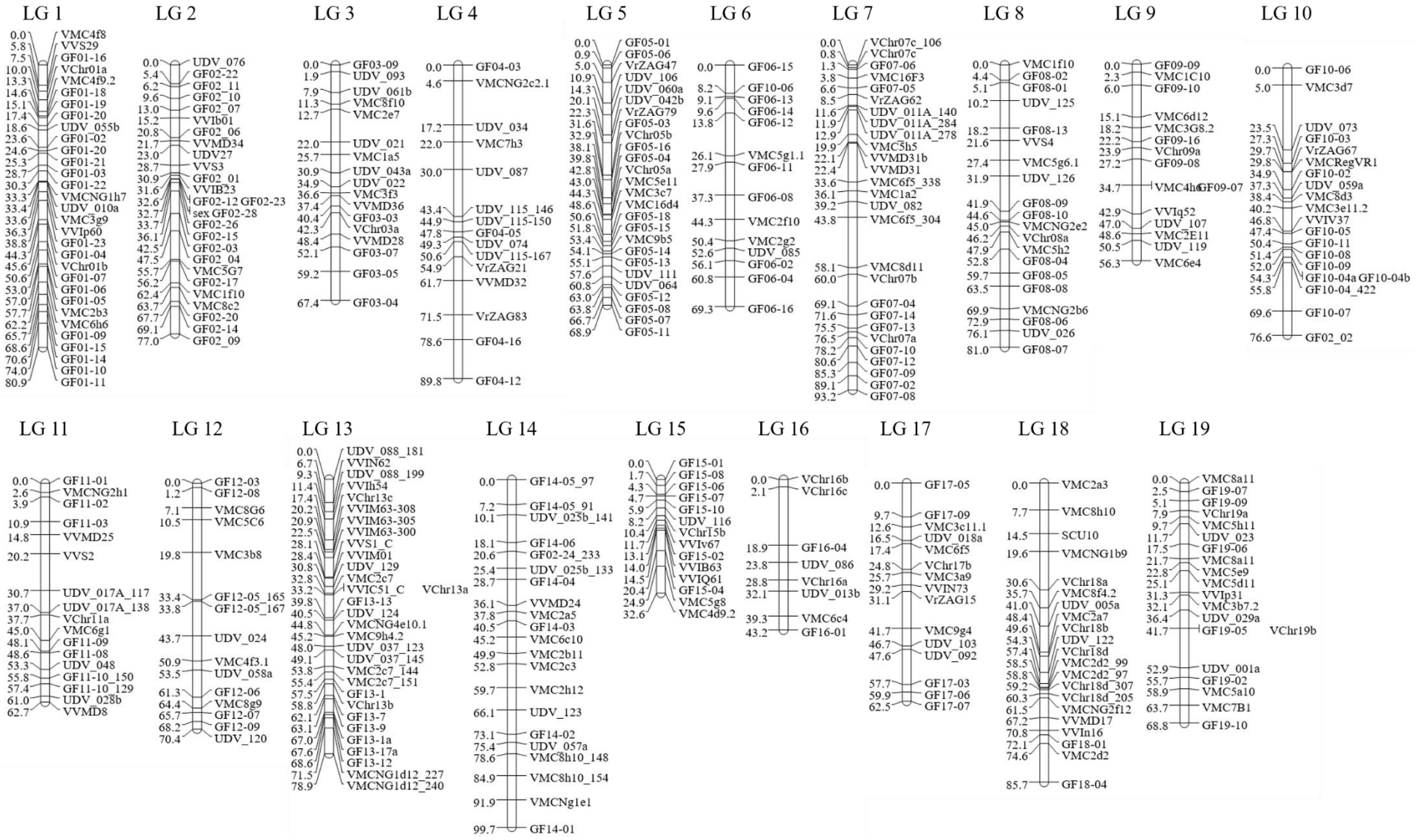

Figure S 12: Genetic map of mapping population 'VB2001' with 374 SSR markers on 19 linkage groups. The population consists of 151 F1 individuals. Marker distances are given in centi Morgan (cM) on the left side of each linkage group.

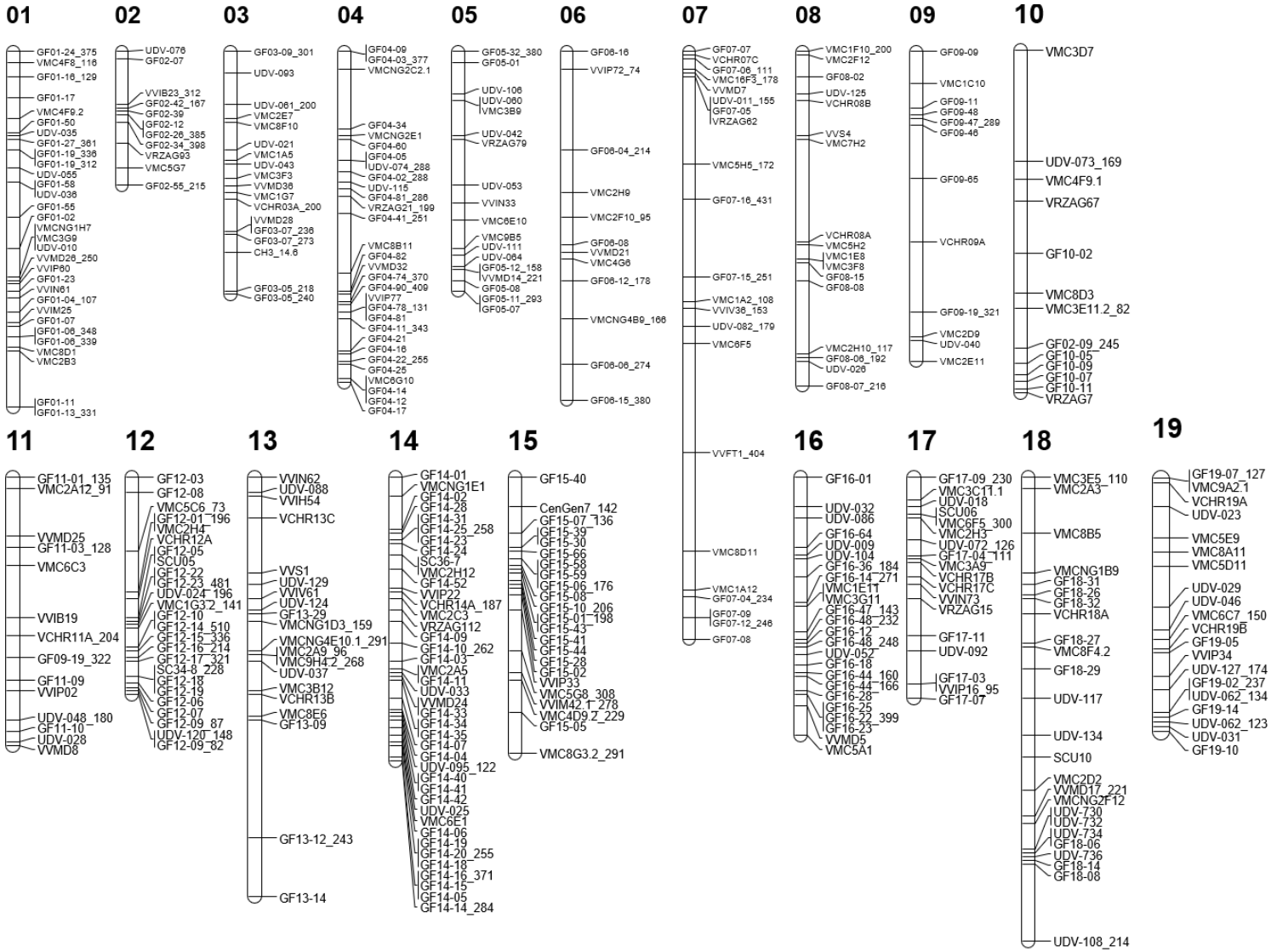

Figure S 13: Genetic map of mapping population 'CMVB1989' with 394 SSR markers on 19 linkage groups. The population consists of 151 F1 individuals.

6.3. Grapevine Root Development in Field Trial

Table S 2: List of 'VB2001' population genotypes, parental genotypes 'V3125' and 'Börner' and reference cultivars with their corresponding number of replicates of experimental years 2018 and 2019. Missing genotypes are indicated with asterisk (*).

genotype	replicates		genotype	replicates		genotype	replicates	
	2018	2019		2018	2019		2018	2019
2001-102-004	1	*	2001-102-055	2	*	2001-102-112	3	*
2001-102-005	5	*	2001-102-056	1	*	2001-102-113	1	*
2001-102-007	5	*	2001-102-060	1	*	2001-102-114	1	*
2001-102-010	4	*	2001-102-061	9	*	2001-102-115	1	*
2001-102-012	1	*	2001-102-064	3	*	2001-102-116	8	*
2001-102-013	4	*	2001-102-065	2	*	2001-102-117	6	9
2001-102-014	3	*	2001-102-066	1	*	2001-102-119	9	*
2001-102-016	1	*	2001-102-067	8	*	2001-102-120	6	10
2001-102-017	1	*	2001-102-068	9	*	2001-102-121	6	*
2001-102-018	4	10	2001-102-069	8	10	2001-102-122	7	6
2001-102-019	5	8	2001-102-070	9	*	2001-102-123	4	7
2001-102-020	4	*	2001-102-071	2	*	2001-102-124	2	*
2001-102-021	4	10	2001-102-072	2	*	2001-102-126	4	10
2001-102-022	5	*	2001-102-075	1	*	2001-102-127	3	11
2001-102-023	3	*	2001-102-079	3	*	2001-102-129	10	*
2001-102-024	3	*	2001-102-080	8	10	2001-102-130	9	*
2001-102-025	4	*	2001-102-081	7	*	2001-102-131	6	*
2001-102-026	6	10	2001-102-082	2	*	2001-102-132	10	*
2001-102-027	3	10	2001-102-083	1	*	2001-102-133	11	*
2001-102-031	4	*	2001-102-084	1	*	2001-102-134	2	*
2001-102-032	1	*	2001-102-085	5	10	2001-102-135	1	*
2001-102-033	1	*	2001-102-087	1	*	2001-102-136	7	*
2001-102-034	1	*	2001-102-089	5	8	2001-102-137	7	*
2001-102-037	1	*	2001-102-090	7	*	2001-102-138	5	*
2001-102-038	1	*	2001-102-091	7	7	2001-102-139	1	*
2001-102-039	2	*	2001-102-094	1	*	2001-102-140	1	*
2001-102-040	4	8	2001-102-095	7	*	2001-102-141	2	*
2001-102-041	3	10	2001-102-096	5	*	2001-102-142	1	*
2001-102-042	10	*	2001-102-097	5	*	2001-102-143	5	*
2001-102-043	4	6	2001-102-098	6	11	2001-102-144	4	*
2001-102-044	9	5	2001-102-100	10	*	'Börner'	4	8
2001-102-045	8	*	2001-102-101	11	*	'V3125'	2	9
2001-102-047	10	10	2001-102-103	7		'1103 Paulsen'	*	10
2001-102-048	2	*	2001-102-105	4	8	'5C Geisenheim'	*	10
2001-102-050	2	*	2001-102-108	1	*	'Couderc 3309'	*	10
2001-102-051	1	*	2001-102-109	6	10	'Calardis Musqué'	*	10
2001-102-052	2	*	2001-102-111	1	*	'Kober 125AA'	*	10
						'Ramsey'	*	9

Colour analysis	Pop	Year	Filters			Colour Specification					
			Smoothing/ Noise Removal	Debris		Background			Root		
				Area	LW Ratio	Hue	Saturation	Intensity/ Brightness	Hue	Saturation	Intensity/ Brightness
Colour analysis on with colour classes and groups defined in „Colour Class File“, classification based on colour	‚VB2001‘	2019	high	2.0	4.00	24	107	43	31	11	158

Table S 3: WinRHIZO settings for image analysis of depth segments based on colour classes

Table S 4: Contributions of principal components for maximal root length (RL), adventitious root number (RN), root dry weight (RDW), maximal root diameter (RD), and shoot dry weight (SDW).

	Dim. 1	Dim. 2	Dim. 3	Dim. 4	Dim. 5
RL	16.11	4.10	54.16	20.86	4.78
RN	11.28	59.91	7.92	14.48	6.40
RDW	33.70	0.59	0.03	1.50	64.18
RD	11.39	35.20	37.88	14.18	1.34
SDW	27.53	0.19	0.01	48.98	23.29

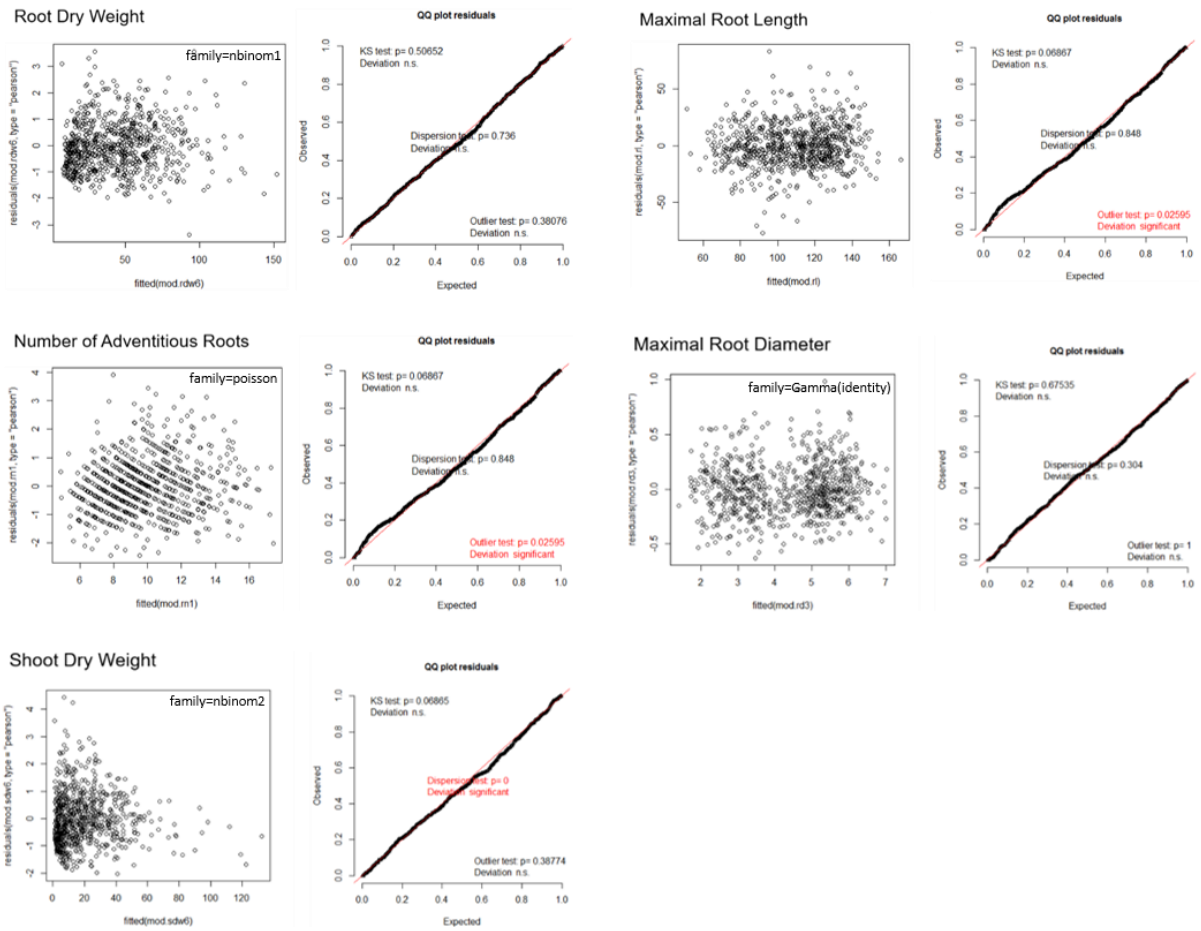

Figure S 14: Model diagnostics of mapping population 'VB2001' for statistic modeling of root system measurements of the field trial

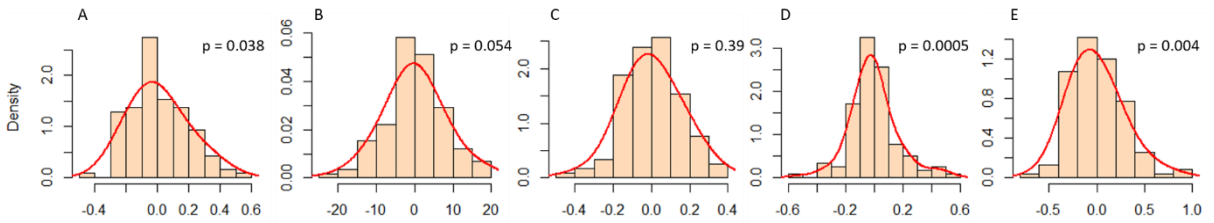

Figure S 15: Histograms of best linear unbiased prediction (BLUP) values of root dry weight (A), maximal root length / rooting depth (B), number of adventitious roots (C), maximal root diameter (D), and shoot dry weight (E) of mapping population 'VB2001'

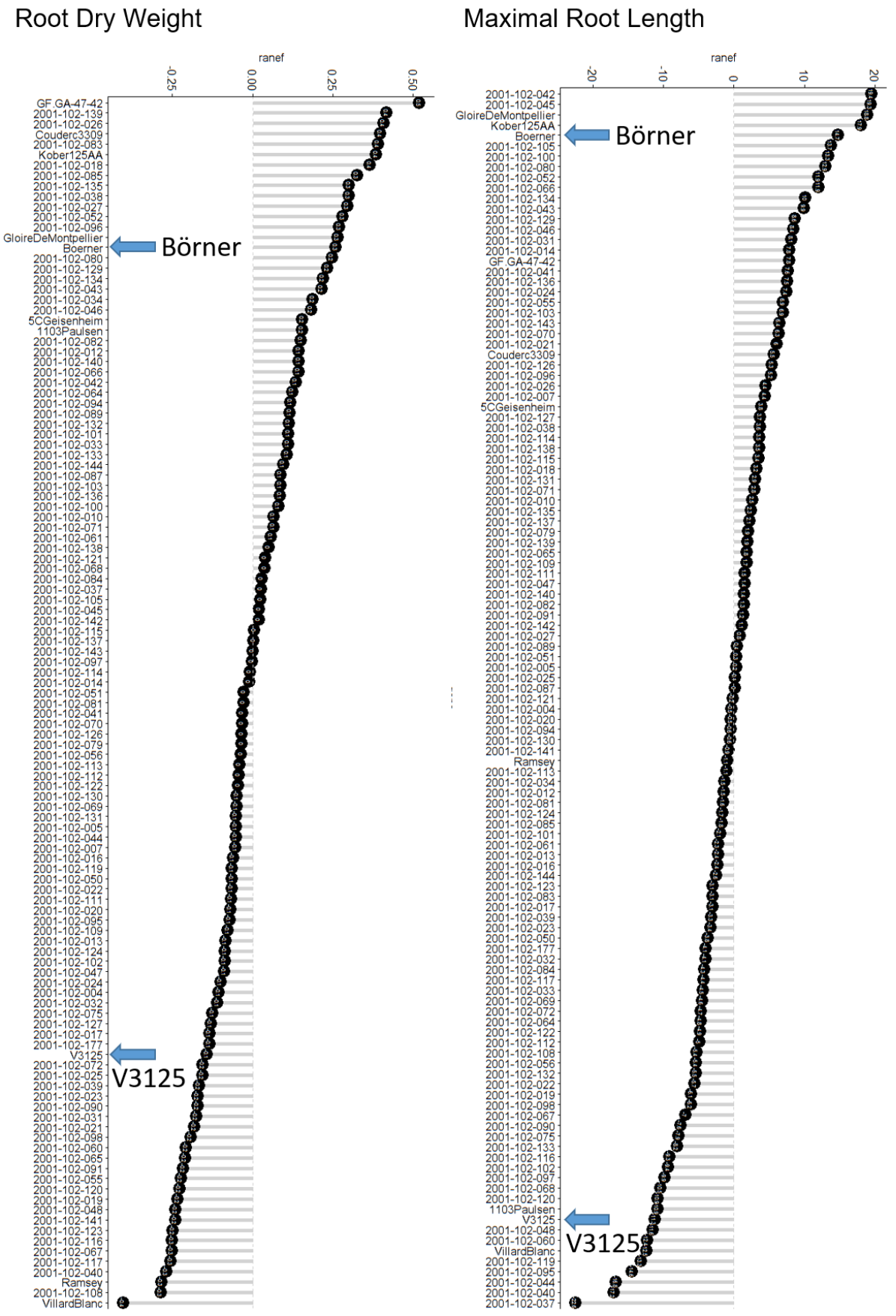

Figure S 16: BLUP values for root dry weight and maximal root length of population and parental genotypes of 'VB2001' grown in the field trial. Genotypes with measurements over population average are at the top of the plot. Genotypes with measurements under population average are at the bottom end of the plot.

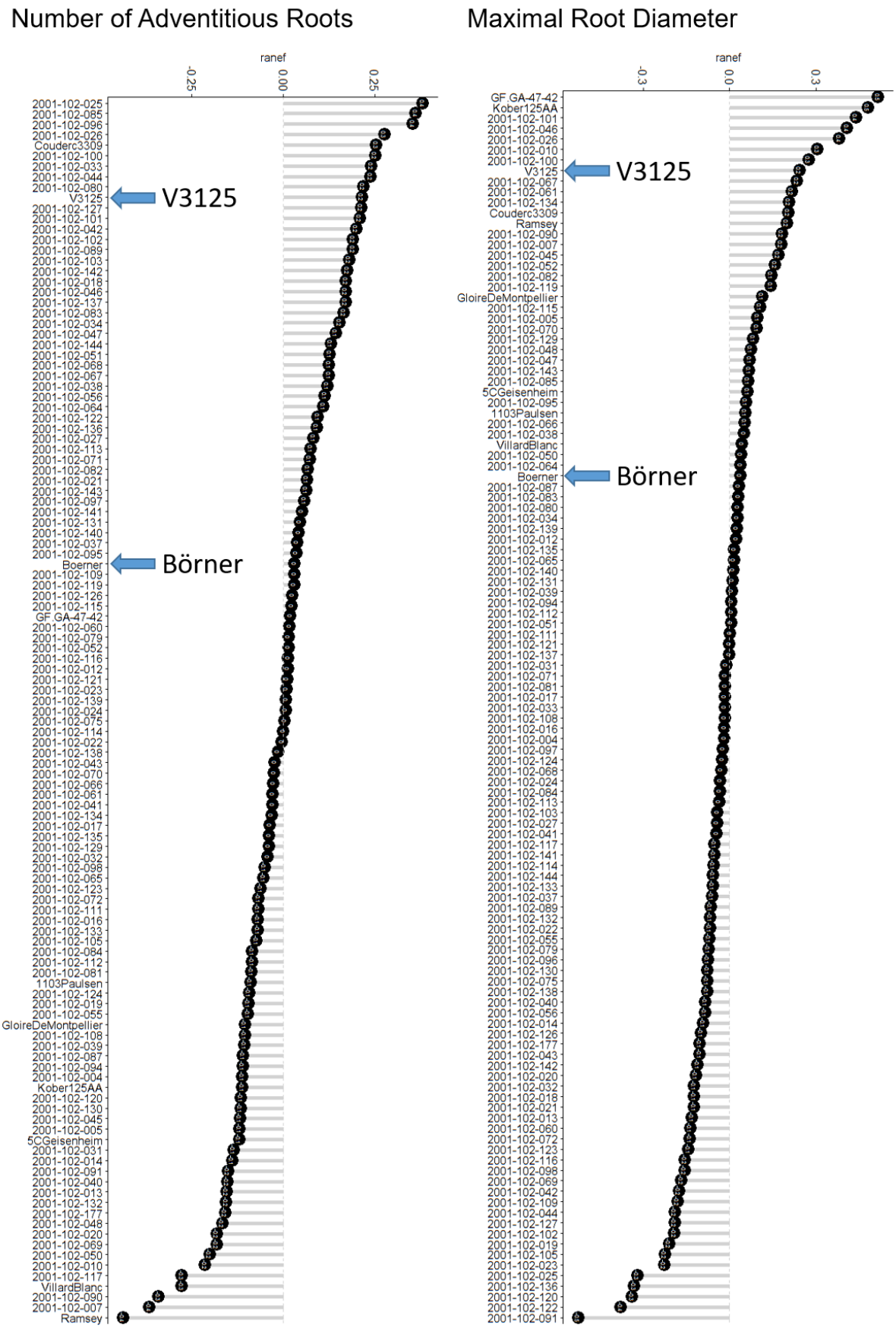

Figure S 17: BLUP values for number of adventitious roots and maximal root diameter of population and parental genotypes of 'VB2001' grown in the field trial. Genotypes with measurements over population average are at the top of the plot. Genotypes with measurements under population average are at the bottom end of the plot.

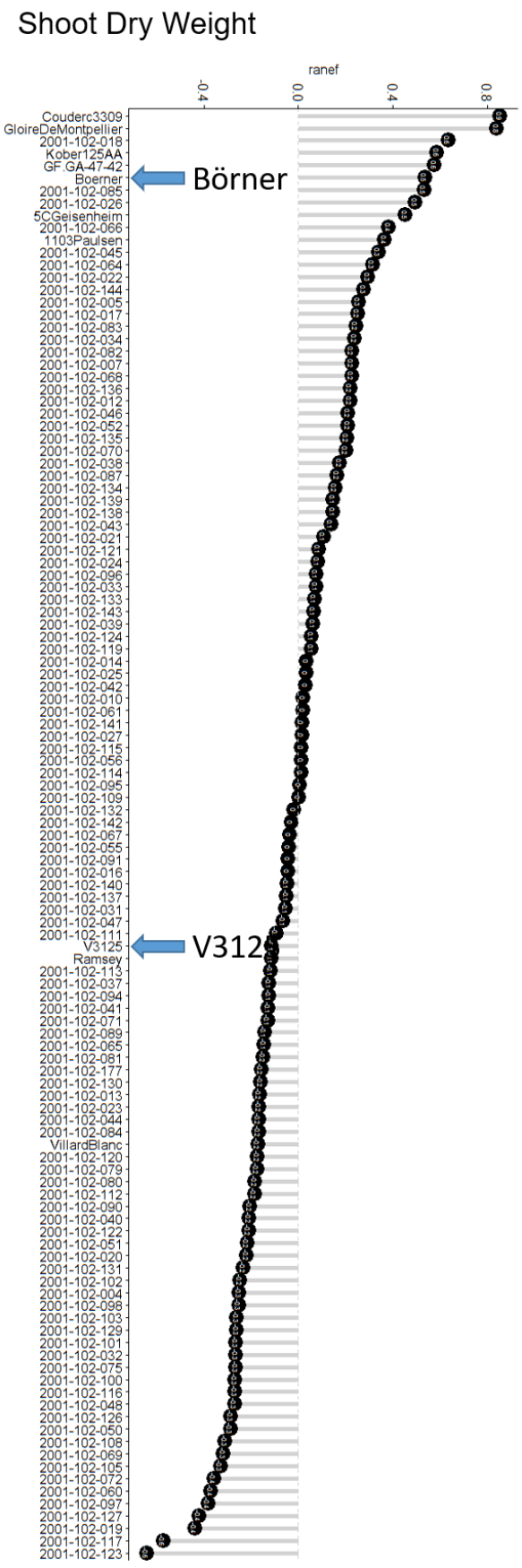

Figure S 18: BLUP values for shoot dry weight of population and parental genotypes of 'VB2001' grown in the field trial. Genotypes with measurements over population average are at the top of the plot. Genotypes with measurements under population average are at the bottom end of the plot.

Acknowledgements

The project was supported by funds of the Federal Ministry of Food and Agriculture (BMEL) based on a decision of the Parliament of the Federal Republic of Germany via the Federal Office for Agriculture and Food (BLE) under the innovation support programme.